CO_2 capture using solid sorbents: Fundamental aspects, mechanistic insights and recent advances

Matthew T. Dunstan[1,*], Felix Donat[2,*], Alexander H. Bork[2,*], Clare P. Grey[1], Christoph R. Müller[2,+]
* Equally contributing authors
+ Corresponding author, muelchri@ethz.ch
[1] Department of Chemistry, University of Cambridge, Lensfield Road, Cambridge CB2 1EW, United Kingdom
[2] Laboratory of Energy Science and Engineering, Department of Mechanical and Process Engineering, ETH Zürich, Leonhardstrasse 21, 8092 Zürich, Switzerland

Abstract

Carbon dioxide capture and mitigation forms a key part of the technological response to combat climate change and reduce CO_2 emissions. Solid materials capable of reversibly absorbing CO_2 have been the focus of intense research for the past two decades, promising stability and low energy costs to implement and operate compared to the more widely used liquid amines. In this Review, we explore the fundamental aspects underpinning solid CO_2 sorbents based on alkali and alkaline earth metal oxides operating at mid- to high temperature: how their structure, chemical composition and morphology impact their performance and long-term use. Various optimization strategies are outlined to improve upon the most promising materials, and we combine recent advances across disparate scientific disciplines including materials discovery, synthesis, and in situ characterization to present a coherent understanding of the mechanisms of CO_2 absorption both at surfaces and within solid materials.

1 Introduction and objectives - CO_2 capture by metal oxides

Humankind faces an urgent challenge to rapidly reduce greenhouse gas emissions in order to reach a carbon neutral society by 2050, the point at which environmental changes caused by climate change may become irreversible [1], [2]. Amongst the many technologies being developed towards this goal, it has been argued that carbon dioxide capture, utilization and storage (CCUS) is a necessary component, being both a mature and relatively inexpensive measure that can support other initiatives in electrochemical storage, renewable energy conversion and improving industrial efficiency [3]–[6]. Not only is CCUS an environmental necessity, but it also represents a significant economic opportunity [7], [8]. Recent governmental and industrial white papers highlight its vital role in "Power to X" (P2X) schemes that seek to harness electricity to synthesize various energy-dense fuel sources by utilizing H_2 from electrolysis combined with CO_2 from capture [9]–[13]. P2X represents just one of several

proposed industrial processes aiming to use CO_2 as a feedstock [14]–[20], underlining the need for efficient CCUS implementation.

Within the area of carbon dioxide capture, liquid amines have seen the most use at scale in pilot plants designed to reversibly capture CO_2 and yielding a purified stream of CO_2 for subsequent sequestration [18], [21]–[23]. However, amines and especially their regeneration incur a relatively high energy cost, and there exist concerns regarding their toxicity [24], motivating research over the past two decades to develop alternative materials. CO_2 capture by metal oxides has been of industrial relevance for more than 150 years, ever since Tessié du Motay and Marechal [25] used CaO to absorb the CO_2 generated in a gasification process to increase the purity of H_2. The use of oxides for CO_2 capture has emerged only recently when Silaban and Harrison suggested using CaO to capture CO_2 from emissions in 1995 [26]. In 1999, Shimizu et al. [27] proposed a post-combustion CO_2 capture process composed of two interconnected fluidized bed reactors, in which CO_2 is continuously absorbed from a flue gas stream by CaO, forming $CaCO_3$, followed by its thermal decomposition to CaO to obtain a stream of sufficiently pure CO_2 (> 96 %) for sequestration (R1 in Table 1) [28]. This process, termed calcium (or carbonate) looping (CaL), formed the basis for research on CO_2 capture by metal oxides at mid- to high temperatures (> 200 °C) to the present day. The higher operating temperatures of metal oxides compared to liquid amines gives the promise of a lower energy penalty incurred if implemented into power plants, driving interest in their further development [29], [30]. There has been a great deal of research aimed at understanding various aspects of the CO_2 absorption reaction at elevated temperature, including the materials that are of potential interest, and various modifications and optimizations that can be performed to achieve benchmarks set by governments and industry.

This review aims to focus on the chemistry, engineering and material science aspects that underpin mid- to high temperature CO_2 capture using solid oxide materials (e.g. CaO, MgO and Li_4SiO_4) in order to consolidate the current state of understanding of the parameters that drive capture performance; for general overviews of solid sorbents suitable for CO_2 capture at low temperature (< 200 °C), e.g. carbon-based materials, zeolites, metal-organic-frameworks (MOF) or hydrotalcite-like compounds, which all do not necessarily form thermodynamically stable carbonates, we refer to relevant review papers [31]–[39]. The different disciplines concerned in the development of metal oxide sorbents can offer complementary insights into CO_2 absorption, but their communities are often disparate; this review aims to bring together the contributions of each field, and to encourage more interdisciplinary studies and experimental approaches.

CaO-based sorbents are by far the most widespread in terms of research literature, much of which is focused on the optimization of the archetypal CaO on an industrial process scale; for summaries of this work, we refer to a number of review papers [40]–[50] and also to papers covering specifically Mg- [51], [52] and Li-based [53], [54] sorbents. In contrast, this review will investigate questions at a much more fundamental level, including the influence of material structure, ionic conduction and particle morphology on CO_2 absorption, and how the structural and operando analysis of a wide range of Ca, Mg and Li containing materials reveals trends tying performance to these chemo-physical properties. This includes theoretical approaches utilizing screening methodologies based on first principle analysis using density functional theory (DFT), as well as large-scale experimental screening which can guide the rational design of novel materials. This review also covers work applying new analytical techniques to study CO_2 capture materials including in situ X-ray diffraction (XRD), Raman spectroscopy, nuclear magnetic resonance (NMR) and synchrotron-based techniques, attempting to uncover causal links between performance and the various chemical and physical features to a material.

The hope is to offer researchers in this field a broad survey of the underlying problems inherent in solid oxide CO_2 capture, and to highlight the most advanced research efforts in material synthesis, structural manipulation and material characterizations to present common findings across different fields providing advances in fundamental understanding.

2 Fundamentals of the carbonation and calcination reactions

The following sections discuss fundamental aspects of the carbonation and calcination reactions for the most widely used sorbents for CO_2 at elevated temperature, i.e. CaO and MgO, including their structural transformations and kinetics. Further, the role of the gas environment and reasons for sorbent deactivation are assessed. In order to simplify the analysis, we chose to focus solely on unmodified CaO-$CaCO_3$ and MgO-$MgCO_3$ as model systems, given that the majority of previous research has involved these materials or modifications thereof, and that they represent the basis of the most advanced systems in terms of practical implementation.

2.1 Thermodynamic properties of alkali metal oxide sorbents

The applicability of any material for CO_2 capture at elevated temperatures (> 200 °C) is driven by the requirements of the process in which the material is to be used. For post-combustion CO_2 capture, CO_2 concentrations in the off-gas from industrial processes typically range from ~ 3 – 15 vol.% CO_2 depending on the type of fuel used, but can reach as high as 35 – 40 vol.% in cement plants or in the iron and steel industry [55]–[58]. Ideally, CO_2 is removed completely from the respective gas stream before it is released to the atmosphere. In pre-combustion CO_2 capture, e.g. for integrated gasification combined cycle (IGCC) power plants, partial pressures of CO_2 from coal gas can range from 0.5 to 10 bar [59]–[61].

Figure 1 plots the equilibrium partial pressure of CO_2, $p_{CO2,eq}$, as a function of temperature T for various single metal oxide sorbents. Combinations of T and p_{CO2} above the respective $p_{CO2,eq}$-curves imply the material exists as carbonate, whereas below the curve the material's thermodynamically stable state is its oxide form.

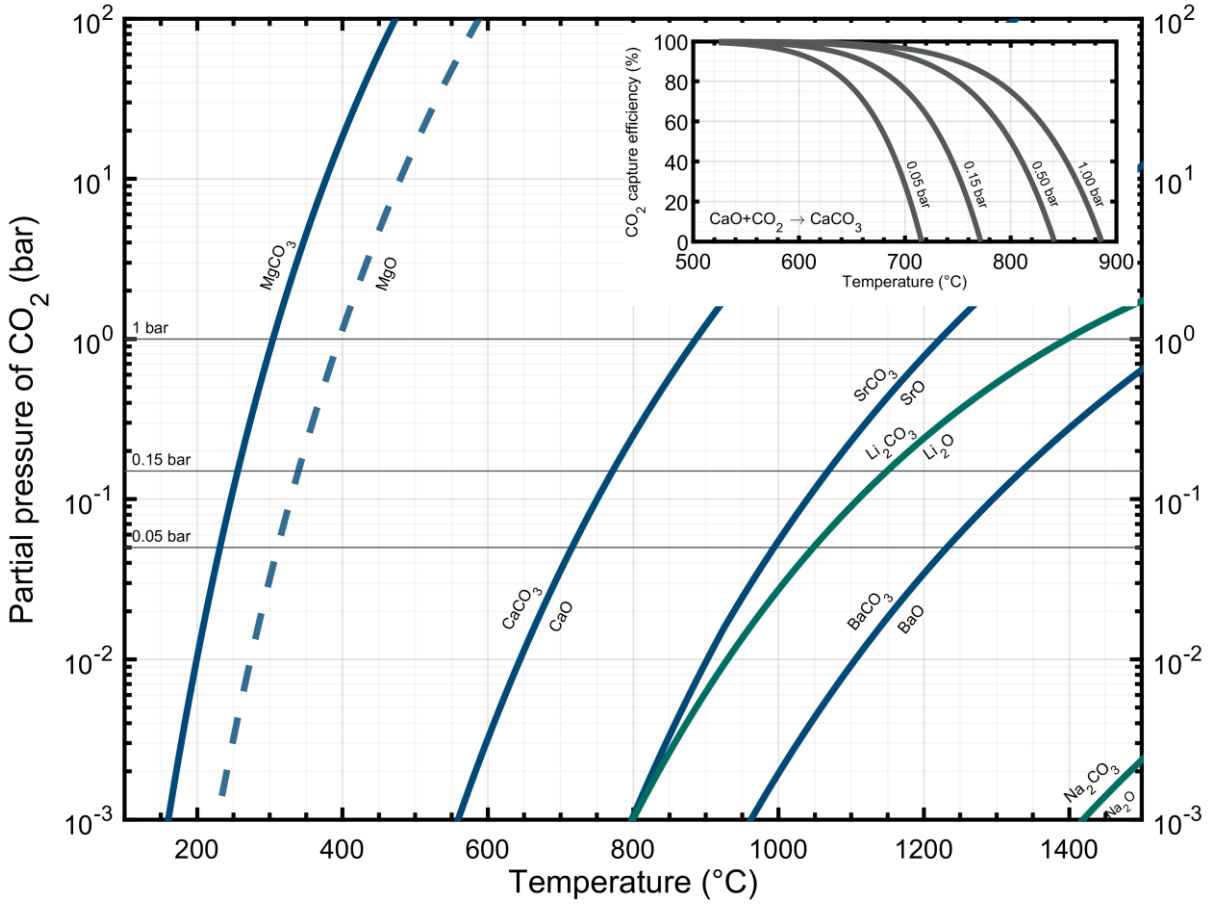

Figure 1. Equilibrium partial pressure of CO_2, $p_{CO2,eq}$, as a function of temperature for alkali (green) and alkaline earth (blue) metal oxide-carbonate systems. Horizontal grey lines indicate p_{CO2} of 0.05, 0.15 and 1 bar, respectively. Note that the $p_{CO2,eq}$ for the systems K_2O-K_2CO_3, Rb_2O-Rb_2CO_3 and Cs_2O-Cs_2CO_3 are < 10^{-3} bar for temperatures 100 – 1500 °C and are thus not seen in the figure. The curves were computed using thermodynamic data provided by the NASA Glenn Research Center [62]. *The blue dashed line indicates the $p_{CO2,eq}$ for the system MgO-$MgCO_3$ reported in* [63], [64]. *The inset plots the maximum CO_2 capture efficiency as a function of temperature for the system CaO-$CaCO_3$ for different p_{CO2}; for a CO_2 capture efficiency of zero the temperature for the transition between CaO and $CaCO_3$ is obtained for the given p_{CO2}.*

Taking the system CaO-$CaCO_3$ and a gas stream containing 15 vol.% CO_2 (equivalent to $p_{CO2} \approx 0.15$ bar at atmospheric pressure), the maximum CO_2 capture efficiency at 600 °C is $(p_{CO2} - p_{CO2,eq})/p_{CO2} = (0.15 - 0.0032)/0.15 = 97.9$ %, but decreases to $(0.15 - 0.0358)/0.15 = 76.1$ % at 700 °C. The removal of almost all (99.9 %) CO_2 from the gas stream is thermodynamically feasible up to temperatures of 570 °C. We note that the thermodynamic properties of the CaO-$CaCO_3$ system enable also the capture of CO_2 from ambient air ($p_{CO2} = 4 \cdot 10^{-4}$ bar) [65]–[67]. Turning to the release of CO_2 from the sorbent (i.e. the decomposition of $CaCO_3$), temperatures greater than ~ 900 °C are required to obtain a pure stream of CO_2 ($p_{CO2} \approx 1$ bar).

Surprisingly, the thermodynamic data for the system MgO-$MgCO_3$ is inconsistent; for temperatures up to 520 °C, the $p_{CO2,eq}$ differ by at least one order of magnitude from references [63], [64] and standard thermodynamic tables (NASA, NIST or HSC Chemistry 6 and later) [68]. The thermodynamic data provided by NASA suggests that CO_2 capture using MgO is

unfavorable at atmospheric pressure at temperatures > 300 °C, while references [63], [64] imply it is unfavorable > 400 °C in 1 bar of CO_2. Experiments have shown that $MgCO_3$ can indeed be formed from MgO at temperatures > 300 °C in 1 bar CO_2 (see Table 6 in Section 3.2) when promoters are added. Although promoters will not affect the thermodynamics of MgO, this suggests that either the thermodynamic data from references [63], [64] are a better predictor of the operation temperature of MgO or that the standard thermodynamic data may practically not be relevant when promoters are added; this is discussed in Section 3.2 where the role of molten salts is elaborated upon. Further, it is worth noting that capturing 99.9 % of the CO_2 in a gas stream containing 15 vol.% CO_2 is thermodynamically unfavorable at temperatures greater than 165 °C or 235 °C, respectively, when using MgO.

The high reaction temperatures required for the decomposition of $SrCO_3$ and $BaCO_3$ in CO_2-rich atmospheres render them unsuitable for post-combustion CO_2 capture, but they are potential candidates for energy storage applications owing to their relatively high energy densities (reaction enthalpy per mass of alkali oxide) [69], [70].

The monometallic oxides involving the alkali metals Li, Na and K have not been considered often as sorbents for large scale CO_2 capture, but do play an important role in altering the CO_2 sorption mechanisms of CaO and MgO (Sections 3.1.1 and 3.2). In their hydroxylated forms, they are important for direct air capture (in aqueous solution) [71]–[74] or in specialized applications such as scrubbing CO_2 within a spacecraft ($Li(OH)_2$) [75], [76]. Monometallic Li-, Na- and K-carbonates do not decompose completely in CO_2-rich environments at practically feasible temperatures (up to ~ 1200 °C) and can thus not be employed as sorbents in a cyclic reaction scheme with CO_2 being the only gaseous reactant [77]. However, CO_2 capture of these carbonates is feasible in the presence of steam [78] and there have been promising experimental investigations where Na_2CO_3 or K_2CO_3 was reacted with equimolar amounts of CO_2 and H_2O to form $NaHCO_3$ or $KHCO_3$ at temperatures < 100 °C [79]–[86]. Li is typically investigated in ternary metal oxide systems [54], e.g. Li_2ZrO_3 or Li_4SiO_4, as is discussed in Section 5.3.

Important physical and chemical properties of the alkali and alkaline earth metal oxides and their respective carbonates are summarized in Table 1; these properties inform the following analysis of mechanistic aspects of the carbonation and calcination reactions in Sections 2.2 and 2.3.

Table 1. Overview of important physical and chemical properties of alkali and alkaline earth metal oxides and their carbonates. If not stated otherwise, the properties were obtained from [68].

Metal oxide / carbonate	Molecular weight (g mol^{-1})	Gravimetric CO_2 uptake capacity (g_{CO2} g_{MeO}^{-1})	Gibbs free energy at 298 K (carbonation) (kJ mol^{-1})	Enthalpy of reaction at 298 K (carbonation) (kJ mol^{-1})	Specific heat capacity at 298 K (J K^{-1} mol^{-1})	Equilibrium temperature for p_{CO2} = 0.15 / 1.00 bar (°C)	Melting point (°C)	Molar volume (cm^3 mol^{-1})	True density (kg m^{-3})	Crystal ionic radius of cation (Å) [87]	Trivial name / Mineral name	Carbonation reaction
MgO	40.304	1.094	-48.55	-100.89	37.24	(255/340)/ (305/395)[1]	2825	11.29	3570	0.86	Magnesia	$MgO + CO_2 \rightarrow MgCO_3$ (R1)
$MgCO_3$	84.314				76.11		990	28.01	3010		Magnesite	
CaO	56.077	0.786	-130.44	-178.17	42.05	770/885	2900	16.74	3350	1.14	Calcia, lime	$CaO + CO_2 \rightarrow CaCO_3$ (R2)
$CaCO_3$	100.087				83.47		1330	36.93	2710		Calcite	
SrO	103.619	0.426	-190.18	-241.49	45.25	1070/1225	2530	20.68	5010	1.32	Strontia	$SrO + CO_2 \rightarrow SrCO_3$ (R3)
$SrCO_3$	147.629				82.42		1495	38.45	3840		Strontianite	
BaO	153.326	0.288	-220.73	-272.49	47.02	1335/1560	1973	25.26	6070	1.49	Baria	$BaO + CO_2 \rightarrow BaCO_3$ (R4)
$BaCO_3$	197.336				85.98		1555	45.79	4310		Whitherite	
Li_2O	29.881	1.476	-174.65	-222.71	54.1	1150/1395	1455	16.24	1840	0.90	Lithia	$Li_2O + CO_2 \rightarrow Li_2CO_3$ (R5)
Li_2CO_3	73.891				98.32		730	35.70	2070		-	
Na_2O	61.979	0.712	-270.60	-321.11	69.12	> 1500	1130	28.43	2180	1.16	-	$Na_2O + CO_2 \rightarrow Na_2CO_3$ (R6)
Na_2CO_3	105.989				112.30		860	41.56	2550		Soda ash	
K_2O	94.196	0.468	-350.31	-396.29	72.00	> 1500	740	40.08	2350	1.52	Potash	$K_2O + CO_2 \rightarrow K_2CO_3$ (R7)
K_2CO_3	138.206				114.43		900	61.73	2239		-	
Rb_2O	186.935	0.236	-354.17	-401.09	74.00	> 1500	505	46.39	4030	1.66	-	$Rb_2O + CO_2 \rightarrow Rb_2CO_3$ (R8)
Rb_2CO_3	230.945				117.60		875	70.63	3270		-	
Cs_2O	281.810	0.156	-348.44	-394.99	76.00	> 1500	495	59.71	4720	1.81	-	$Cs_2O + CO_2 \rightarrow Cs_2CO_3$ (R9)
Cs_2CO_3	325.820				123.85		795	76.66	4250		-	

[1] For the system MgO-$MgCO_3$, conflicting thermodynamic data has been reported [64], [68].

From a practical point of view, there is a trade-off between thermodynamics and kinetics when identifying the optimum reaction conditions for CO_2 capture applications (e.g. for post-combustion or pre-combustion CO_2 capture). The Arrhenius term of any kinetic expression increases with temperature, while the thermodynamic driving force for carbonation ($p_{CO2} - p_{CO2,eq}$) decreases; the latter determines the maximum theoretical CO_2 capture efficiency of the process, as is shown for the system CaO-$CaCO_3$ in the inset of Figure 1. The rates at which CO_2 is captured by the sorbents need to be sufficiently high for the carbonation reaction to be limited only by thermodynamics and ensure high process efficiencies. Even when a sorbent is observed to transition rapidly between its oxide and carbonate state in experimental test equipment, this does not automatically entail the efficient removal of CO_2 from a gas stream (see Section 6).

2.2 Carbonation

2.2.1 CaO-$CaCO_3$ system

The carbonation reactions (R1 – R9 in Table 1) are exothermic and thus generate a significant quantity of heat that can be utilized within the carbon dioxide capture process. Being a (theoretically) reversible reaction, the decomposition of the carbonate (the calcination step) is equally endothermic and is favored at higher temperatures (Figure 1). The heat of reaction increases with the molecular weight of the alkaline earth metal oxide used as the sorbent, but the energy density decreases.

Computational studies have suggested that during carbonation the nucleation of calcite ($CaCO_3$), occurs on the (111) surface of CaO with CO_3^{2-} groups spreading laterally layer-by-layer [88]; note that of the three $CaCO_3$ polymorphs aragonite, vaterite and calcite, only calcite is thermodynamically stable under typical carbonation conditions (but also has the lowest adsorption preference for CO_2 of the three polymorphs [89]). At temperatures < 300 °C, amorphous $CaCO_3$ can be formed, which crystallizes exothermally > 300 °C [90]. The initial surface reaction is fast and measuring intrinsic kinetics requires precise control of the reaction conditions [91]–[93]. Gradually increasing rates of carbonation that would imply the formation and growth of nuclei have seldomly been observed [94]–[96]. The intrinsic rate constant for the CaO-CO_2 reaction has been found to be first order with respect to p_{CO2}, but changes to a zero-order dependence for ($p_{CO2} - p_{CO2,eq}$) > 0.1 bar [91]. Reported activation energies for the carbonation reaction are low and typically < 30 kJ mol^{-1}, often ~ zero [97]–[99]. Various conceptually different reaction models were found suitable for the kinetic modelling of the carbonation reaction [46], [96], [100], including shrinking core, pore and grain models. Similar to many gas-solid reactions, the observed rate of carbonation decreases once all readily

available surface CaO has been covered with a product layer of $CaCO_3$. As is shown in Table 1, the molar volume of $CaCO_3$ is roughly twice that of CaO. The concept of a critical product layer thickness of ~ 20 – 90 nm [101]–[104] has been widely adopted to explain the transition from a fast (i.e. kinetically-controlled) to a slow (i.e. diffusion-controlled) carbonation regime that is typically observed when investigating the sorbent's long-term cyclic stability (i.e. repeated cycles of carbonation and calcination). Biasin et al. [97], [105] measured the crystallite size of $CaCO_3$ using synchrotron X-ray diffraction (XRD) and showed that the increase in crystallite size correlated with the observed transition from the fast to slow carbonation regime. They showed that both the reaction temperature and the initial CaO crystallite size affect the critical $CaCO_3$ crystallite size (when the observed rate of carbonation decreases substantially), which varied between 12 nm (at low temperature and/or for large CaO crystallite sizes) and 282 nm (at high temperature and/or for small CaO crystallite sizes); the final crystallite size of $CaCO_3$ was thus not necessarily greater than the initial crystallite size of CaO. These results agree well with atomic force microscopy (AFM) studies on single CaO crystals by Li and Cai [106], who observed that (i) the surface of CaO is not covered uniformly with $CaCO_3$ product during carbonation, and (ii) $CaCO_3$ grows as islands on the CaO surface, with the island density decreasing with increasing temperature while their size increases. Grain boundary diffusion dominates the initial product layer diffusion when the average $CaCO_3$ crystallite size is small, whereas lattice diffusion becomes more dominant as the product layer diffusion continues [107], [108]. Through inert marker experiments, Sun et al. [109] confirmed the hypothesis made by Bhatia and Perlmutter [110] that product layer diffusion is dominated by the inward counter-current diffusion of CO_3^{2-} anion groups (and not individual C, O or CO_2 [111], [112]) and outward current of O^{2-} anions; gaseous CO_2 thus reacts with O^{2-} anions on the solid surface to form CO_3^{2-} anion groups, which then diffuse inward through the $CaCO_3$ layer to the $CaO/CaCO_3$ interface where new $CaCO_3$ is formed.

The idea that a critical product layer thickness causes the drop in carbonation rate ignores the fact that the solid-state diffusion – grain boundary or lattice diffusion or both – of CO_2 (or more precisely, CO_3^{2-} anion groups) through the $CaCO_3$ product layer is several orders of magnitude slower than the diffusion of CO_2 through a narrow pore inside a sorbent particle [107], [113], [114]. What is therefore considered as product layer diffusion is, on a particle scale, rather the diffusion of CO_2 through the pore network to the nearest unconverted CaO site, possibly also between existing islands of $CaCO_3$ product. True product layer diffusion becomes rate limiting typically much later into the carbonation reaction [107], and the transition period between

surface kinetic control and product layer diffusion is characterized by a mix of pore diffusion and the gradual blocking of small pores by the $CaCO_3$ product [115], [116].

Figure 2 illustrates four exemplary cases of how the carbonation reaction proceeds, as observed often in laboratory testing using thermogravimetric analyzers (TGA). Such measurements give a good indication of the structure of the pore network of the sorbent particle, and do not necessitate any N_2 sorption or Hg porosimetry measurements that would quantitatively yield pore volume and surface area as a function of the pore dimension. Note that if only the final CO_2 uptake is compared for different sorbents, there is typically no clear correlation with the initial pore volume and surface area of the material [117].

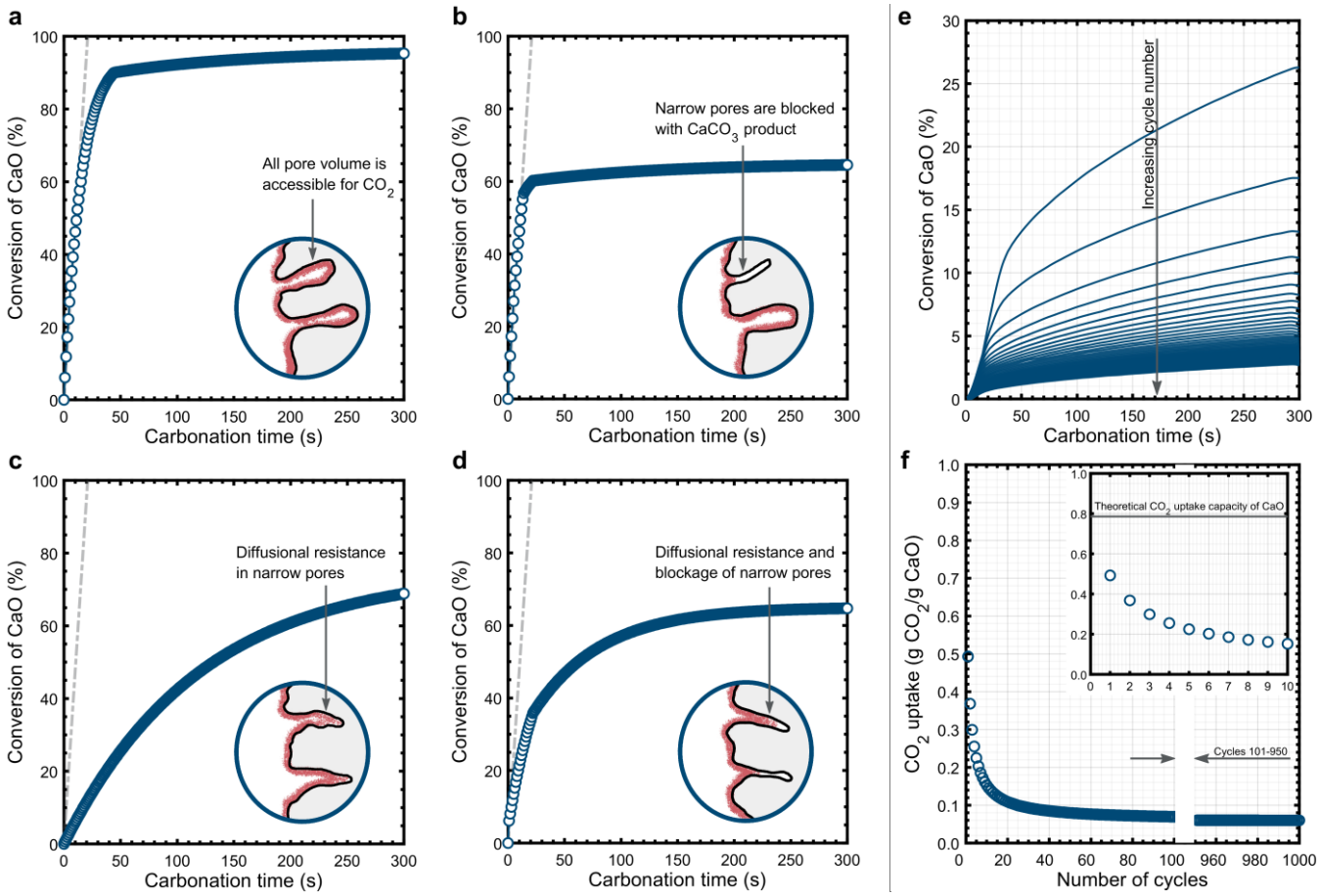

Figure 2. (a) – (d): Illustration of conversion profiles of CaO typically observed for different pore size distributions. The carbonation time of 5 min is used for illustration purpose only and the true carbonation time depends on the actual amount of sorbent used. The dashed grey line represents the maximum rate of carbonation under kinetic control. Cartoons in the bottom right corner of each plot illustrate qualitatively the differences in the size of the pores; red color indicates $CaCO_3$ product. Note that to put emphasis on the pores, the grey CaO skeleton is drawn unrealistically thick. (e) Conversion of CaO measured in the TGA using natural limestone as the sorbent under very harsh reaction conditions (calc. at 950 °C in pure CO_2) over 100 cycles; original, unpublished data. (f) Illustration of the cyclic decrease in CO_2 uptake of CaO-based sorbents over 1000 cycles. The data was computed using the correlation given by Grasa and Abanades [118] *(Section 2.5.1) with values reported for limestone ($k = 0.73$ and $X_r = 0.075$). The inset focuses on the first ten cycles, during which the decrease in CO_2 uptake is most significant.*

Figure 2a presents an ideal case where almost all CaO is immediately converted to $CaCO_3$. The sharp transition from a fast to a slow carbonation regime suggests a rapid change in the rate-

limiting step from kinetic control to product layer diffusion control. Figure 2b shows a similar trend in conversion of CaO with time, but the conversion value at which the sharp transition from a fast to a slow carbonation regime occurs is much lower [119]–[121]. This implies that a relatively large fraction of CaO is inaccessible to CO_2, e.g. because it can only be reached through small pores that become blocked with $CaCO_3$. Figure 2c shows a case where only a small fraction of CaO is converted under kinetic control. The carbonation reaction proceeds at a slower rate than in the other three cases due to diffusion limitations and CO_2 moving through a network of narrow pores, but reaches near completion within a reasonable time [122]. Lastly, Figure 2d shows a case which is most frequently observed with natural CaO-based sorbents [99], [123]. A reasonably large amount of CaO is accessible for CO_2 under kinetic control, followed by a gradual decrease in the observed rate of carbonation due to increasing diffusional transport resistance within the pore network. Eventually, the smallest pores are blocked with $CaCO_3$, leaving some unconverted CaO inaccessible for CO_2, and the observed rate of conversion is governed by product layer diffusion.

Based on our knowledge of the carbonation reaction, the implications for a CO_2 capture process with CaO are the following: (i) Intrinsic surface kinetics of pure CaO are extremely fast and are usually not rate-limiting at temperatures > 500 °C; measuring and determining the intrinsic kinetics becomes important if the CaO is modified for other reasons, e.g. when improving the cyclic stability which might have a negative effect on the surface reaction kinetics in the fast regime. (ii) Small CaO crystallites allow for a higher conversion of CaO within the fast reaction regime than do large crystallites. (iii) Diffusional transport of CO_2 through the pore network lowers the rate of carbonation with time. CaO associated with large mesopores or macropores is accessible for CO_2 for a longer time and is less likely to be blocked with $CaCO_3$ product; this requires the size of the pores to be approximately twice the diameter of the typical critical product layer thicknesses that tend to increase with temperature. (iv) The greater the porosity of a CaO-based sorbent is, the smaller is the average thickness of the CaO skeleton, which ensures higher effective CO_2 uptakes (provided that most of the pore volume is within the mesoporous/microporous range). (v) The rate of diffusional transport of CO_2 increases with increasing temperature and enables higher conversions of CaO, but lowers the CO_2 capture efficiency (Figure 1). (vi) True product layer diffusion is of little practical relevance as the rate of carbonation under solid-state diffusion control is near zero.

2.2.2 MgO-$MgCO_3$ system

Magnesium oxide (MgO) is another alkaline earth oxide that has gained considerable attention for CO_2 capture [31], [51], [77], [124]–[130] (see Table 1). Pure MgO adsorbs CO_2 at lower

temperatures than CaO, i.e. between 25 – 400 °C, and is regenerated at temperatures between 450 – 500 °C under a N_2 atmosphere. The cyclic operation temperature is defined by the equilibrium thermodynamics of the reaction $MgO + CO_2 \rightarrow MgCO_3$ as shown in Figure 1. The lower energy requirement for regeneration (Table 1) makes the use of MgO attractive compared to CaO due to its potentially lower energy consumption for the entire system [31], [51], [131]. In addition to its low operating temperature, magnesium oxide is abundant, low cost and has a high theoretical maximum CO_2 uptake of 110 wt% [51]. Recent work published on various aspects of MgO used in CCUS include a comprehensive summary of performance enhancements and optimization of MgO sorbents [51], a review of the kinetics of carbon dioxide capture of solid sorbents including MgO [49] and a critical analysis of the mechanisms of CO_2 interaction with the MgO surface [31]. In this review, we provide an updated review of papers that have brought new insight into the fundamental understanding of CO_2 capture by MgO and elaborate on which questions still remain unanswered.

Table 2. Selected porous MgO sorbents adapted from [51].

Sorbent	Surface area	Instrument (cycles)	Carbonation conditions	Decarbonation conditions	Capacity last cycle ($g_{CO2}\ g^{-1}$)	Ref.
MgO	250 $m^2\ g^{-1}$	TGA (5)	25 °C, 100 % CO_2	500 °C, N_2	0.01-0.02	[127]
MgO	1073 $m^2\ g^{-1}$	TGA (5)	25 °C, 100 % CO_2	500 C, N_2	0.08	[127]
MgO	373 $m^2\ g^{-1}$	TGA (20)	200 °C, 20 % CO_2/N_2, 30 min	450 °C, N_2, 30 min	0.022	[129]
MgO	130 $m^2\ g^{-1}$	TGA (6)	25 °C, 100 % CO_2 60 min	600 °C, Ar, 60 min	0.093	[128]
MgO	306 $m^2\ g^{-1}$	TGA (19)	80 °C, 100 % CO_2 90 min	600 °C, N_2, 30 min	0.201	[130]

Although magnesium oxide has a high theoretical capacity, the actual CO_2 uptake of commercially available MgO (surface area of ~ 250 $m^2\ g^{-1}$) is < 2 wt% [127]. The low CO_2 uptake has been ascribed to a low basicity, a high lattice enthalpy and a surface unidentate carbonate layer creating a high CO_2 diffusion resistance towards unreacted MgO [132]–[134]. For reference, the surface basicity of alkali oxides increases in the order MgO < CaO < SrO < BaO [135] and MgO has a lattice energy of 3795 kJ mol^{-1} which is in fact only slightly higher than the lattice energy of CaO (3414 kJ mol^{-1}). MgO is the more sensible choice for carbonation at low temperature (< 400 °C) because the temperature for regeneration is comparatively lower than for CaO, SrO and BaO (Figure 1). The high lattice energy implies that the activation barrier for ion detachment from MgO is high and it is only the outer layer of atoms that react with CO_2. Molecular modelling has furthermore shown that CO_2 adsorption on MgO is more likely to occur at an edge or corner site than on flat terraces, which is similar for

CaO [136]–[139]. That the carbonation reaction of MgO is limited to its surface has been substantiated experimentally by the strong correlation between CO_2 uptake and surface area [140]. It is possible to improve the CO_2 uptake of MgO by fabricating materials with a high surface area of up to 1000 $m^2 g^{-1}$, achieving capacities of 20 wt% at temperatures between 25 – 400 °C [59], [127]–[129], [140]–[142]. In Section 5.1, we describe how infrared spectroscopy has been used to gain further insight to how CO_2 is adsorbed on the surface of pure MgO.

The fact that MgO can capture CO_2 at low temperatures, even reaching 80 $mg_{CO2} g^{-1}$ at room temperature, may prove useful for applications such as separation of CO_2 in aircraft, submarine, train and spacecraft technologies [127]. Unfortunately, the uptake appears to be too low for application as sorbent in pre- or post-combustion CO_2 capture technologies, especially considering the low CO_2 concentrations found in many CO_2-emitting processes, which implies a lower quantity of adsorbed CO_2 [31], [143]. Section 3.2 describes the research efforts aimed at modifying MgO to overcome its surface-limited adsorption in order to have both adsorption and absorption reaching capacities of 40 – 65 wt% at higher temperatures of 300 – 400 °C. In addition, we assess critically the hypotheses that seek to explain the mechanisms underpinning this significant improvement.

2.3 Calcination

2.3.1 CaO-$CaCO_3$ system (calcite)

The endothermic decomposition of calcite ($CaCO_3$), termed the calcination reaction, occurs if the p_{CO2} falls below the respective $p_{CO2,eq}$ for a given temperature (Figure 1) and proceeds typically very rapidly with an activation energy roughly equivalent to its reaction enthalpy (Table 1) [144]. Impurities in $CaCO_3$ can lower its decomposition temperature slightly [145]. Temperature and p_{CO2} affect the rate of decomposition, but do not affect the topotactic decomposition mechanism of $CaCO_3$ (i.e. there is a preferred crystallographic orientation between the carbonate and the oxide product) [146], [147]. Calcination is initiated by the loss of CO_2 at the surface of the calcite – the rate limiting step – which, due to strain accumulation, undergoes a diffusionless collapse to form a mesoporous structure made up of rod-shaped, metastable CaO nanocrystals. Stress release causes the ejection of the remaining CO_2 that diffuses outwards and induces porosity, and results in the oriented aggregation of the metastable CaO nanocrystals to form crystal bundles [148]. Further aggregation and sintering leads to a reduction in surface area and porosity, the closing of mesopores and the development of micrometer-sized pores. The structural transformation of the metastable CaO nanocrystals during calcination is exothermic, which may explain the overall negative activation energies

for the calcination reaction that have been observed at high decomposition temperatures (> 850 °C) [149], [150]. For further information on the origin of the metastability of the CaO phase we refer to a detailed experimental study by Dash et al. [151].

The reaction conditions during calcination (e.g. temperature, p_{CO2}, reaction time) and the impurities present in the sorbent have a direct impact on the structural and morphological properties (e.g. crystallite size, surface area, porosity) of the nascent CaO, which in turn determine its subsequent sorption properties for CO_2 [148], [152]–[154]; this is elaborated in Section 2.5.1. On a plant level, the high endothermicity of the calcination reaction requires the co-combustion of a fuel, e.g. natural gas, which was shown to be feasible also under oxy-fuel combustion conditions [155]–[157].

2.3.2 MgO-$MgCO_3$ system (magnesite and dolomite)

Naturally, magnesium carbonate exists in the form of hydromagnesite ($Mg_5(CO_3)_4(OH)_2 \cdot 4H_2O$), huntite ($Mg_3Ca(CO_3)_4$) or dolomite ($CaMg(CO_3)_2$), and studies have mostly investigated the decomposition mechanism of these compounds due to their industrial importance [158]. Once decomposed to the metal oxides and gaseous CO_2 (and H_2O), these types of carbonates do not re-form within reasonable timeframe under typical carbonation conditions. Hydromagnesite has often been used as a precursor for MgO-based sorbents for CO_2 capture [134], [159], [160], whereas dolomite has been used as an alternative sorbent to limestone with only the CaO component (but not the MgO component) being active for cyclic CO_2 sorption [161]–[166].

Dolomite decomposes topotactically in one ("full decomposition") or two ("half decomposition) steps, subject to the specific combination of T and p_{CO2} [167]. The combinations of T and p_{CO2} corresponding to these two modes of decomposition behavior of dolomite are in good agreement with the thermodynamic properties of its individual (hypothetical) components $MgCO_3$ and $CaCO_3$ (Figure 1). Thus, under conditions at which $CaCO_3$ is predicted to be stable (e.g. for T = 750 °C and p_{CO2} = 0.5 bar), only the "Mg component" of the dolomite undergoes decomposition to MgO ("half decomposition"). Rodriguez-Navarro et al. [167] note that the term "half decomposition" (or "half calcination") is misleading, because it does not reflect the actual structural transformations occurring within the material. Using 2D-XRD and transmission electron microscopy (TEM), they observed that $CaMg(CO_3)_2$ decomposes first to a cubic mixed oxide ($Ca_{0.5}Mg_{0.5}O$), which then rapidly undergoes de-mixing into oriented crystals of Mg-poor CaO and Ca-poor MgO solid solutions [167]–[169]. Eventually, pure CaO and MgO crystals are formed during coarsening via oriented aggregation and sintering. CaO nanocrystals form as a solid solution with up to ~ 9 mol% Mg,

as the solubility of Ca in Mg (and vice versa) is relatively low [170]. Performing the decomposition under conditions that predict $CaCO_3$ to be thermodynamically stable, these CaO nanocrystals react readily with the CO_2 released from the dolomite decomposition to form Mg-calcite (similar observations were made for the decomposition of the triple carbonate $(Ba,Sr,Ca)CO_3$ [171]). Upon increasing the temperature further (such that thermodynamically CaO is favored over $CaCO_3$), the Mg-calcite transforms into $CaCO_3$, which then undergoes decomposition as described in Section 2.3.1.

Turning to pure $MgCO_3$, its topotactical decomposition yields MgO with multiple orientational relationships; there has been no evidence for any preferential alignment of MgO with respect to $MgCO_3$ [170], [172]. This is different from the decomposition of $Mg(OH)_2$, which has shown to yield a single orientational relationship between $Mg(OH)_2$ and MgO [172]. The actual decomposition mechanism of $MgCO_3$ is similar to that of $CaCO_3$ (and also $SrCO_3$): Upon heating, the CO_2 released from the CO_3^{2-} layers induces strain that leads to a rearrangement of the rhombohedral cell into a cubic configuration [173]. Metastable MgO nanocrystals are formed, followed by their aggregation and sintering. Comparing the crystallite size of the oxides derived from the decomposition of carbonates under vacuum, the size increases in the order magnesite < dolomite < calcite and thus follows their decomposition pressure and temperature [170], [174]. The decomposition of $MgCO_3$ is largely irreversible [175], as is discussed above in Section 2.2.2.

The transformation from $MgCO_3$ to MgO is endothermic, yet, sometimes an exothermic peak has been observed at the onset temperature of this transformation under certain conditions [158], [176]. The exotherm is typically observed when hydromagnesite (and not crystalline $MgCO_3$ or dolomite) is heated up; hydromagnesite undergoes several morphological transitions when CO_2 and H_2O are released upon heating, including the crystallization of amorphous magnesium carbonate at ~ 200 °C [177]. As soon as crystalline $MgCO_3$ is formed, the decomposition occurs, and so the exotherm coincides with a sharp decrease in sample weight. Further, grinding (i.e. surface activation) of $MgCO_3$ [178], the addition of Na-salts [179], [180], and the presence of steam (Section 2.4.3) were all found to lower the decomposition temperature.

2.4 Role of the flue gas environment

Fuel gas or flue gas from combustion processes is composed of many species, the quantity of which vary with the nature and the origin of the fuel. Besides the effects of SO_2 and steam, which have been extensively studied in the context of CaO-based sorbents, few other gaseous species have been reported to influence the cyclic carbonation-calcination reaction. There has

been no evidence that unburnt fuel gases (e.g. CH_4, H_2 or CO) or O_2 affect the cyclic CO_2 uptake capacity of CaO-based sorbents; this is expected because neither CaO nor $CaCO_3$ react with these species chemically. The inert gas He has been shown to increase the rate of decomposition of $CaCO_3$ over air, N_2, O_2 or CO_2 atmospheres, and lower the temperature at a given p_{CO2} for the calcination reaction to be initiated [181], [182]. The enhancement effect of He was ascribed partially to its higher thermal conductivity that improves heat transfer, but mostly to an enhanced CO_2 diffusivity in He.

2.4.1 Effect of SO_2 on CaO

Up to 2005, far more literature has dealt with the sulfation of CaO than its carbonation because the emission of SO_2 from fossil fuel-fired boilers was an important environmental problem [183]–[185]. In high-temperature flue gas desulfurization, limestone is added to the combustion zone of a boiler, where it decomposes to CaO and CO_2. CaO reacts with SO_2 and O_2 to form $CaSO_4$ in an exothermic reaction during the combustion process and so prevents the release of SO_2 into the atmosphere.

$CaO + SO_2 + 0.5\ O_2 \rightarrow CaSO_4 \qquad \Delta H_{850°C} = -481.4$ kJ/mol (R10)

If SO_2 is present in a CO_2-rich flue gas stream, both species compete for reaction with CaO [186], [187]. Rates of carbonation are typically faster than are rates of sulfation at temperatures of 600 – 700 °C, but the rate of R10 increases with temperature and is thermodynamically feasible also under $CaCO_3$ decomposition conditions [188], [189]. The molar volume of the sulfation product $CaSO_4$ is ~ 25 % higher than that of the carbonation product $CaCO_3$, which increases the diffusion resistance for CO_2 when carbonation and sulfation occur simultaneously. An interesting consequence of the difference in molar volumes is that deactivated CaO-based sorbents for CO_2 often possess a higher reactivity for SO_2, because the optimal pore size for sulfation is greater than for carbonation [190]–[192]. Thus, the reactivity of the sorbents towards SO_2 increases upon carbonation-calcination cycling. An additional problem with SO_2 present in a flue gas is that the sulfation product $CaSO_4$ is thermodynamically stable under typical calcination conditions, which lowers the effective CO_2 uptake capacity over repeated cycles.

2.4.2 Effect of steam on CaO

It is well-established that the presence of steam enhances the extent of the carbonation reaction within a given time, for both natural, synthetic and chemically modified sorbents [193]–[219]. Similar to He, steam was found to accelerate the calcination reaction and to lower the thermodynamic driving force for its initiation [181], [220]–[225]. Unlike He, steam does affect the physical (i.e. structural and morphological) properties of the CaO formed [182], [225],

[226]. Champagne et al. [227], [228] observed that the CO_2 uptake was improved when the subsequent carbonation was performed under dry conditions.

The main experimental works dealing with the influence of steam have been summarized by Zhang et al. [229]. The enhancement during carbonation becomes apparent in the diffusion-controlled regime [230]–[232] and is usually not noticeable in the fast, kinetically-controlled regime. Remarkably, only small amounts of steam present during carbonation, < 1 vol.%, are sufficient to improve the rate of conversion significantly [193], [205], [212]. Furthermore, the driving force ($p_{CO2} - p_{CO2,eq}$) needed for carbonation to commence is lowered substantially in the presence of steam, suggesting that steam potentially affects the reaction pathway for carbonation [193]. Morphological analyses of sorbents collected after repeated cycles of sorption and desorption of CO_2 revealed that samples cycled in the presence of steam possessed a greater surface area and pore volume in the pore diameter range 10 – 100 nm [193], [211], [233]–[235]. Larger pores lower the diffusional resistance when $CaCO_3$ forms and permit higher CO_2 uptake capacities over a given time; however, very high steam concentrations (> 20 vol.%) present during calcination accelerate sintering and pore growth to an extent that the sorbent's activity is affected negatively [236], see Section 2.5.1.

It has been reported that steam has a "catalytic" effect (both on the carbonation [209], [214], [237] and calcination reaction [221], [223], [238]–[240]). Indeed, both experimental [238] and computational [240] studies found substantially lowered activation energies for the calcination reaction in the presence of as little as 0.015 % steam, which provides an alternative pathway for $CaCO_3$ decomposition involving the dissociative adsorption of steam on the $CaCO_3$ surface.

Turning to the carbonation reaction, it was proposed that steam is dissociatively adsorbed on the surface of CaO through oxygen vacancies, forming H^+ and OH^- [241]–[243]. H^+, given its small size, diffuses easily through the $CaCO_3$ product layer to the $CaO/CaCO_3$ interface and reacts with O^{2-} to form OH^-. OH^- diffuses outward to the $CaCO_3$/gas interface and reacts with CO_2 to form CO_3^{2-} anion groups, which eventually diffuse inward through the $CaCO_3$ layer to the $CaO/CaCO_3$ interface where new $CaCO_3$ is formed. The faster diffusion of OH^- over O^{2-} is believed to enhance the carbonation reaction, but experimental proof is yet to be provided. As mentioned above, the beneficial morphology formed during calcination in the presence of steam contributes to a synergistic effect of a higher CO_2 uptake when steam is present during both the carbonation and calcination stages.

Lastly, it has been suggested that CaO and steam could form $Ca(OH)_2$ as an intermediate species, which improves the formation of $CaCO_3$ [244]–[246]. Under typical carbonation conditions (> 650 °C) employed for the calcium looping cycle, $Ca(OH)_2$ cannot exist stably

from a thermodynamic point of view, making this pathway an unlikely reason for the improved CO_2 uptake in the presence of steam [237]. However, for carbonation performed at lower temperatures, e.g. for MgO to $MgCO_3$, hydroxide species can be thermodynamically stable and affect the carbonation mechanism on the metal oxide; this is discussed in the following section. It is worth mentioning that in a modification of the two-step calcium looping process, a reaction step is included in which the spent CaO is re-activated through the exothermic hydration reaction R11 [247]–[252].

$CaO + H_2O \rightarrow Ca(OH)_2$ $\Delta H_{400°C} = -102.8$ kJ/mol (R11)

The $Ca(OH)_2$ product reacts faster with CO_2 than does CaO owing to morphological differences, but also tends to possess a lower mechanical strength [253].

2.4.3 Effect of steam on MgO

Several experimental studies have shown that the reactivity of MgO-based sorbents increases in the presence of steam, introduced either via a pretreatment step or during carbonation [59], [64], [160], [254]–[258]. For example, Zarghami et al. [59] observed a 38 % higher uptake after 100 seconds of carbonation when 10 % steam was added during carbonation and a 30 % higher uptake after 5 min of carbonation when a MgO sorbent was pretreated in 30 vol.% H_2O/N_2 at 330 °C (Figure 3a and Figure 3b, respectively). Most of these studies have shown that it is necessary to use a steam concentration above 5 vol.% during carbonation in order to observe a beneficial effect [64], while the use of a lower concentration of 1 vol.% steam had no measurable impact [63], in contrast to CaO described above. MgO-based sorbents promoted with alkali metal salts show a similar behavior evidenced by a higher CO_2 uptake and enhanced reaction rates with CO_2 in the presence of steam [160], [254], [255]. Interestingly, introducing steam at strategic times during carbonation and calcination has also shown to be a suitable method to reactivate the capture performance of MgO-based sorbents after repeated cycling [64], [160], similar to what has been reported for CaO when including a steam hydration step in the process (Section 2.4.2).

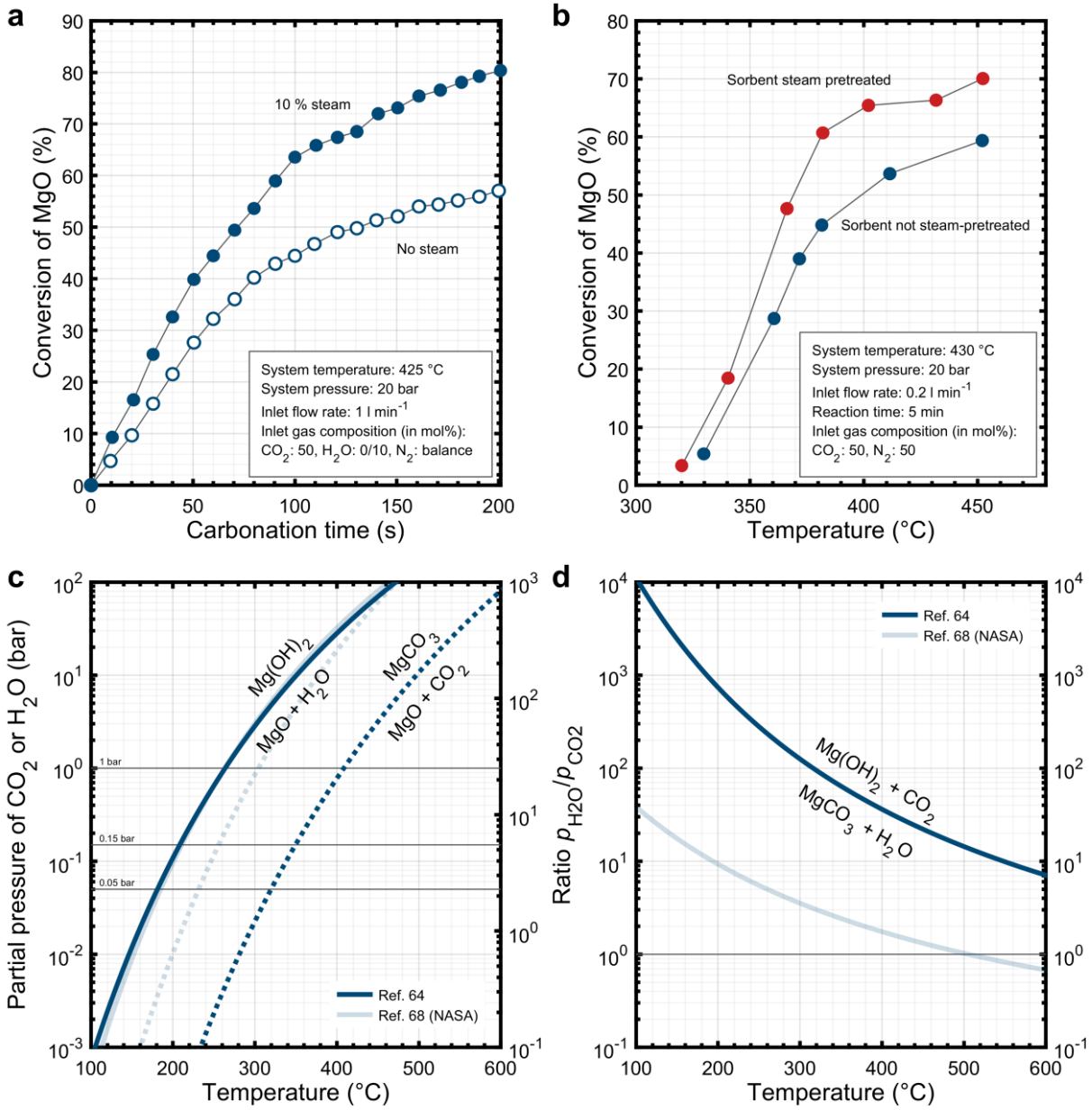

Figure 3. (a) and (b): Influence of steam, either during carbonation or pretreatment, on MgO conversion at 20 bar. a) Initial stage of carbonation with a steam concentration of 0 mol% or 10 mol%. b) Comparison of MgO conversion for MgO and steam pretreated MgO; pretreatment at 330 °C, 20 bar using 30 mol% steam in N_2 for 1 h. Figures (a) and (b) were reproduced with permission from [59]*, copyright (2015) American Chemical Society. (c) and (d): Equilibrium curves for reactions R12 – R14 showing the thermodynamically most favorable reaction products in the presence of H_2O and CO_2. (c) The dark blue lines correspond to the equilibrium pressure and temperature for the reactions $Mg(OH)_2 \leftrightarrow MgO + H_2O$ (solid) and $MgO + CO_2 \leftrightarrow MgCO_3$ (dotted), respectively. (d) Equilibrium curve for the reaction $Mg(OH)_2 + CO_2 \leftrightarrow MgCO_3 + H_2O$ plotted as a function of p_{H2O}/p_{CO2}. Figures (c) and (d) were reproduced using thermodynamic data from* [64]*; lines in pale color are shown for comparison only and were computed using thermodynamic data from* [68].

The enhancement of the CO_2 uptake of MgO has been associated with the formation of an intermediate reaction product, viz. $Mg(OH)_2$, that reacts more readily with CO_2 than MgO, and to changes in the morphology of MgO [59], [64], [259]. Zarghami et al. [59] found a higher activity of the MgO sorbent when it was pretreated in a mixture of H_2O/N_2 (30 mol% H_2O) for 1 h at 20 bar and 330 °C and then dried in N_2. Although the pore size distribution was not measured it was speculated that the pretreatment in H_2O provided a more "favorable" pore

structure as any formed $Mg(OH)_2$ should decompose after drying in N_2 at 330 °C. To investigate the influence of intermediate reaction products, Fagerlund et al. [64] compared the reactivity of MgO and $Mg(OH)_2$ and found that $Mg(OH)_2$ reacts ~ 50 % faster than MgO in the first 4 min of reaction although MgO had a smaller particle size and larger surface area. Reactions R12 – R14 describe the simplest reaction products of MgO and $Mg(OH)_2$ in the presence of steam and carbon dioxide.

$Mg(OH)_2 \rightarrow MgO + H_2O$ $\Delta H_{400°C} = -74.7$ kJ/mol (R12)

$MgO + CO_2 \rightarrow MgCO_3$ $\Delta H_{400°C} = -97.6$ kJ/mol (R13)

$Mg(OH)_2 + CO_2 \rightarrow MgCO_3 + H_2O$ $\Delta H_{400°C} = -22.9$ kJ/mol (R14)

The thermodynamic equilibria for reactions R12 – R14 are shown in Figure 3c. Conditions (pressure and temperature) at the left side of the dotted equilibrium curve lead to the formation of $MgCO_3$ in the presence of CO_2. For instance, in a 1 bar CO_2 atmosphere, $MgCO_3$ is stable below 408 °C. The thermodynamic equilibrium curve for the dissociation of $Mg(OH)_2$, R12, is similar to that of $MgCO_3$, reverse reaction R13, albeit shifted by ~ 140 °C towards lower temperatures. Importantly, if the conditions are such that both $MgCO_3$ and $Mg(OH)_2$ are thermodynamically favorable, Figure 3d can be used to determine the most stable reaction product in the presence of both H_2O and CO_2 (given as the ratio p_{H2O}/p_{CO2}). In the area above the equilibrium line in Figure 3d, magnesium hydroxide is the most likely reaction product, while magnesium carbonate is most likely to form under the conditions that lie below the equilibrium line. Considering these two possible products in the presence of both steam and carbon dioxide, the steam partial pressure p_{H2O} must be several orders of magnitude higher than p_{CO2} for $Mg(OH)_2$ to be the most stable phase. This indicates that $MgCO_3$ is likely to form from $Mg(OH)_2$ under most relevant reaction conditions.

It is worth mentioning that the curves in Figure 3d indicate the most stable product when the reaction has reached thermodynamic equilibrium and under the assumption that the only possible reactions are those considered in R12 – R14, while in practice other reaction products may form, including intermediates such as lamella oxyhydroxide $Mg_{x+y}O_x(OH)_{2y}$ [64][258], [260].

2.5 Deactivation

2.5.1 CaO

The dominant reasons for the observed decrease in the cyclic CO_2 uptake of CaO-based sorbents are (i) the loss of pore volume and surface area associated with pores of 50 – 150 nm, and (ii) the increase of CaO crystallite size [101], [261], [262]. Consequently, the conversion curve for the carbonation reaction shifts towards lower values, as illustrated in Figure 2e, whereas the

rate of the calcination reaction is usually not affected. The closure of pores and the increase of the $CaCO_3$ crystallite size during the carbonation reaction is shown in Figure 4. Deactivation curves (i.e. the plot of CO_2 uptake as a function of cycle number, Figure 2f) are generally well approximated by simple mathematical expressions reminiscent of sintering theories describing the reduction of surface area with time [118], [263]–[267], e.g. $X_N = (1/(1–X_r)+k\cdot N)^{-1}+X_r$, where X_N is the conversion of CaO in cycle N and the two parameter k and X_r refer to the deactivation constant and the residual conversion, respectively. The conversion of CaO after thousands of carbonation-calcination cycles does not fall to zero, but levels off at $X_r \approx 5 – 10$ % [118], [268]. In the absence of mechanical deterioration, ~ 100 cycles are sufficient in most cases for a good estimate on the long-term reactivity of the sorbent (Figure 2f).

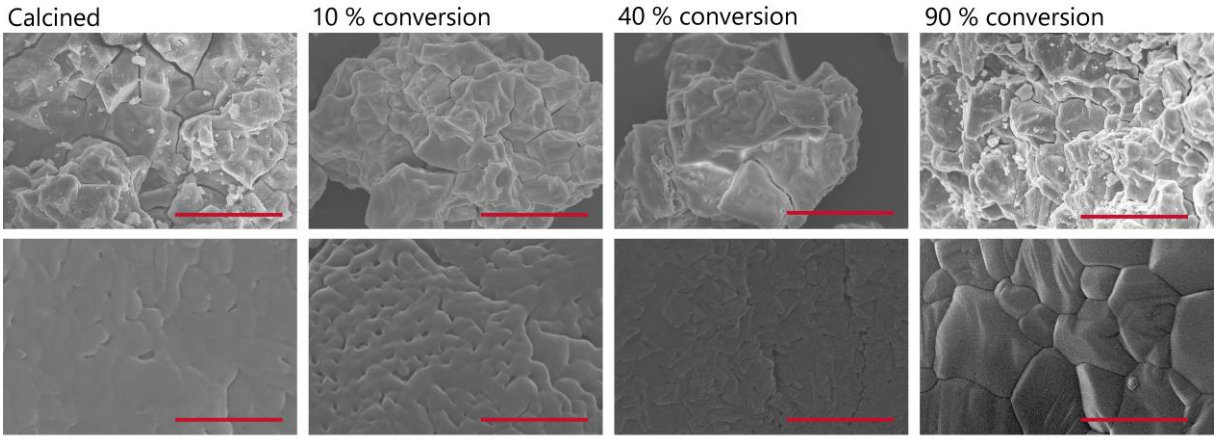

Figure 4: Scanning electron microscopy images of limestone-based sorbent (Havelock) exposed to 15 vol.% CO_2 for different durations in a fluidized bed at 650 °C. The length of the red scale bar is 30 μm in the top row, and 500 nm in the bottom row. The images show the formation of a carbonate layer (10 % conversion), and the development and growth of carbonate grains due to sintering (40 % and 90 % conversion) [269].

Sintering of CaO and $CaCO_3$ has been studied for decades owing to its relevance for the cement industry [270]–[273]. The smaller the CaO grains are and the higher the temperature is, the more pronounced the sintering is (i.e. the increase in grain size) [274]. Borgwardt found that CaO derived from $Ca(OH)_2$ sinters faster than CaO derived from $CaCO_3$ [275], and that the sintering of CaO is enhanced in the presence of steam and CO_2 over a long period [276]. From a carbon dioxide capture process point of view, the sintering of the CaO phase (once formed) is insignificant and does not impair appreciably the sorbent's long-term cyclic activity because calcination times are short (of the order of minutes rather than hours) [148], [152]. $CaCO_3$ possesses a lower sinter temperature than CaO (Table 1), and hence the conditions during which $CaCO_3$ transforms to CaO determine its activity for CO_2 sorption. High calcination temperatures, calcination times and CO_2- or steam-rich atmospheres enhance sintering, or, more precisely, the aggregation of metastable CaO nano-/microcrystals that form during the decomposition of the $CaCO_3$ [148], [277]. The faster the transition from $CaCO_3$ to CaO occurs

(e.g. by using a higher heating rate), the larger is the surface area of the CaO produced, which in turn enables a higher CO_2 uptake in the carbonation reaction [152], [278]. In contrast, high carbonation temperatures and long carbonation times were found to lower the rate of deactivation due to the formation of thicker product layers that yield a higher porosity after their decomposition [279]–[283].

On the process scale, a further form of deactivation occurs when sorbent particles of low mechanical strength and abrasion resistance break or disintegrate into small pieces and dust; these small pieces are readily entrained from the reactor, requiring continuous addition of fresh sorbent particles to maintain the reactor inventory [284], [285]. The dominant reasons for the breaking up of sorbent particles are the high particle and gas velocities, collisions with other particles, the reactor walls and particle transfer equipment, thermal stress (due to the heating and cooling), and bulk phase changes (when transitioning between oxide and carbonate of different molar volumes). Various means to reduce the extent of deactivation and prolong the lifetime of CaO-based sorbents are discussed in Section 3.

2.5.2 MgO

Cyclic tests of pure MgO-based sorbents reveal a similar decay in the CO_2 capture performance as for CaO, i.e. losing $30 - 45$ % of their initial CO_2 uptake capacity after 20 cycles. The mechanism of deactivation has mainly been attributed to the loss of surface area [128], [129], [141]. In the course of carbonation, MgO will change volume which has been shown to affect the pore size distribution [64] but its contribution to the decay has not been studied systematically so far. Concerning changes in surface area, Gao et al. [129] performed carbonation at 120 °C in 100 % CO_2 and regeneration at 450 °C in N_2 and found that the specific surface area of the sorbent decreased from 372 $m^2\ g^{-1}$ to 197 $m^2\ g^{-1}$ after 10 cycles which resulted in a decay of 30 %. This is in turn implies that there is not linear relationship between the reduced surface area and lower uptake. When the same authors tested for carbonation at 200 °C and calcination at 450 °C in 50 vol.% CO_2, they reported a progressive decline in the CO_2 uptake from 48 mg g^{-1} to 26 mg g^{-1} over 20 cycles. Further reducing the CO_2 concentration to 20 vol.%, the overall uptake was lower at 35 mg g^{-1}, but also had a lower relative amount of decay to 22 mg g^{-1}, but here the surface area and pore volume was not determined after the experiment. It is possible that the reduced rate of decay in CO_2 uptake at diluted CO_2 concentrations stems from a lower MgO conversion, leading to a reduced extent of sintering, but finding the underlying explanation for this difference is missing. To understand this observation better, it would be valuable for future work to describe in detail how various CO_2

concentrations affect the surface area over cycling and at which point the most severe sintering occurs as function of temperature and pressure.

3 Material optimization

3.1 CaO-based sorbents

Recent review articles by Liu et al. [47] and Salaudeen et al. [44] have summarized various approaches and techniques used to enhance the cyclic CO_2 uptake of CaO-based sorbents, therefore these approaches are only described in brief here [44], [47], [247]. Generally, these attempts fall into three broad categories: (i) Process modifications, (ii) tuning of reaction conditions, and (iii) sorbent modifications. Recent results are summarized in Table 3.

Table 3. Selected CaO sorbents modified with structural supports.

Main sorbent	Support (wt%)	Instrument (cycles)	Carbonation conditions	Decarbonation conditions	Capacity last cycle ($g_{CO2}\ g_{sorbent}^{-1}$)	Ref.
CaO	Al_2O_3 (9 %)	TGA (30)	750 °C, 55 % CO_2/N_2, 20 min	750 °C, N_2, 20 min	0.51	[286]
CaO	$Ca_{12}Al_{14}O_{33}$ (25 %)	TGA (45)	690 °C, 15 % CO_2/N_2, 30 min	850 °C, N_2, 10 min	0.26	[287]
CaO	SiO_2 (35 %)	TGA (13)	800 °C, 15 % CO_2/N_2, ~ 40 min	800 °C, N_2, ~ 40 min	0.21	[288]
CaO	ZrO_2 (40 %)	TGA (100)	700 °C, 100 % CO_2, 30 min	700 °C, 30 % CO_2/He, 30 min	0.30	[289]
CaO	Y_2O_3 (86 %)	TGA (100)	740 °C, 25 % CO_2/N_2, 10 min	740 °C, Ar, 10 min	0.08	[290]
CaO	MgO (26 %)	TGA (50)	758 °C, 100 % CO_2, 30 min	758 °C, He, 30 min	0.53	[291]
CaO	La_2O_3 (20 %)	Packed Bed (11)	850°C, 100 % CO_2, 30 min	850 °C, N_2, 10 min	0.58	[292]
CaO	Li_2CO_3 (5 %)	TGA (17)	765°C	765 °C	0.1	[293]

Process modifications refer to changes of the principle, two-step (carbonation and calcination) layout of the calcium looping process to accommodate additional reactors for sorbent regeneration via hydration [294], [295] (Section 2.4.2) or improved heat integration using additional redox-active metal oxides (oxygen carriers) [296]–[298].

The reaction conditions can be tuned to maximize a sorbent's cyclic CO_2 uptake and/or lifetime based on the parameters discussed in Sections 2.1 – 2.5. Unfortunately, there has often been a tendency in the field to employ "mild" reaction conditions that would lead to higher reported cyclic CO_2 uptakes (and thus ease advertising of a new material composition) than employing "harsh", but more realistic reaction conditions. Such studies can be misleading in properly gauging the advancement of the technology itself, but may provide useful insights to better understand the inherent properties of the material being studied (see Section 5). Ultimately, sorbents need to perform well under the reaction conditions determined by the requirements of the CO_2 capture process and the sorbent's thermodynamic properties, leaving limited room for optimization. For certain applications of the cyclic CO_2 capture and release process, e.g. thermochemical energy storage with a closed CO_2 circuit, it may be beneficial to release the

CO_2 from the sorbent at low temperature (< 800 °C) and low p_{CO2} (< 0.01 bar, possibly at absolute pressures ≪ 1 atm) to enable a high long-term cyclic stability of the sorbent material [299]–[302], but we note that closed CO_2 circuit process designs are typically not considered to be part of CCUS.

The most actively researched sorbent modifications are discussed in the following sub-sections. In Section 3.1.1 the subject of alkali metal doping of CaO-based sorbents is discussed, where the term "dopant" is used interchangeably with "promoter". Strictly speaking, a dopant is located within the crystal lattice of CaO, which is not the case in most of the studies presented below. In Section 3.1.2, "stabilizers" are discussed, of which the main purpose is to stabilize the CaO skeleton.

3.1.1 Alkali metal doping

In one of the first systematic studies on the effect of alkali metal promotion of CaO sorbents for CO_2, CaO was impregnated with up to 20 wt% of Li, Na, K, Rb or Cs using chloride and hydroxide precursors. The corresponding CO_2 uptake was determined at 600 °C in pure CO_2 [303]. Doping with Cs improved the CO_2 uptake significantly, while the other alkali metal dopants affected the CO_2 uptake negatively. The performance of the sorbents followed the order Li < Na < K < Rb < Cs and thus improved with increasing electropositivity/atomic radii of the alkali metals. Florin and Harris found that doping CaO with 1 wt% Li_2CO_3 lowered the cyclic CO_2 uptake capacity of CaO [304]. Similarly, the CO_2 uptake capacity of Li_2CO_3-doped (8.6 wt%) CaO prepared by Derevschikov et al. [305] decayed at a faster rate than did pure CaO. After the isothermal TGA experiments over 18 cycles of carbonation and calcination at ~ 760 °C, there was almost no Li left in the sorbent. Salvador et al. [306] observed that doping natural limestones with NaCl or Na_2CO_3 had a negative effect on the sorption performance in a pilot-scale fluidized bed combustor, whereas for some limestone-dopant combinations positive effects were observed in TGA experiments (e.g. for Havelock and Cadomin limestone doped with NaCl). Manovic et al. [282] doped natural limestone (Kelly Rock) with 5 wt% Na_2CO_3 to explain the poor cyclic performance of a Na-rich limestone (La Blanca) after thermal pretreatment, as observed in their previous work [261]; pronounced sintering facilitated by the presence of Na^+ ions was identified as the main reason for deactivation. Using NaBr as the dopant of CaO, Xu et al. [307] found that the cyclic CO_2 uptake capacity over 100 cycles increased with an increasing amount of NaBr added (up to 10 mol %). NaCl and KCl were also found to be effective performance enhancers, whereas NaOH and KOH did not improve the cyclic CO_2 uptake capacity significantly and even accelerated the deactivation of the doped sorbent [308]. Seawater contains various dissolved Na- and K-salts and has been used in

attempts to improve the cyclic stability of CaO-based sorbents. Most studies concluded that doping by seawater affects the cyclic CO_2 uptake capacity negatively owing to the enhancement of sintering [309], [310], however, an improvement in CO_2 sorption has been observed when only small amounts of seawater were used [311]–[313].

The examples above show that currently there is little consensus whether the addition of alkali species improves CO_2 sorption or not. Common amongst the studies is a strong dependence of CO_2 sorption on the reaction conditions, the synthesis method, and the type and amount of the alkali metal salt precursor. To predict the sorbent's cyclic behavior upon doping, it is important to understand how the dopants transform physically and chemically under carbonation and calcination conditions and whether they react with the CaO host structure.

Alkali metal hydroxides or nitrates used as dopant precursors decompose to the respective oxides under high calcination temperatures (~ 850 – 950 °C). From Figure 1 it is apparent that in the presence of small amounts of CO_2, the oxides transform to their carbonate forms, i.e. their thermodynamically most favorable state. Once formed, the alkali metal carbonates Na_2CO_3 and K_2CO_3 are very stable and do not decompose, even in N_2, until approaching their melting points [314], [315]. The melting points of Li_2CO_3, Na_2CO_3 and K_2CO_3 are relatively low (Table 1), and eutectic mixtures of the three components possess melting points as low as ~ 400 °C [316]–[318]. Importantly, single alkali metal carbonates (specifically Na_2CO_3 and K_2CO_3) readily react with CaO and CO_2 under typical carbonation conditions, forming alkali metal-Ca double carbonates (e.g. $Na_2Ca(CO_3)_2$ or $K_2Ca(CO_3)_2$) [319]–[321]. The very fast formation of such Na/K-Ca carbonates (the double salts or double carbonates) appears to depend on surface area to a much lesser extent than does the formation of $CaCO_3$ from CaO. Double carbonates have similar melting temperatures as the single alkali metal carbonates, but possess different thermodynamic properties: in a N_2 atmosphere, they decompose to CaO and the single alkali metal carbonate at temperatures similar to, or even lower than, $CaCO_3$, whereas in a CO_2 atmosphere, they do not decompose even when they reach their melting point (in contrast to many Mg-based double carbonates [322]–[325]). Double carbonates have therefore been used as sorbents for CO_2 achieving higher cyclic CO_2 uptake capacities than those that were observed for the reference CaO sorbent even at lower sorption temperatures [321], [326]; the regeneration of the sorbents was always performed under N_2. Other studies utilized the low eutectic temperatures of the carbonate mixtures to fabricate sorbents coated with molten salts under reaction conditions [327] – a similar approach to what is typically employed to enable fast sorption rates for MgO-based sorbents (Section 3.2).

The rate and extent of CO_2 uptake under pure CO_2 was found to be highest when the binary or ternary alkali metal carbonates were molten at the carbonation temperatures > 600 °C. The optimum molar loading of alkali metal carbonates was 7.5 mol %, with loadings > 10 mol % resulting in a significantly reduced CO_2 uptake [327]. Calcination was performed in N_2 and the maximum calcination temperature that ensured a high subsequent CO_2 uptake capacity was 750 °C; at higher calcination temperatures the binary or ternary alkali carbonates were assumed to decompose and thus lose their ability to promote CO_2 sorption. Clearly, such reaction conditions are unsuitable for CCUS schemes (see Section 6.3), and so the applicability of molten salt layers on CaO to enhance CO_2 sorption may be limited to process optimization employing Le Chatelier's principle, e.g. in the sorption-enhanced steam methane reforming (Section 6.3), where producing a pure stream of CO_2 is usually not the primary goal. A follow-up paper by Huang et al. [328] demonstrated that alkali metal salts can only promote CO_2 sorption when they are (i) in a liquid (i.e. molten) state, and (ii) possess high O^{2-} and CO_3^{2-} conductivities, consistent with the mechanism of the carbonation of CaO discussed in Section 2.2.1. Most alkali metal chlorides investigated were thus no suitable promoters although they were molten. Furthermore, there was no experimental evidence that binary or ternary molten alkali metal carbonates react chemically with CaO to form a new phase, implying that the molten salts function only as gateway for CO_2 to the CaO surface. Both CO_2 and CaO were speculated to dissolve in the liquid molten salts, followed by $CaCO_3$ formation which accumulates until saturation is reached within the solution. Eventually, $CaCO_3$ precipitates out forming a layer that can be permeated by the molten salts [327]. In the presence of a molten salt layer, the carbonation reaction does therefore not become limited by diffusion through a $CaCO_3$ product layer.

From the different studies using alkali metal salts to enhance the CO_2 uptake capacity of CaO-based sorbents, there is a consensus to several key findings. Firstly, alkali metal precursors that decompose to an alkali metal oxide under typical carbonation/calcination temperatures readily form double carbonates with CaO in the presence of CO_2; these double carbonates have lower melting temperatures and enable higher diffusivities of CO_3^{2-} ions than the single alkali or alkaline earth metal carbonates. Performing the calcination reaction in N_2 results in the decomposition of the double carbonate. The alkali metal carbonate (e.g. Na_2CO_3 or K_2CO_3) tends to separate from the bulk CaO with cycling and accumulate on the surface, from where it can detach completely from the sorbent eventually [329]. Hence, the alkali metal content in the sorbent decreases with cycling [305].

Secondly, double carbonates form, but do not decompose in CO_2 during calcination. Since the melting temperature of the double carbonates is lower than typical calcination temperatures (> 900 °C), they melt and thus contribute significantly to the sintering of the calcium species [330]. Under CO_2, double carbonates do not undergo cyclic phase transformations and are less mobile within the sorbent. The alkali metal content in the sorbent hence decreases to a lesser extent than when calcined in N_2 and as a consequence promotes sintering for a longer time.

Thirdly, using binary or ternary alkali metal carbonates impregnated within CaO-based sorbents (or applied as coatings) can enhance CO_2 transport within the sorbent, as the conductivity of CO_3^{2-} increases significantly above the eutectic temperature [331], [332]. However, when the molten salts decompose under high calcination temperatures, there is a risk of double carbonate formation with Ca, leading to accelerated sintering which causes the deactivation of the material for CO_2 sorption. It is well known from CO_2 transport membranes that the immobilization of the molten alkali metal carbonate phases strongly depends on the microstructure of the host structure (here: CaO) and the physical properties of the molten carbonates, e.g. the wettability [333]. Capillary forces, which decrease with increasing pore diameter, need to be high to withhold the molten alkali metal carbonates, and so sintering is expected to contribute to the loss of the alkali metals [334].

With these findings in mind, doping CaO with alkali metal salts will inevitably enhance sintering. An improvement in the cyclic CO_2 uptake capacity is only feasible if the amount of alkali metal salt added is extremely low, < 1 mol %, and even then its effect will depend strongly on the CaO microstructure and the synthesis method employed. The sintering and growth of pores needs to occur in a way that it benefits the carbonation reaction and aspects related to the transport of CO_2 (or CO_3^{2-}/O^{2-}) within the sorbent. In the context of sulphation, a clear increase in pore size was observed upon doping limestone with Na_2CO_3, which was more beneficial for the penetration of sulfur into the particles [335]–[337]. Similar effects were observed also for CO_2 sorption [338], [339]. Alkali metal halides (e.g. NaCl or KCl) appear to enhance sintering more than do alkali metal carbonates [306], [340], [341]. Al-Jeboori et al. [342], [343] found that doping limestones with as little as 0.167 mol % hydrogen halides (HBr or HI) and other inorganic salts improved the cyclic performance significantly owing to an sintering-induced optimization of the pore structure, showing that different promoters can be beneficial provided they have an appropriate influence on the microstructure of $CaO/CaCO_3$. This differs from structural stabilizers discussed in Section 3.1.2, which ideally remain entirely inert upon cycling. Sorbent modification via coating requires greater amounts of alkali metal salts (typically binary or ternary carbonates) to ensure the coverage of the entire sorbent surface.

The formation of mixed phases with CaO needs to be avoided by employing low calcination temperatures.

Generally, the immobilization of dopants in the sorbent is difficult and the choice of dopants should thus consider the possibility of the formation of harmful by-products (e.g. chlorine species) that may be released to the atmosphere. Furthermore, species with low melting temperatures (such as alkali metal salts) that exist in the liquid or even gas phase under typical carbonation/calcination conditions may condensate and accumulate in downstream pipework or heat exchangers and accelerate corrosion and fouling [335], [336]. Experience from coal or biomass combustion may be helpful in predicting the possible interactions of the alkali metal salts with other components of the sorbent [344]–[346].

3.1.2 Structural stabilization

Sintering is one of the dominant mechanisms responsible for the rapid decay in the activity of CO_2 sorbents with increasing number of carbonation and calcination cycles [118], [160], [250]. In the simplest case of a single phase material, the driving force for sintering is the reduction of surface free energy of the sintered particles, which involves grain growth, densification and reduction in porosity [347]. Sintering of $CaCO_3$ (upon calcining to CaO) cannot be prevented owing to the high temperatures required to recover the active CaO phase for CO_2 sorption; note that $CaCO_3$ has a Tammann temperature of only 533 °C. For reference, the Tammann temperature is defined as half the melting point of a solid in Kelvin and as a general rule of thumb can be used to predict the onset of rapid sintering [348]. Impurities in the sorbent that induce structural defects and/or interact chemically with the Ca phases may amplify sintering and accelerate the deactivation of the sorbent upon cycling.

However, sorbents can be engineered such that the negative effects of the sintering of $CaCO_3$ are reduced and the sorbent's long-term activity is improved. There are two principal strategies for modifying sorbents synthetically: (i) Stabilization of the active Ca phases through inclusion of species with high melting points (as opposed to doping with low melting point materials such as alkali metal salts that are discussed in Section 3.1.1) described in this section, and (ii) structuring of the CaO-based sorbent such that contact points between $CaCO_3$ grains are minimized, which is covered in Section 3.1.3.

A combination of the two strategies yields the most active synthetic sorbents that have been produced thus far [119], although they may not automatically be the most suited sorbents for a practical CO_2 capture process. For any modification of CaO it is worth benchmarking against a sorbent derived from natural limestone that predominately consists of $CaCO_3$.

When using stabilizers or support materials, the possibility of a chemical reaction with CaO (or $CaCO_3$) must be considered. A prominent example is Al_2O_3, which reacts with CaO to form calcium aluminum oxides [185], [349]. Calcium aluminum oxides do not possess any capacity for CO_2 sorption at high temperature and once formed remain inert under typical reaction conditions. Since active CaO is consumed to form the inert mixed oxide phase, the maximum theoretical CO_2 uptake capacity decreases accordingly. Other oxides potentially forming mixed phases with CaO include the oxides of the elements Mn, Ti, Zr or Si [45], [350].

In order to not compromise a sorbent's maximum CO_2 uptake capacity, inert support materials that do not react with CaO (or $CaCO_3$) are more desirable. MgO is one of the most frequently used stabilizers, because it possesses a very high melting temperature (~ 2850 °C, Table 1). It does not react with CO_2 nor forms a stable mixed carbonate or oxide with Ca under typical CaO carbonation calcination conditions [167], [351]. Also, the maximum degree of substitution between the oxides of Ca and Mg in solid solutions is relatively low (< 17 mol%) due to the large difference in cation radii (Table 1). Although the beneficial influence of stabilizers like MgO has been known for a long time from the comparison of the cyclic performances of natural limestones and dolomites [26], [118], [352], [353], synthetic sorbents with structural stabilizers were not been synthesized until the early 2000s [354]–[357] and have only been an active area of research since 2008 [358], [359].

The following two subsections – dealing with stabilizers that alternatively do not or do form mixed phases with CaO or $CaCO_3$ – review recent works that have led to a better understanding of how stabilizers function within a sorbent; for a comprehensive list of works on synthetic sorbents we refer to some recent reviews on the topic [44]–[46], [360].

3.1.2.1 Inert stabilizers

Conceptually, a stabilization of the cyclic performance of a CaO-based sorbent can be achieved with every type of metal oxide, provided its melting point is higher than that of $CaCO_3$, its solubility in CaO is low and (ideally) it does not interact chemically with CaO. Accordingly, oxides of the elements Mg, Y, La, Ce, Pr, Yb and Nd have previously been investigated as potential stabilizers for CaO with varying success [163], [286], [291], [350], [361]–[365]. La_2O_3, for example, was found to stabilize CaO while being also active (to some extent) for CO_2 sorption [359], [366]–[368]. Besides structural stabilization, metal oxides (e.g. CeO_2) have also been observed to improve O^{2-} transport within the sorbent and therefore enable faster carbonation rates [369], [370]. From purely geometrical considerations, ~ 80 % of the grains within a sorbent particle should be stabilizer and ~ 20 % CaO such that direct contact between CaO is prevented, assuming the grains are of similar size. Practically, the amount of stabilizer

used is much smaller (typically ~ 10 – 25 wt%) to avoid excessive loss in the theoretical, maximum CO_2 uptake capacity; thus, contacting between individual CaO grains and sintering is never eliminated completely. For the support to be effective in acting as a physical barrier between CaO grains and to prevent subsequent sintering upon calcination, it needs to be dispersed uniformly within the particle. Wet chemistry methods (e.g. sol-gel or co-precipitation) enable a much higher degree of dispersion than mechanical mixing or impregnation methods, which is reflected by the higher cyclic stability of stabilized sorbents when prepared through such methods [46]. One aspect that has not been given much attention yet is the potential segregation of the support and the active phases upon cycling, such that the stabilizer would no longer function as intended [371]. The melting temperatures of the phases are usually very different, corresponding to different strengths in their atomic bonding and hence different rates of atomic diffusivity – this is commonly known as the Kirkendall effect and has often been observed in the context of chemical looping using CuO-based materials [372], but also been exploited in the synthesis of hollow nanostructures [373] (see section 3.1.3). Therefore, effective stabilizers do not necessarily possess the highest melting temperatures [43], [350], but rather they do not segregate from the active metal oxide phase upon repeated cycling [374]. The higher the porosity of the sorbent particle, the less pronounced the Kirkendall effect is.

3.1.2.2 Reactive stabilizers

Oxides of the elements Al, Mn, Ti, Zr and Si do potentially form ternary oxides with CaO upon cycling, or during the initial synthesis of the sorbent [375]–[377]. When the stabilizing ternary phase forms under reactive conditions, its dispersion within the sorbent particle is usually relatively uniform and thus less dependent on the synthesis method employed. Compared to inert stabilizers, the ternary phase does not typically segregate from the CaO phase and so naturally provides a better stabilizing function, as well as tending to have a higher mechanical stability. However, ternary oxides formed from reactive stabilizers and CaO, e.g. calcium aluminates or calcium silicates, often have lower melting temperatures than binary oxides and themselves may be more prone to sintering. Deactivation mechanisms may thus differ from that of binary oxide stabilizers and explain why no consistent trend between the cyclic performance and the melting temperature of the support has been observed [43], [350], [378]–[381]. Ternary (Ca-containing) oxides functioning as structural stabilizers can also be produced separately from the actual sorbent, and then combined with CaO during synthesis [354], [358], [382]–[384]; this functions similarly to using inert binary oxides as stabilizers.

There exists some uncertainty whether the chemical composition of the sorbent is cyclically stable when relying on a reactive stabilizer. Taking Al_2O_3 as example, different calcium aluminate phases can form upon calcination, which may then transform into other, thermodynamically more favorable, calcium aluminate phases upon cycling: Kim et al. [385] synthesized a CaO-based sorbent in which $Ca_3Al_2O_6$ was formed after the initial calcination at 800 °C. Using in situ XRD and DNP-SENS ^{27}Al NMR, the gradual transformation of $Ca_3Al_2O_6$ into $Ca_{12}Al_{14}O_{33}$, was observed with cycling. During that transformation Al_2O_3 also formed, which segregated from the CaO and $Ca_{12}Al_{14}O_{33}$ phases and accumulated on the surface of the sorbent particle. The cyclic CO_2 uptake decreased accordingly. Interestingly, the Al_2O_3 phase did not react with CaO to form calcium aluminate, probably because the kinetics for this reaction were too slow (note that the calcination step at 900 °C lasted only 4 min before switching to carbonation at 650 °C).

3.1.3 Nano- and microstructured morphologies

Several researchers have been successful in improving cyclic stability using template-assisted techniques to obtain a highly porous sorbent that incorporates structural stabilizers. The overarching goal in these studies has been to synthesize nano- and micro-structured sorbents that exhibit reduced sintering during repeated carbonation-calcination cycles. First we describe morphologies achieved by template-assisted techniques, which may further be distinguished by the distribution of the stabilizer: (i) A homogenously distributed stabilizer to retard sintering in a nanostructured sorbent [119], [120], [378], [386]–[396] or (ii) a surface layer of the stabilizer, which acts as a physical barrier around the sorbent at the core, referred to as core-shell structures [120], [390], [397]–[400]. Secondly, we discuss the use of so-called polymorphic spacers, where the stabilizer is a second separate phase which undergoes a volume change during cycling [401]–[403]. An overview of the different approaches for morphology stabilization are shown schematically in Figure 5.

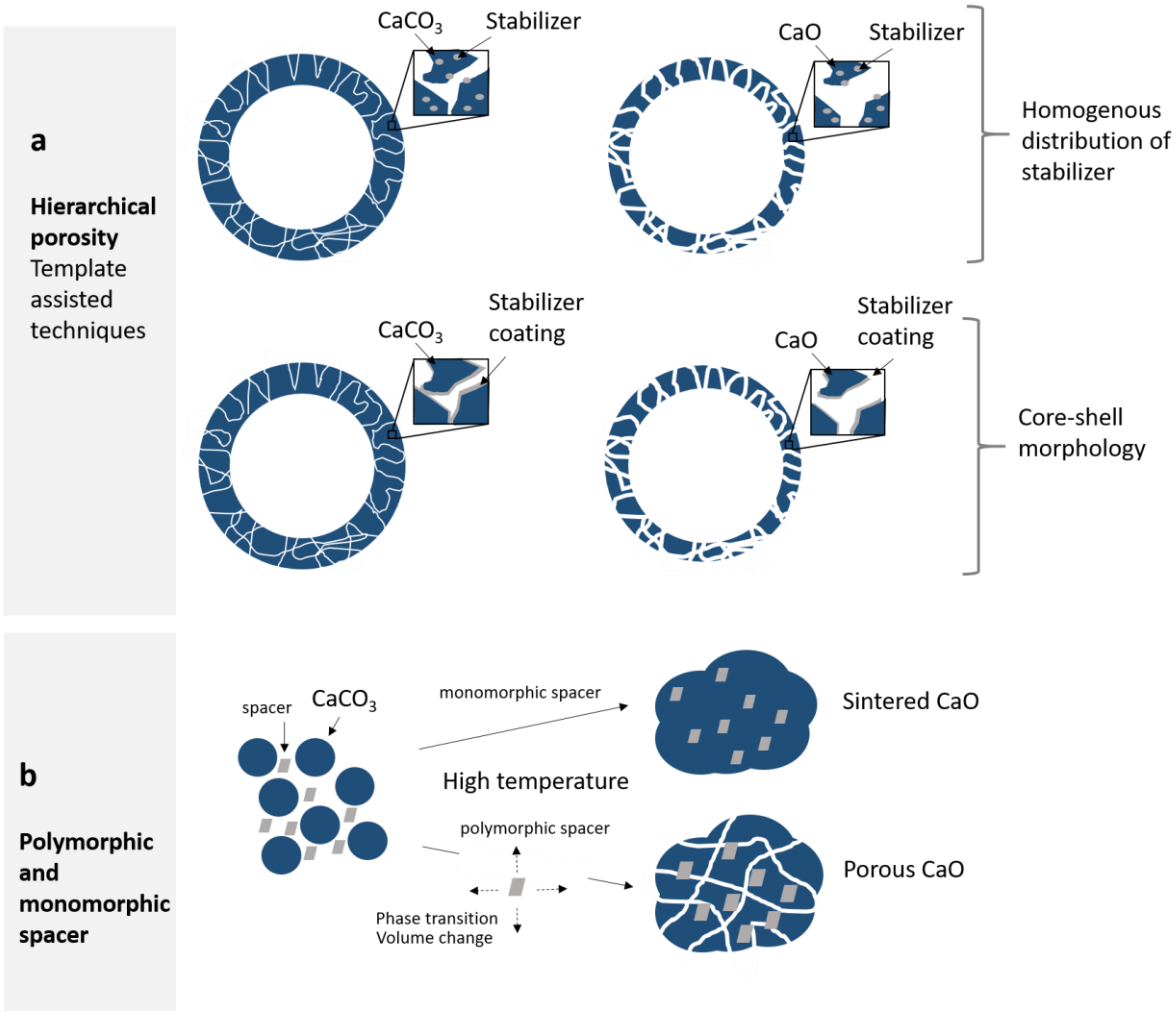

Figure 5. Schematic of nano- and microstructured morphologies to improve cyclic stability. The left and right column show the carbonated and calcined states, respectively. a) Hierarchical porosity obtained by template-assisted techniques with a homogenous distribution of the stabilizer or a stabilizer coating providing a core-shell morphology, respectively, adapted from [119] *and* [120]*. b) Polymorphic and monomorphic spacer used for a CaO sorbent, adapted from* [401]*.*

Sacrificial templates have been used to synthesize nanostructured sorbents with homogenously distributed stabilizers [119], [120], [378], [386]–[388], [390]–[396]. The resulting morphologies have been characterized as microspheres [119], [391], [394], [396], [397], [404], microtubes [393], cage-like structures [392], [405], and nanosheets [387]. The structures are principally a product of the shape of the templates such as carbonaceous spheres [286], [388] or hard templates of biomass including cotton [393], willow, straw and wheat [395], but there have also been examples where hollow structures were obtained without using carbonaceous templates by exploiting the Kirkendall effect [406], [407]. However, in the context of CO_2 capture, carbonaceous templates have been used much more frequently. For example, to ensure a homogenous mixing of the stabilizing phase, Broda et al. [286] used a one-pot synthesis method using aluminum and calcium nitrate precursors mixed with a gelating agent. At the end of the gelation step, carbonaceous spheres were produced covered with an amorphous Ca-Al-

based film. Pyrolysis of the gel at 500 °C in N_2 resulted in a crystalline film containing polymorphs of $CaCO_3$, which was followed by a final step in which the carbon template was removed by calcination at 800 °C in air leaving a porous nano- and microstructured CaO-based crystalline film in the shape of a hollow sphere.

Another approach to limit deactivation as a result of sintering is the fabrication of core-shell structures, [398], [400], [408]–[410]. Here, the template-assisted technique is likewise used to create a highly porous sorbent, but instead of a homogenous distribution of the stabilizer, the active sorbent material is covered with a thin layer of stabilizer material. The motivation for this particular morphology is to use a small amount of inert material to retain a high capacity, while sintering is impeded due to a thin physical barrier, the shell, which limits the contact between the calcium carbonate grains [411]. A brief summary of various approaches to achieve core-shell structures is provided in Table 4. Vapor phase deposition techniques such as atomic layer deposition (ALD) and chemical vapor deposition (CVD) offer the possibility to introduce a layer of stabilizer on the core sorbent material. The advantage of the ALD technique is that it enables control of the layer thickness at the atomic scale and can provide a thin conformal coating. The technique has been applied to layer coatings of thickness between 1 nm to 30 nm of stabilizer oxides on a porous CaO support to create core-shell structures for CO_2 capture [119], [120], [378], [397], [399], [410]. It is worth mentioning that the core-shell structure is formed in the as-prepared materials but it also tends to collapse during multiple cycle operation [412]. Despite this collapse, the initial core-shell morphology provides a relatively higher CO_2 uptake stability compared to sorbents without ALD coatings. Han et al. [398] notes that while the ALD processing technique produces a sorbent with a high activity and excellent regenerability, it is a complex and expensive synthetic procedure. Instead, they proposed to use chemical vapor deposition as a relatively more scalable and inexpensive technique. The CVD technique was used to cover CaO particles of 60 – 80 μm in diameter with nanoparticles (4 – 8 nm diameter) of Al_2O_3. Although the cyclic capacity was improved by 300 % compared to the benchmark CaO, the capacity was not as high as for the material resulting from the ALD technique (Table 4). From these results, the question arises whether the benefit of the added capacity over numerous cycles in sorbents stabilized by ALD outweighs the higher cost and whether such sorbents can be practical (see Section 6.3). To that end, impregnation, wet coating or self-assembly template assisted techniques are promising alternatives providing high capacity at a lower cost. For example, the self-assembly template synthesis (SATS), Table 4, provides a high CO_2 uptake capacity of 0.46 g g^{-1} over 104 cycles. Contrary to the other core-shell materials, the core is made of Al_2O_3 while the outer shell is made of the active CaO. To

minimize the reaction between CaO and Al_2O_3, a third nano-sized TiO_2 phase is introduced as a physical barrier. Here, self-assembly refers to the ordered structure that is achieved under an adjusted pH of 6 resulting in a core of Al_2O_3 which is completely coated in TiO_2. Finally, the active CaO phase is added as calcium acetate monohydrate and is mixed with the excess nano-sized TiO_2.

Table 4. Preparation techniques to achieve core-shell structures. [(a)] SATS: Self-assembly template synthesis; EISA: Evaporation-induced self- assembly; ALD: atomic layer deposition; CVD: chemical vapor deposition. [(b)] CO_2 uptake capacity in the last cycle of the experiment compared to theoretical maximum 0.786 g_{CO2} $g_{sorbent}^{-1}$ for CaO.

Core material	**Shell material**	**[(a)]Coating preparation technique**	**CO_2 capture equipment (cycles)**	**[(b)]Capacity last cycle (g_{CO2} $g_{sorbent}^{-1}$)**	**Temperature Carbonation/ Calcination**	**Ref.**
CaO	SiO_2/ZrO_2	Impregnation	TGA (20 cycles)	0.32	675 °C / 850 °C	[408]
Al_2O_3	TiO_2/CaO	SATS	TGA (104 cycles)	0.46	700 °C / 900 °C	[400]
CaO	TiO_2/SiO_2	Wet coating and EISA	TGA (30 cycles)	0.22	675 °C / 850 °C	[409]
CaO	Al_2O_3	ALD	TGA (30 cycles)	0.55	650 °C / 900 °C	[410]
CaO	Al_2O_3	CVD	TGA (20 cycles)	0.41	650 °C / 950 °C	[398]

The term polymorphic spacers was introduced by Zhao et al. [401] to describe the stabilization of CaO by Ca_2SiO_4. In this case, "spacer" refers to particles of a second phase forming a physical barrier that inhibits sintering, while "polymorphic" refers to a phase transformation the stabilizing material undergoes during the temperature change between carbonation and calcination. Ca_2SiO_4 exhibits a reversible phase transition between the α' and β polymorphs between 630 – 690 °C that results in a volumetric change of ~ 2 %, with the higher volume α' phase forming at temperatures near that of the calcination of $CaCO_3$. The authors proposed that this volume change results in microporous channels that enable CO_2 to access CaO, leading to a higher stability over repeated cycling. While promising, a critique of the study points out that the testing conditions are not relevant for those used in an industrial context [402]. The material was tested in a TGA with calcination at 850 °C in pure N_2 for 30 min, which is not representative of a commercial scale setup were the goal is to produce a concentrated steam of CO_2. In response to this critique the authors performed thermogravimetric tests in pure CO_2 and demonstrated a higher performance of the CaO modified by polymorphic spacers in this case as well [403]. Other studies contradict these results, showing CaO modified with Ca_2SiO_4 to still show the typical decay of unmodified CaO [402], [413], clearly highlighting the need for more analysis of these materials.

3.2 MgO-based sorbents

Given the lower sorption temperatures of MgO compared to CaO, a popular approach to enhance the kinetics of CO_2 uptake of MgO is its promotion with alkali metal nitrates such as $LiNO_3$, $NaNO_3$, and KNO_3 [133], [414]–[418]. Webley and co-workers [419], [420] studied adsorbents based on double salts of $MgCO_3$ with either K_2CO_3 and Na_2CO_3 prepared by wet mixing; others investigated also Cs_2CO_3 or Rb_2CO_3 [421], [422]. K-Mg double salts reached a CO_2 uptake of 8 wt% at 375 °C in pure CO_2 [420], while Na-Mg double salts showed higher CO_2 uptakes reaching between 15 wt% [423] and ~ 20.7 wt% [419]. Zhang et al. [423] noted difficulties in reproducing the performance for these materials, and argued that a modified synthesis route must be developed in order to improve the reproducibility of the material and to allow scale up to larger quantities. Recent results in this area are shown in *Table 5* and Table 6, while Figure 6 shows the CO_2 capture performance of MgO promoted with $NaNO_3$ using thermogravimetric analysis.

Table 5. Selected MgO sorbents modified with an inert support.

Main sorbent	Support (wt%)	Instrument (cycles)	Carbonation conditions	Decarbonation conditions	Capacity last cycle (g_{CO2} $g_{sorbent}^{-1}$)	Ref.
MgO	Al_2O_3 (56 %)	TG-MS (6)	200 °C, 10 % CO_2, 10 % H_2O, 60 min	600 °C, Ar, 60 min	0.131	[141]
MgO	TiO_2 (86 %)	TGA (7)	25 °C, 100 % CO_2 200 min	150 °C, N_2, 200 min	0.022	[424]
MgO	CeO_2 (30 %)	TPD (1)	200 °C, 100 % CO_2, 30 min	150 °C, He, -	0.024	[425]
MgO	CuO (18 %)	U-tube reactor (1)	200 °C, 14 % CO_2, 2 sec	200 °C, N_2, 120 min	0.035	[426]

Table 6. Selected MgO sorbents modified by alkali metal salt (AMS). For further comparison see [417].

Main sorbent	Dopant (wt%)	Instrument (cycles)	Carbonation conditions	Decarbonation conditions	Capacity last cycle (g_{CO2} $g_{sorbent}^{-1}$)	Ref.
MgO	$NaNO_3$ (20 %)	TGA (9)	330 °C, 100 % CO_2, 45 min	385 °C, N_2, 30 min	0.267	[134]
MgO	KNO_3 (34 %)	TGA (12)	325 °C, 100 % CO_2, 20 min	450 °C, N_2, 30 min	0.078	[415]
MgO	$LiNO_3$/$NaNO_3$/KNO_3 (6/4/15 %)	TGA (40)	300 °C, 100 % CO_2, 60 min	350 °C, N_2, 30 min	0.306	[133]
MgO	AMS:MgO (0.15:1 molar ratio) $CaCO_3$ (wt%)	TGA (50)	350 °C, 100 % CO_2, 45 min	400 °C, N_2, 15 min	0.650	[427]
MgO	AMS:MgO (0.2:1) CeO_2 (10 wt%)	TGA (30)	325 °C, 100 % CO_2 60 min	425 °C, N_2 15 min	0.430	[142]

Vu et al. [415] investigated MgO modified by various alkali metal salts and found that the highest CO_2 uptake in the MgO/KNO_3 system (molar ratio of MgO:KNO_3 = 5:1) was 13.9 wt% at 325 °C in 100 % CO_2 (120 min of carbonation). The morphology of MgO was modified by variations in the synthesis procedure. For example, the BET surface areas of the different MgO

materials produced ranged between 128 to 380 $m^2 g^{-1}$ and the BJH pore volume between 0.6 and 1.9 $cm^3 g^{-1}$. Contrary to earlier works on MgO-based CO_2 sorbents in which an increased CO_2 uptake for an increasing pore volume was observed [428], [429], Vu et al. could not identify a clear relationship between the CO_2 sorption capacity and the pore volume or surface area of MgO. Therefore, future studies of materials with well-defined pore structures would be very valuable to delineate accurately the effect of promoters while excluding effects due to differences in the pore structure and/or surface area.

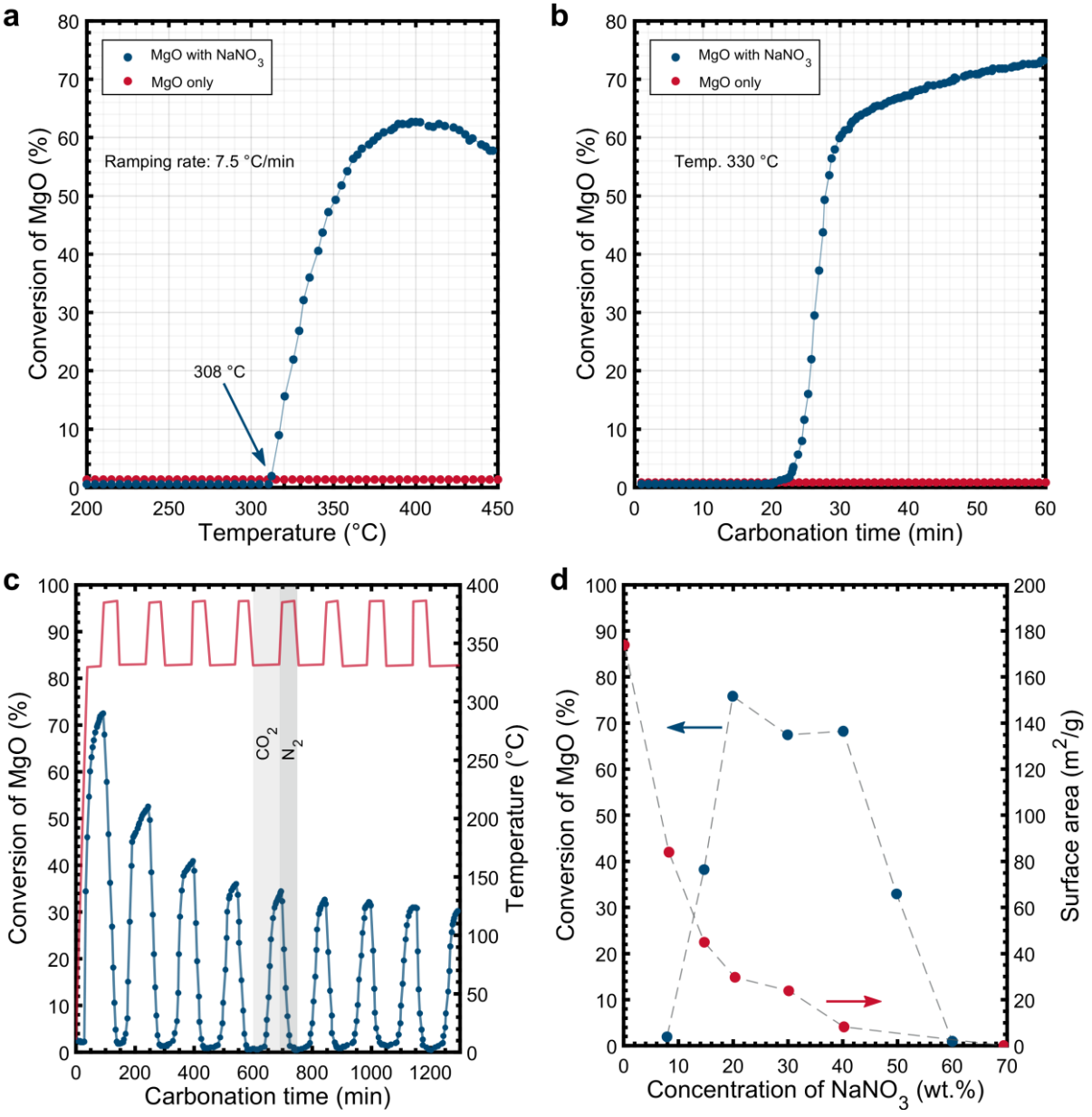

Figure 6. Thermogravimetric analysis of MgO powder with and without a $NaNO_3$ promoter. CO_2 uptake during (a) heating in CO_2 and (b) isothermal CO_2 absorption at 330 °C. (c) Multiple temperature-pressure swing cycles of MgO promoted with 20 wt.% $NaNO_3$ for carbonation at 330 °C in 1 bar CO_2 and regeneration in N_2 at 385 °C. (d) CO_2 uptake and BET surface area of $NaNO_3$-MgO as a function of $NaNO_3$ weight percent. Figures (a) – (d) were reproduced with permission from [134], *copyright (2014) Wiley-VCH.*

There have been several theoretical studies aimed at understanding CO_2 absorption at the surface of different promoted MgO sorbents. Kim et al. [430] calculated the absorption energy of various alkali oxide promoters on MgO surfaces, and the corresponding CO_2 absorption energy. They found that absorption energies of promoters must exceed 0.52 eV in order to be thermally stable in binding to MgO, that the CO_2 absorption energy must be lower than 1.86 eV to ensure regenerability, and that Li, Ca and Sr-promoted MgO best fits these criteria. A similar study on MgO-CaO(100) solid-solution surfaces found Li-promotion to result in CO_2 binding that is too strong, and that Sr-promotion was optimal for sorbent regeneration [431]. Although there is consensus that alkali metal nitrates and carbonates promote the CO_2 capture of MgO, there is an on-going debate regarding the mechanism(s) behind this promotional effect [133], [134], [160]. As discussed in Section 2.1, thermodynamic equilibrium considerations (Figure 1) suggests that $MgCO_3$ should not form at 1 bar CO_2 for temperatures > 300 °C. Most of the experimental works on MgO-based CO_2 sorbents that include alkali metal nitrate promoters contradict this prediction as $MgCO_3$ undeniably forms above 300 °C at atmospheric pressure, implying that equilibrium thermodynamics of the simple MgO-$MgCO_3$ system cannot be applied to predict the carbonation temperature of alkali metal nitrate promoted MgO. Figure 7 highlights two mechanisms with different rate-limiting steps that have been proposed to describe the carbonation of promoted MgO. One hypothesis, Figure 7a, assumes that the promoter (i.e. the alkali metal nitrate) lowers the energy barrier to dissociate bulk MgO into $[Mg^{2+} \cdots O^{2-}]$ ionic pairs, which migrate to the triple phase boundary (i.e. MgO|$NaNO_3$|CO_2) and react with adsorbed CO_2 on the surface of MgO to form $[Mg^{2+} \cdots CO_3^{2-}]$ ionic pairs that in turn form solid $MgCO_3$ when reaching saturation. Since the triple phase boundary will have the highest concentration of $[Mg^{2+} \cdots CO_3^{2-}]$ ionic pairs it is reasonable to assume that it is the most favorable reaction site for the formation of solid $MgCO_3$. However, it has been hypothesized that $MgCO_3$ may also precipitate away from the original dissolution site as to not inhibit any further reaction [134]. The importance of the triple phase boundary was highlighted by showing that an intermediate content of $NaNO_3$ (20 – 40 %) provides the highest CO_2 uptake. Assuming this theory to hold, one would have to manufacture materials that have a very long triple phase boundary length in order to maximize the amount of favorable reaction sites for $MgCO_3$ formation. A large triple phase boundary length could be achieved e.g. by dispersing the promoter very finely on high surface area MgO. There are experimental observations that may contradict this hypothesis, and it was shown that solid $MgCO_3$ forms even in the absence of a triple phase boundary, e.g. on a MgO(100) single crystal covered completely by $NaNO_3$ [159].

A second hypothesis concerning the carbonation mechanism of promoted MgO was proposed by Harada et al. [133] and others [415], [432]. Here, it is argued that the molten promoter layer impedes the formation of a unidentate carbonate layer, which is CO_2-impermeable, on the MgO surface. It is hypothesized that the molten promoter layer dissolves CO_2 which can react with a high concentration of oxide ions (O^{2-}) present in the nitrates (from the reaction $NO_3^- \leftrightarrow NO_2^+ + O^{2-}$) thereby generating carbonate ions (CO_3^{2-}). To substantiate this model, the authors combined TGA with in situ FT-IR and XRD experiments. Non-promoted MgO displayed only surface unidentate carbonate in the entire duration of the experiment. Promoted MgO exhibited different carbonate species as function of time in a two-stage reaction process. In the first stage (<4 min), promoted MgO displayed FT-IR peaks indicative of surface unidentate carbonate, while strong peaks associated with carbonate ions (CO_3^{2-}) and crystallized $MgCO_3$ were detected in the second stage (> 4 min) by FT-IR and XRD respectively. Based on the insights from FT-IR and XRD, TGA measurements quantified the captured carbonate species as function of time. Here, promoted MgO displayed a plateau in the CO_2 uptake of < 3 mg g^{-1} in the first minutes (< 4 min) of carbonation associated with the formation of unidentate carbonate layer on the MgO surface that is not covered in promoter. This CO_2 uptake is lower than that of pure MgO (~ 15 mg g^{-1}) under similar conditions. This indicates that promoted MgO has a lower coverage of CO_2-impermeable unidentate carbonate. Further, in the second reaction regime (> 4 min), promoted MgO displayed a strong increase in the uptake >300 mg g^{-1} which could be related to the carbonate ions and crystalline $MgCO_3$ compared to the non-promoted MgO which did not see a noticeable uptake above 15 mg g^{-1} related to the unidentate carbonates formed in the first minutes of carbonation. Based on previous work showing oxide ion (O^{2-}) concentrations of $2 \cdot 10^{-7}$ M in molten alkali metal nitrates [433], it is possible that the generation of carbonate ions (CO_3^{2-}) is indeed a product of oxide ions and dissolved CO_2 [434], but this has not been proven unequivocally by direct observation for the promoted MgO system. Alternatively, the oxide ions may have originated from MgO instead of the promoter. Further, this model is not very specific about where the carbonate ions generated react with the MgO surface to form crystalline $MgCO_3$. An implication of this model is that the interface between MgO and the alkali metal salt is the most favorable reaction site and the reaction rate is limited by the diffusion of CO_2 through the promoter layer. Assuming that this hypothesis is valid, a very active sorbent requires the maximization of the interface area between MgO and the promoter, e.g. by uniformly coating the surface of MgO by a promoter. Further, the thickness of the promoter layer should be thin to shorten the diffusion path. Assuming a full surface

coverage of MgO particles with a diameter of e.g. 500 nm, and a loading of 20 wt.% promoter would imply a coating thickness of 50 nm [133].

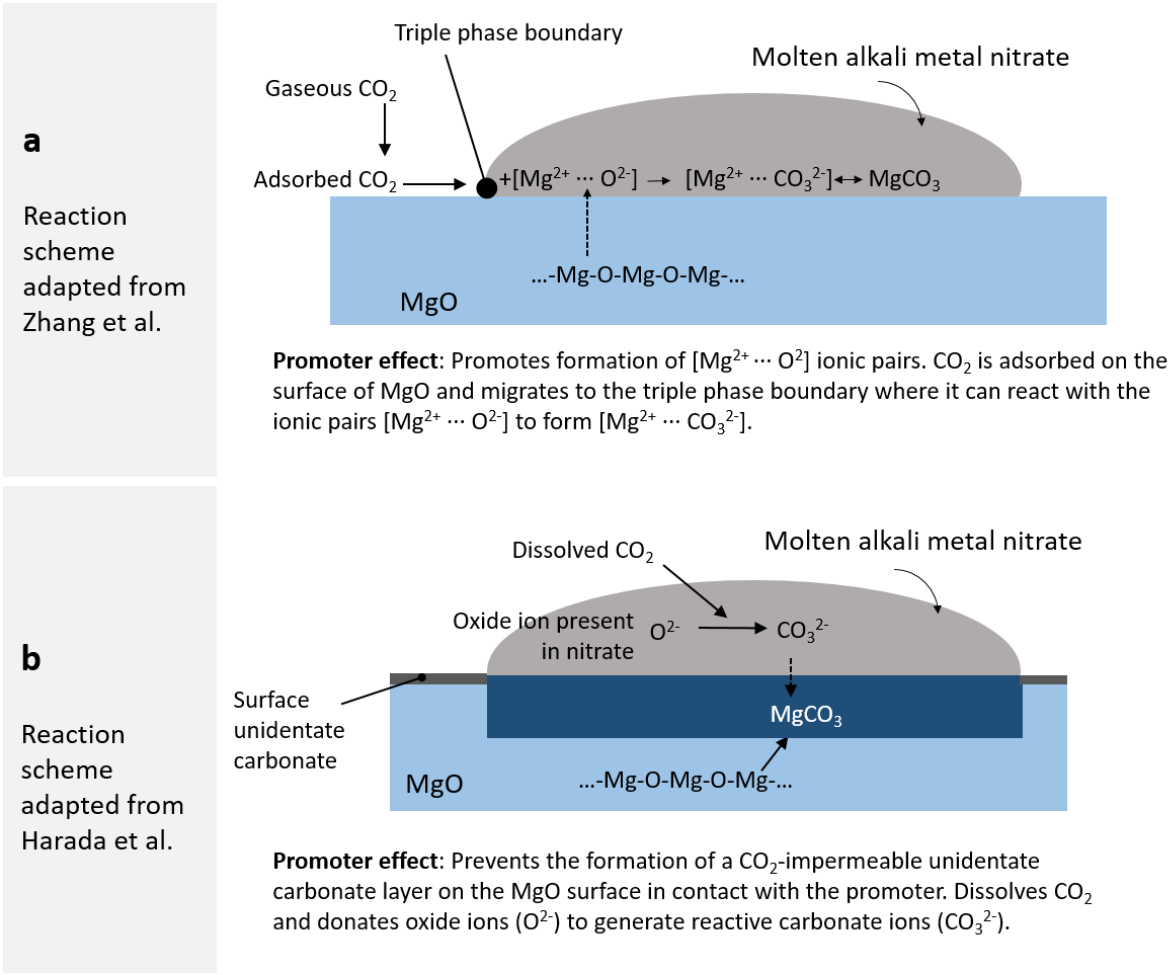

Figure 7. Schematics of two proposed carbonation mechanisms of promoted MgO. a) The first mechanism is adapted from [134]. *The main role of the promoter is to dissolve MgO and enhance the formation of $[Mg^{2+} \cdots O^{2-}]$ ionic pairs. Gaseous CO_2 is adsorbed on the MgO surface and migrates to the triple phase boundary to form $[Mg^{2+} \cdots CO_3^{2-}]$ ionic pairs that precipitates as solid $MgCO_3$ upon reaching saturation* [134]. *b) This mechanism is adapted from* [133]. *Here, the promoter has several roles. It reduces the surface area of MgO covered in a CO_2-impermeable unidentate layer. Further, it dissolves CO_2 that can react with oxide ions (O^{2-}) present in the alkali metal nitrate (i.e. $NO_3^- \leftrightarrow NO_2^+ + O^{2-}$) to form carbonate ions (CO_3^{2-}). For this mechanism, there is no description or experimental evidence showing how and where the generated carbonate ions (CO_3^{2-}) react with MgO to form $MgCO_3$. For completeness, the formation of $MgCO_3$ is depicted here as a product layer in the interface between MgO and $NaNO_3$ to reflect the illustration in the original reaction scheme.*

Dal Pozzo et al. [160] critically assessed the validity of the two carbonation mechanisms sketched in Figure 7, by synthesizing and testing a wide range of MgO alkali metal nitrate systems. They found a direct correlation between the solubility of MgO in the molten nitrates and the CO_2 uptake, and an inverse correlation between the melting point of the nitrates and the CO_2 uptake capacity. These findings provide some evidence for the dissolution of MgO into the promoter to be the rate limiting step as proposed in the mechanism of Zhang et al. [134].

To obtain a better understanding of the promotional mechanism of alkali metal salts on the CO_2 uptake of MgO, experiments that run over multiple carbonation and calcination cycles are also

informative. It has been reported that MgO promoted by alkali metal nitrates and carbonates display a decay in the CO_2 uptake; often in the range of 30 – 60 % of the initial uptake over 10 cycles [133], [435], [436]. In these works, deactivation has been associated to sintering similar to what has been observed for pure MgO and CaO-based sorbents [133], [255], [437]. However, more recent work suggests that changes in the morphology of MgO cannot explain fully the observed deactivation, instead also changes in the distribution of the molten salt promoters on the surface of MgO have to be taken into consideration [159], [160]. For example, Jo et al. [159] observed that in a N_2 atmosphere $NaNO_3$ had a lower contact angle (higher affinity) on a model MgO(100) surface compared to the same surface that has been exposed to CO_2 (carbonated sample), Figure 8.

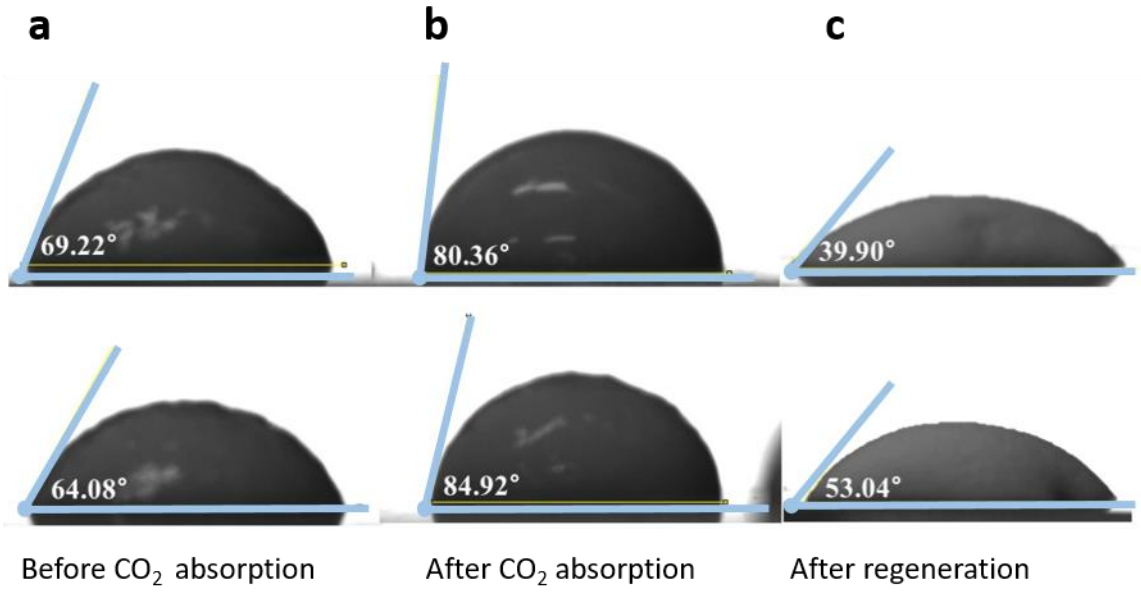

Figure 8. Optical measurement of contact angle between a MgO wafer and droplet of molten (Li, Na, K)NO_3. (a) before CO_2 absorption, (b) after carbonation, (c) after calcination. Note that two measurements were made for each set point after cooling the wafer with the molten droplet to room temperature. Figure reproduced with permission from [159]*, copyright (2017) PCCP Owner Societies.*

Hence, it is conceivable that a repulsive force between $MgCO_3$ and the promotor would lead to segregation of the molten promoter away from the newly formed $MgCO_3$. Following this, the deactivation observed with increasing cycle number would be a result of the segregation and agglomeration of the promoter leading to a reduced surface area covered by the promoter (i.e. MgO and $NaNO_3$ interface). This hypothesis was supported experimentally by the work of Dal Pozzo et al. [160] characterizing the surface of an as-prepared MgO-$NaNO_3$ sorbent and after 10 cycles using energy dispersive X-ray (EDX) spectroscopy. Here, in the as-prepared sample $NaNO_3$ was well-dispersed on the surface, which upon ten carbonation-calcination cycles agglomerated into larger particles. To which extent the agglomeration is driven by the repulsion from the $MgCO_3$ surface or perhaps simple Ostwald ripening has not been quantified so far.

Further, it is worth noting that the particle size of $NaNO_3$ and its surface coverage was characterized ex situ, which may differ from the actual morphology of $NaNO_3$ under working conditions as the temperature of carbonation and calcination conditions exceed the melting point of $NaNO_3$ of 308 °C. However, with an increasing degree of agglomeration of the promoter both the length of the triple phase boundary and the area of the interface between the promoter and MgO decrease, making it difficult to draw any conclusions about the prevailing carbonation mechanism from these experiments. Here, molecular dynamic simulations may prove helpful to understand the rheological behavior and coverage of the molten salt promoter on the surface of MgO and $MgCO_3$, respectively, under operating conditions [438]. Recently, in situ TEM was utilized to observe directly the growth of $MgCO_3$ at the triple phase boundary [435]. Although these results confirm that $MgCO_3$ can grow at the triple phase boundary, it does not prove the hypothesis that the triple phase boundary is the only reaction site as the interface was inaccessible for TEM as it is buried under the $NaNO_3$ promoter.

Similar to the discussion in Section 2.4.3, the effect of water-based treatments on the CO_2 uptake capacity on alkali salt promoted MgO has been explored. For example, Dal Pozzo et al. [160] compared the potential of three methods to (partially) re-activate the sorbent, viz. mechanical grinding, hydration and filtration followed by re-coating the sample with fresh $NaNO_3$. Grinding the MgO-$NaNO_3$ sample after the 10^{th} cycle resulted in a small improvement of the CO_2 uptake in the 11^{th} cycle, while immersing the sample into water, followed by drying in air at 80 °C, nearly doubled the uptake compared to the previous cycle. For these two experiments, the sample maintained its "original" $NaNO_3$. In the last experiment, the water-soluble $NaNO_3$ was removed from the cycled MgO-$NaNO_3$ sample by filtration and re-coated with "fresh" promoter, which had a similar impact on the CO_2 uptake as hydration. Two possible explanations were proposed to rationalize the observation. Immersing the sample into water dissolves $NaNO_3$, leading to a potentially more favorable redistribution of $NaNO_3$ on the surface of MgO upon drying. However, it was found that hydration also affected the crystallite site of MgO. The as-prepared sample had an average MgO crystallite size of 24 nm, which increased to 39 nm after 10 cycles. After hydration, the crystallite size of MgO was decreased to 29 nm. The exact reason for the decrease in crystallite size upon hydration is unknown, yet it was hypothesized that the formation of $Mg(OH)_2$ during hydration may be linked to the reduced size of MgO. To explore further the effect of steam on promoted MgO, a constant stream of 2 vol.% steam was introduced. The presence of a continuous flow of steam during carbonation and calcination improved the CO_2 uptake in the first cycles, but the CO_2 uptake decreased after the sixth cycle. Although the reason for the higher rate of the decay in the CO_2

uptake in the presence of steam is currently not understood, the potentially promising effect of adding steam at strategic times should promote further works in this area. So far, the highest CO_2 uptake of an MgO-based sorbent of 0.65 g_{CO2} g^{-1} was obtained when adding alkali metal salt promoters and $CaCO_3$ [427], Figure 9.

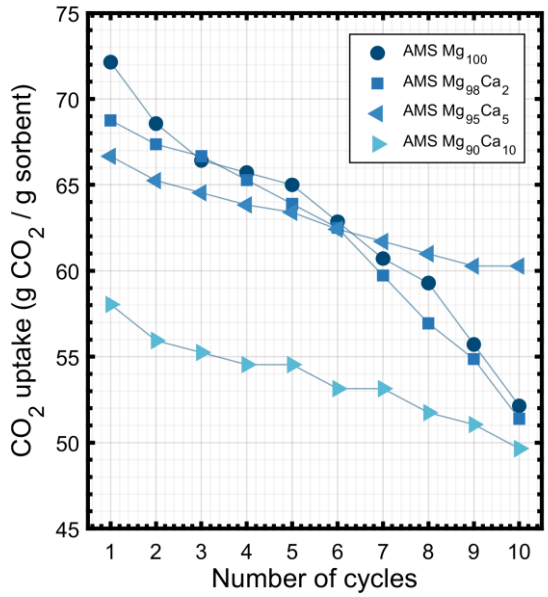

Figure 9. CO_2 absorption test of MgO powder promoted with alkali metal salt, (Na,Li,K)NO_3 and varying content of $CaCO_3$ for 10 temperature-pressure swing cycles with carbonation at 350 °C in 1 bar CO_2 for 45 min and regeneration at 500 °C in 1 bar CO_2 for 5 min. Figure produced using data from [427].

The optimum molar ratio of MgO/$CaCO_3$ was found to be 0.95:0.05. The authors attributed the improved performance to (i) the promoting effect of the alkali metal salts, (ii) the rapid formation of a $CaMg(CO_3)_2$ double carbonate and (iii) a plate-like morphology of the material. The plate-like morphology was hypothesized to prevent the agglomeration of the promoter and thus stabilize the sorbent over multiple carbonation and calcination cycles. The acceleration of the carbonation kinetics was observed to correlate with the formation of a $CaMg(CO_3)_2$ double carbonate, as observed by in situ XRD in the initial 2 min of carbonation (i.e. the time period in which the three-phase material showed the most significant improvement over the material without $CaCO_3$). Interestingly, Jo et al. [159] found that adding $SrCO_3$ to $NaNO_3$-promoted MgO also strongly accelerated the carbonation kinetics. However, under the experimental conditions employed in that study, $SrCO_3$ is not expected to react with $MgCO_3$ to form $SrMg(CO_3)_2$ [159], [439], which is different from group I alkali metal carbonates that can indeed readily form double carbonates with Mg at the beginning of the carbonation reaction [422]. Therefore, the authors reasoned that $SrCO_3$ acted as a nucleation seed for $MgCO_3$ crystallization. Ex situ XRD confirmed the absence of any other Sr-phase besides $SrCO_3$, which indicates that carbonates may also enhance the carbonation kinetics without the formation of double carbonates. An alternate approach to stabilize the cyclic uptake of AMS-promoted MgO

has been shown through the addition of hydrotalcites or TiO_2. Here, the composite structure (e.g. MgO-TiO_2) enhanced the growth of more but small crystallites of $MgCO_3$, thereby reducing sintering. Although a stable cyclic performance was obtained, it came at the expense of a lower CO_2 capture capacity of ca. 0.3 g_{CO2} $g_{sorbent}^{-1}$ [440], [441].

Overall, the reports summarized above show clearly that a better fundamental understanding of the mechanisms through which alkali-based promoters and carbonates enhance the uptake of CO_2 in MgO and the influence of the morphology of both the MgO skeleton and the promoter is very much needed. An improved understanding of these aspects and the identification of the most active MgO sites will facilitate the formulation of more effective MgO-based CO_2 sorbents.

4 Sorbents beyond CaO and MgO

Although CaO- and MgO-based materials have been the subject of most of the research in mid- to high-temperature CO_2 sorbents, they are not the only systems that can undergo cyclic carbonation and calcination reactions. In fact, most other alkali and alkaline earth metal-containing oxides (Li, Na, Ba, …) are capable of some level of CO_2 absorption as shown above and represent an underexplored parameter space compared to the more heavily investigated CaO and MgO systems. Thus, a different strategy for materials optimization is to widen the pool of explorable sorbent materials, both for improving the fundamental understanding of how CO_2 absorption and desorption proceeds, and to find suitable materials for practical use.

4.1 Experimental studies

Iron oxide-based perovskites ($AFeO_3$, where A is an alkaline earth metal such as Ca or Sr) and related structures have been used frequently as oxygen carriers in hydrocarbon conversion schemes (termed chemical looping), in which the materials undergo cyclic redox reactions [442]–[445]. Upon exposure to a strongly reducing gas, the perovskite (e.g. $SrFeO_3$) transforms to metallic Fe and the respective alkaline earth metal oxide, which can readily carbonate in a CO_2-containing environment if thermodynamically feasible [446], [447]. Surface area and pore volume of such materials are naturally low owing to the structural transformations and the high reaction enthalpies associated with the redox reactions; thus, the observed CO_2 uptake capacity is typically relatively low (of the order of $\sim 10 - 20$ % of the theoretical capacity of the respective alkaline earth metal oxide). A positive aspect of these materials is that in an oxidative environment, where $p_{CO2} < p_{CO2,eq}$, the CO_2 is released and the perovskite structure is recovered, thereby avoiding the sintering of the Ca-phases and ensuring a high cyclic stability.

Other, similar mixed oxides containing Ca include calcium cobalt oxide ($Ca_3Co_4O_9$, $Ca_2Co_2O_5$) and calcium copper oxide (Ca_2CuO_3, $Ca_3Cu_7O_{10}$), which possess multiple functionalities. Calcium cobalt oxide has been used in the sorption-enhanced steam reforming of glycerol to produce hydrogen of high purity [448]. Under reforming conditions, the calcium cobalt oxide decomposes to cobalt (oxide) and CaO, which absorbs the CO_2 co-produced and thereby enables higher yields of the reforming product hydrogen; the cobalt functions as a reforming catalyst. Subsequently, the calcium cobalt oxide phase is regenerated under oxidizing conditions while releasing CO_2. Calcium copper oxide is present in CaO/CuO composites that have been investigated for schemes to reduce the energy requirements for sorbent regeneration of the conventional calcium looping process [122], [397]. Here, the exothermic reduction of CuO with a reducing gas such as CH_4 is used to provide the heat required for the regeneration of $CaCO_3$ in the same particle. The calcium copper oxide phase readily segregates into CaO

and CuO under carbonation conditions and does therefore not impair the theoretical CO_2 uptake capacity of the sorbent.

CaO and MgO already have high gravimetric CO_2 absorption capacities, given the relatively low atomic mass of Ca and Mg and the fact they are simple binary compounds. Beyond these two oxides, the most studied materials for high-temperature CO_2 capture, viz. Li_2ZrO_3 [449]–[458] and Li_4SiO_4 [456], [459]–[461], suffer from an intrinsically lower capacity due to the presence of tertiary elements; the same applies to Na_2ZrO_3 [462], [463]. One approach to overcome this problem is to synthesize materials with a higher fraction of alkali metals. A number of such materials have been synthesized and subjected to thermogravimetric studies, including Li_6WO_6 [464], $Li_6Si_2O_7$ [465], Li_8SiO_6 [465], [466], $Li_6Zr_2O_7$ [455], [467], Li_8ZrO_6 [467]–[469], Li_5AlO_4 [470], [471] and Li_5FeO_4 [472], [473]. Thermogravimetric studies have shown that these materials generally have relatively high CO_2 gravimetric capacities and, in many cases, have stable cycling capacity, at least for the small number of cycles tested. An overview of these materials is shown in Table 7.

Table 7. Overview of selected lithium-containing sorbents and their CO_2 uptake capacities. For further comparison see [474].

Main sorbent solid solution	**Instrument (number of cycles)**	**Carbonation conditions**	**Decarbonation conditions**	**Capacity last cycle (g_{CO2} $g_{sorbent}^{-1}$)**	**Ref.**
Li_4SiO_4	TGA (1)	600 °C, 100 % CO_2, ~ 1000 min	Not regenerated	0.45	[459]
Li_8SiO_6	TGA (1)	650 °C, 100 % CO_2, 120 min	Not regenerated	0.52	[475]
Li_4SiO_4	TGA (50)	600 °C, 20 % CO_2/N_2, 60 min	800 °C, N_2, 60 min	0.07	[476]
$Li_6Zr_2O_7$	TGA (3)	750 °C, 100 % CO_2, 60 min	850 °C, N_2, 60 min	0.09	[467]
Li_8ZrO_6	TGA (10)	750 °C, 10 % CO_2, 30 min	900 °C, N_2, 65 min	0.19	[469]
Li_6WO_6 nanowires	TGA (4)	710 °C, 60 % CO_2/N_2, 10 min 710 °C, 60 % CO_2 + water vapor, 10 min	730 °C, 60 % CO_2, 10 min 760 °C, 60 % CO_2 + water vapor, 10 min	0.10 0.02	[464]
α-Li_5AlO_4	TGA (20)	700 °C, 100 % CO_2, 20 min	750 °C, N_2, 20 min	0.19	[474]
Li_5FeO_4	TGA (1)	800 °C, 20 % CO_2/N_2, 180 min	Not regenerated	0.50	[473]
Li_3BO_3 + 10 mol% (Na-K)NO_2	TGA (10)	580 °C, 100 % CO_2, 60 min	650 °C, N_2, 60 min	0.35	[477]
$Li_4Si_{0.85}Ge_{0.15}O_4$	TGA (9)	550 °C, 100 % CO_2, 15 min	550 °C, N_2, 15 min	0.25	[478]
$Li_{3.7}FeO_{0.1}SiO_4$	TGA (5)	650 °C, 100 % CO_2, 60 min	750 °C, He, 30 min	0.05	[479]

Examples of such high-lithium content materials are Li_8ZrO_6 and $Li_6Zr_2O_7$, with combined theoretical and experimental studies showing excellent initial CO_2 uptake capacities [480].

However, there remains the question of regeneration, which was found to not occur; at a calcination temperature of 600 °C, the only reaction with $\Delta G < 0$ is the formation of Li_2ZrO_3:

$Li_2CO_3 + ZrO_2 \rightarrow Li_2ZrO_3 + CO_2$ $\Delta G_{600°C} = -1.7$ kJ/mol (R15)

with all other reactions, including the regeneration of the initial Li_8ZrO_6 and $Li_6Zr_2O_7$ sorbents, requiring a higher energy input to be reformed.

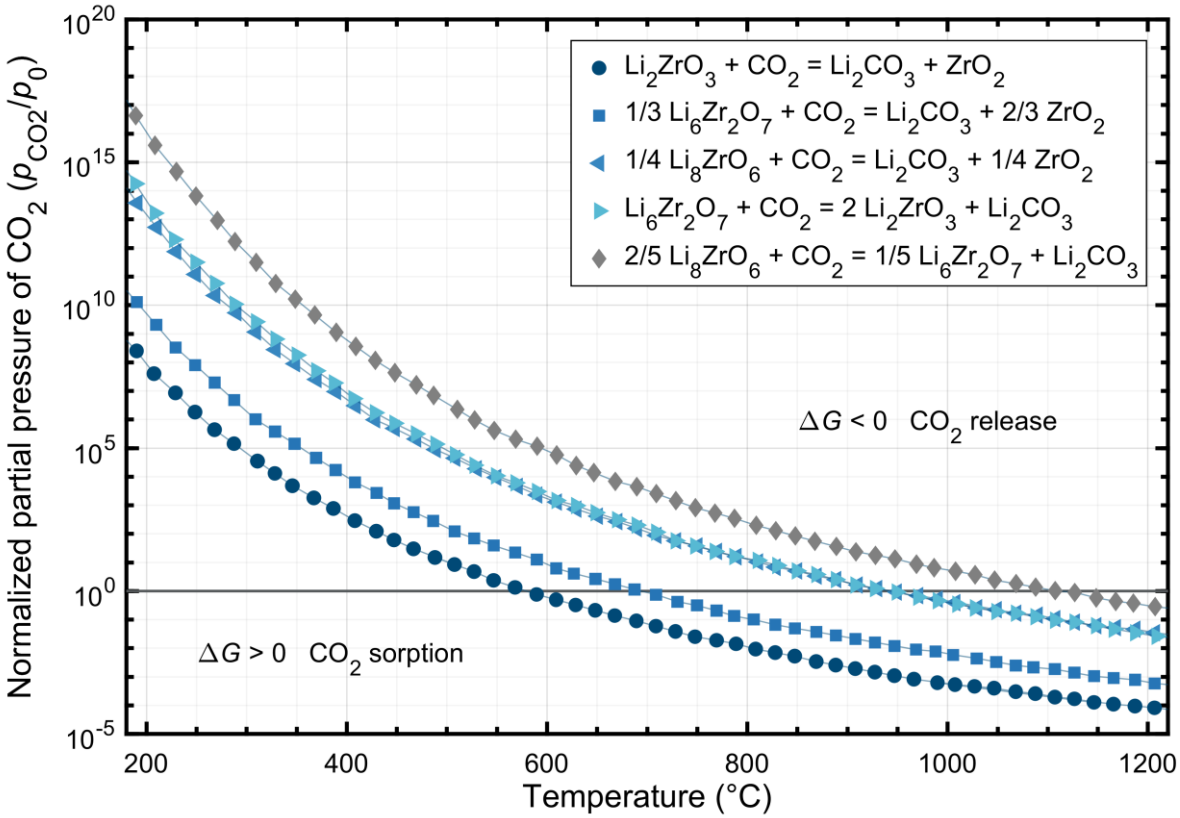

Figure 10: Theoretical carbonation equilibrium curves for the various reactions in the Li_8ZrO_6 and $Li_6Zr_2O_7$ systems. DFT calculations are a useful technique to assess sorbent utility in silico, in this case predicting that these Li-rich materials, while beneficial in terms of gravimetric capacity, do not regenerate after carbonation. At 600 °C and p_{CO2} = 1 atm the only equilibrium curve which predicts sorbent regeneration is the formation of Li_2ZrO_3 from Li_2CO_3 and ZrO_2 (●). Figure reproduced with permission from [480]*, copyright (2015) PCCP Owner Societies.*

This raises the question as to whether the use of high lithium content materials is feasible as their full regeneration could lead to higher energy penalties incurred in their use. While it is beyond the scope of this review to fully explore all studies on Li and Na containing oxides, readers are directed to a number of excellent recent reviews that cover these materials in much more depth [54], [481].

4.2 In silico large scale theoretical screening

There are several different approaches to searching the available chemical space for optimal CO_2 absorption materials, with the two main ones being the sequential, experimental optimization within defined families of material (as exemplified by the various studies of modifications to CaO and MgO described in Section 3), and large-scale screening studies often driven by first-principles calculations. The benefit of the former is that by investigating fewer

materials, their performance can be characterized more thoroughly, and better inferences made about the influence of the chosen modifications. The latter sacrifices depth for the ability to sample the chemical space in more breadth, being better suited to materials discovery that can feed into further experimental investigations. These two approaches are complementary, and both fundamentally seek to correlate structure, morphology and chemistry with the CO_2 capture performance in order to produce more effective materials.

One of the main methods of calculating the ground state energy of materials is using density functional theory (DFT), which allows various properties including the enthalpy of carbonation (at 0 K), volume change and gravimetric capacity to be determined and compared for many different materials. The main difference between these studies is the source of the data, and the scope of materials considered in the screening. With a sufficiently rich data set, such materials discovery methods can be much more efficient than sequential experimental studies in finding new materials with favorable CO_2 capture properties and can also elucidate overall principles or limitations such as targeting materials with intermediate carbonation temperatures which balance energy penalty and kinetic considerations [482], that can guide further studies.

Lin et al. [483] generated their own database of potential zeolite-like structures that were subsequently analyzed via interatomic potentials to determine their thermodynamic stability. CO_2 absorption isotherms were constructed using molecular simulations that allowed the calculation of the parasitic energy cost of the thermodynamically stable materials, corresponding to the penalty imposed on a power plant if fitted with a CCS process using the material. Their screening showed a theoretical limit to the minimum parasitic energy (~ 750 kJ kg^{-1} CO_2^{-1}) that can be obtained with zeolite and zeolitic imidazolate framework (ZIF) type materials.

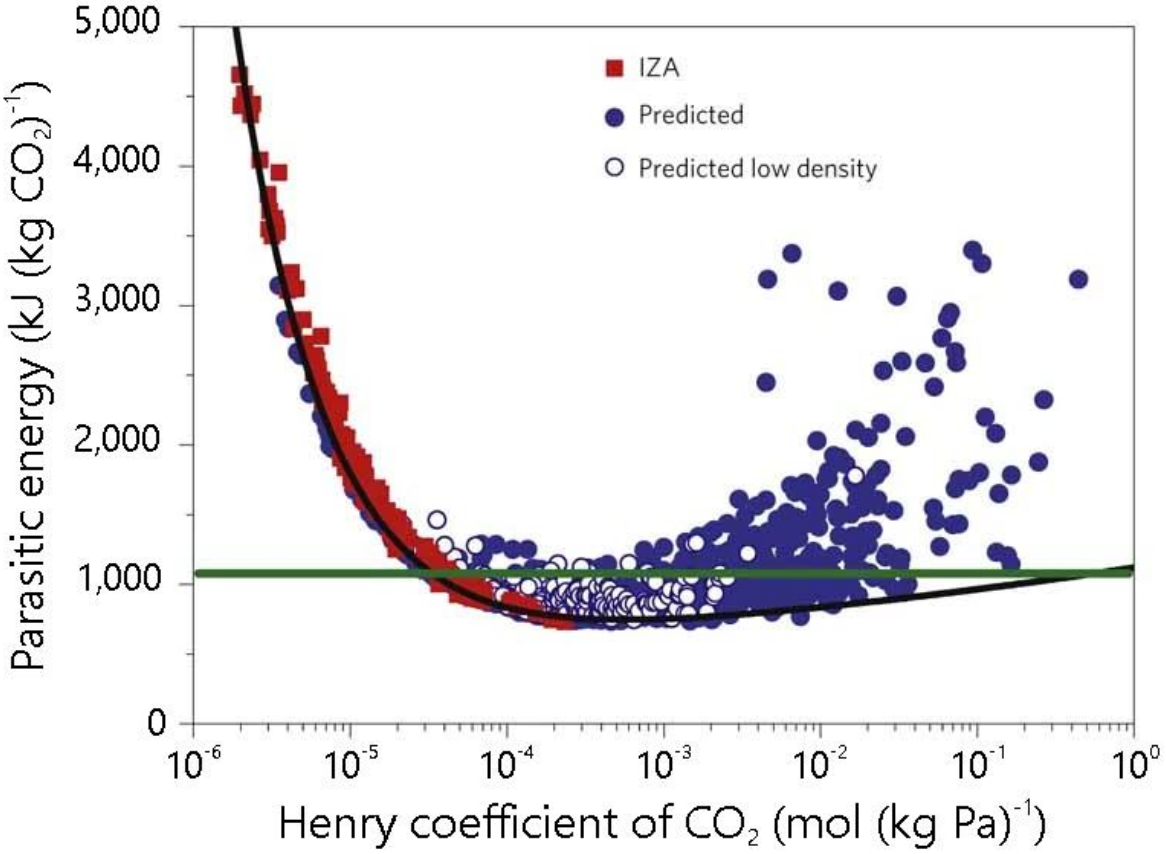

Figure 11: Large-scale in silico screening of theoretically predicted (●) and experimental (■) zeolite structures by Lin et al. The Henry coefficient can be obtained from the CO_2 adsorption isotherm for each material; at sufficiently low pressure the Henry coefficient multiplied by the pressure gives the number of adsorbed molecules. The horizontal green line gives the parasitic energy of the current monoethanolamine (MEA) technology, i.e. the energy penalty imposed through their use in post-combustion CO_2 capture, and the black line is the minimal parasitic energy observed for a given value of the Henry coefficient in the all-silica structures. These results show how large-scale theoretical studies can optimize future materials design efforts. Figure reproduced with permission from [483]*, copyright (2012) Springer Nature.*

Several other studies have also been performed on similar framework materials, albeit on smaller sets, with some comparison between theoretical and experimental results for CO_2 uptake [484]–[486], along with high-throughput synthesis methods being used to find novel ZIF materials for CO_2 capture [487]. The group of Duan et al. has focused on lithium-based oxide materials for high-temperature CCS applications, using density functional theory (DFT) and phonon calculations to determine the carbonation reaction thermodynamics of these materials, and comparing them to tabulated experimental data [78], [468], [488]. Another study looked at a set of potential magnesium-based ternary oxides Mg_2BO_4 (B = Si, V, Ge) for use in pre- or post-combustion CO_2 capture, finding that the critical carbonation temperature decreased with the increasing electronegativity of the B site [489]. Other studies have also outlined a possible screening process based on theoretical DFT and phonon calculations to search for suitable materials with $T_{carbonation}$ < 300 °C given a large starting set, with screening performed on smaller sets of alkali-based oxides [490], [491]. The limitation of these studies is that they are applied to a relatively small number of materials, many of them already well known

experimentally as being promising compounds for CO_2 capture.

The recent creation of large, publicly accessible databases of DFT-calculated inorganic materials such as the Materials Project [492], OQMD [493], [494], AiiDA [495], AFLOW [496], the Computational Materials Repository [497] and others made larger materials discovery efforts possible for the first time, being able to consider tens of thousands of materials at a sufficiently advanced level of DFT accuracy to predict material properties in silico. The first screening to utilize such databases for CO_2 capture was that of Dunstan et al. [498], where data from the Materials Project was used to simulate carbonation enthalpies of thousands of potential materials and subsequently to calculate the energy penalty that would arise from their use in an industrial CCS process. The study utilized the construction of open phase diagrams in the Materials Project, which considered the effect of a changing CO_2 chemical potential (equivalent to changing temperature or CO_2 partial pressure) on the phases present to efficiently enumerate all possible carbonation reactions, and select for energy penalty, stability with respect to p_{O2}, and gravimetric CO_2 uptake capacity. In total 640 compounds were found to reversibly react with CO_2 in a temperature range suitable for high-temperature CO_2 absorption, with several compounds chosen for further experimental testing which validated the CO_2 absorption properties output by the screening. This screening motivated further experimental studies [499] that found several new materials, such as Li_5SbO_5, which showed excellent CO_2 cycling stability, and the screening results are publicly available as a reference and starting point for future exploration.

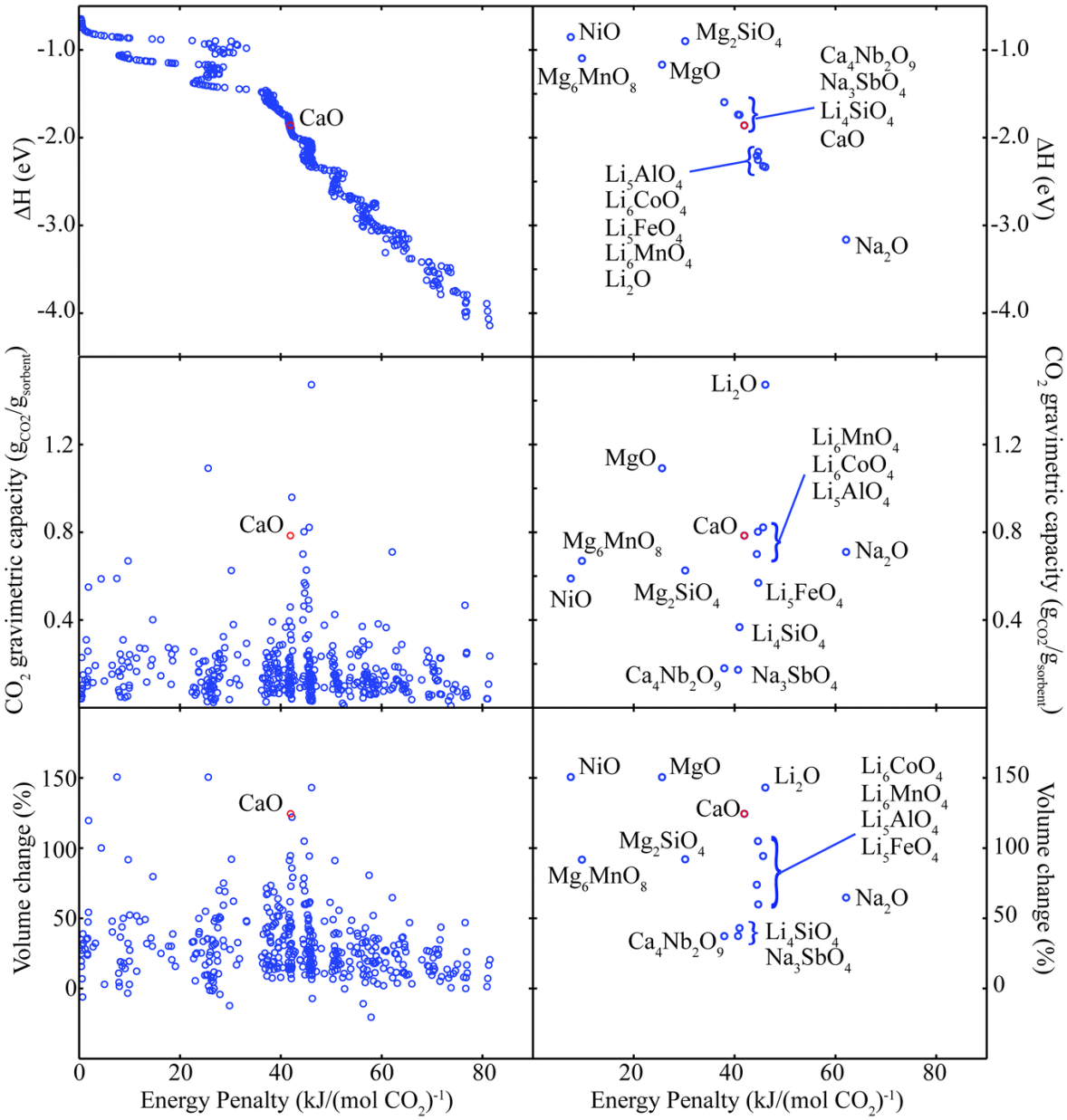

Figure 12: Overview of results from the screening of the Materials Project database for compounds that undergo carbonation. Each data point represents the carbonation reaction for each distinct compound with the most negative ΔH. The calculated energy penalty, Ep, for each reaction is plotted against $\Delta H_{carbonation}$ (top), CO_2 gravimetric capacity (middle) and volume change (bottom). The plots on the left are for the complete 640 distinct compounds in the screening, and the plots on the right are for specific compounds of interest. Figure published by The Royal Society of Chemistry [498].

Apart from theoretical databases, there are also many experimental data repositories such as the NIST-JANAF thermochemical tables [500], NASA Glenn Research Center [501] or Barin and Knacke's tables [502], or commercial software packages [503], [504] to use as the basis for determining promising candidate materials for CO_2 capture. Usually, these databases give very similar results, but in specific cases, such as for the MgO-$MgCO_3$ system, can differ significantly (Section 2.1). Venkatramen et al. [505], [506] used the NIST ionic liquid database as the main source for a large screening of ionic liquids (ILs) for use in CO_2 absorption, compiling properties for over 2600 ILs and finding a number of materials comparable in

performance to liquid amines for CCS and also for use in CO_2/H_2S gas separation [507]. Another study used experimental databases (as well as the Materials Project) as the input for a model chemical looping air separation (CLAS) power plant to perform a parameter sweep of relevant thermodynamic properties, identifying a number of previously unexplored oxide materials which were particularly promising for future use [508].

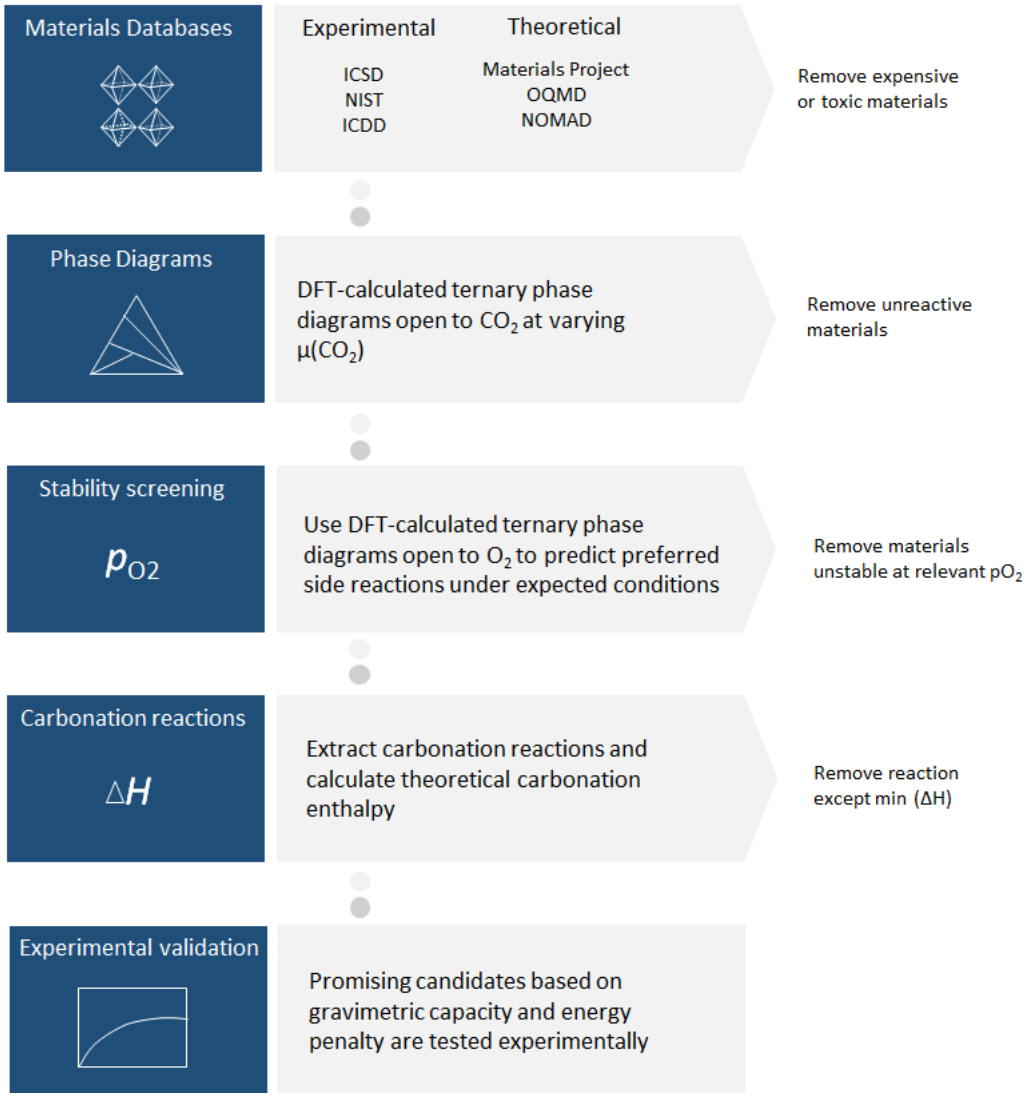

Figure 13: Overview of in silico screening process for novel CO_2 absorption materials, based on the work of Dunstan et al. [498]. *Firstly, materials data are extracted from relevant experimental and theoretical databases, discarding materials containing expensive or toxic elements. Then ternary phase diagrams are constructed for each of the remaining materials, open to CO_2, which outputs predicted carbonation reactions. Once any unreactive materials are removed, a further round of phase diagram construction, this time open to O_2, allows the prediction of any likely side reactions that would prevent the use of the material for CO_2 absorption. Finally, the lowest reaction enthalpy (most negative) for each remaining material is selected, and ranked based on its corresponding gravimetric capacity and energy penalty.*

5 Mechanistic insights into parameters influencing CO_2 absorption and desorption

In order to further improve and optimize materials for CO_2 absorption, advances are needed both in the fundamental understanding and in the application of novel characterization techniques aimed at observing structural and morphological changes during carbonation. The first parts of this section explore a number of recent examples of in situ experimentation applied to CO_2 absorption, while the latter parts explore important concepts linked to sorbent performance, including ionic conduction, crystallite size and facets and alternative reaction pathways.

5.1 In situ experimental methods for new mechanistic insights

The majority of experimental studies on CO_2 capture materials use a handful of analytical methods, with thermogravimetric analysis, N_2 sorption measurements and scanning electron microscopy being the most common ones. While these techniques are suitable for routine characterization, the observation of subtler structural and morphological features require additional techniques that have only started to be employed. However, ex situ studies are inherently limited as they cannot probe the structure and morphology of the sorbents in their active state (i.e. under reactive conditions). Hence, the development and use of in situ/operando methods is crucial to observe the evolution of the sorbent under real operating conditions. This section is intended as an overview of some of these recently introduced techniques to the fields of CCS and the insights they have uncovered when applied to CO_2 capture materials aiming at connecting composition, structure, morphology and performance.

5.1.1 X-ray diffraction and other synchrotron-based X-ray techniques

Synchrotron radiation offers extremely intense X-rays, allowing them to penetrate a wide variety of materials to facilitate the practical use of a wide range of in situ sample environments, with the additional capability of selecting the incident radiation to a specific energy range. This allows a wide range of both ex and in situ analyses of the structure and morphology of potential sorbents for CO_2. X-ray diffraction (XRD) is one of the most used techniques, with the brilliance of synchrotrons enabling high time resolution, in situ monitoring during CO_2 absorption and desorption. More recently, further synchrotron-based techniques, such as X-ray absorption spectroscopy (XAS) [509], X-ray total scattering/pair distribution function (PDF) analysis [177], [510], [511] or small angle X-ray scattering (SAXS) [512] have been applied to CO_2 sorbent research (or relevant materials) to obtain structural information and mechanistic insights on phase transformations.

The work of Cova et al. [472] has focused on using in situ XRD to track the carbonation reaction, observing a multi-step process for the carbonation of Li_5FeO_4. In the initial step, in

the temperature range 100 – 650 °C, Li_5FeO_4 and CO_2 forms Li_2CO_3 and $LiFeO_2$. Above 300 °C the carbonation of $LiFeO_2$ to Li_2CO_3 and Fe_2O_3 was observed; the reverse reaction was activated above 550 °C, re-forming $LiFeO_2$ and releasing CO_2. Similar observations were made for the carbonation of Li_4SiO_4, where the intermediate carbonation products of Li_2SiO_3 and Li_2CO_3 first formed at ~ 645 °C before the complete conversion of Li_4SiO_4 to SiO_2 and Li_2CO_3 occurred only beyond ~ 700 °C [513]. Carbonation of Li_8SiO_6 initially results in the formation of Li_4SiO_4 and Li_2CO_3, before eventually converting to Li_2SiO_3 and Li_2CO_3 [514]. In situ XRD allows these complex multistep reactions to be observed, finding the specific carbonation temperature at which the total CO_2 absorption is maximized.

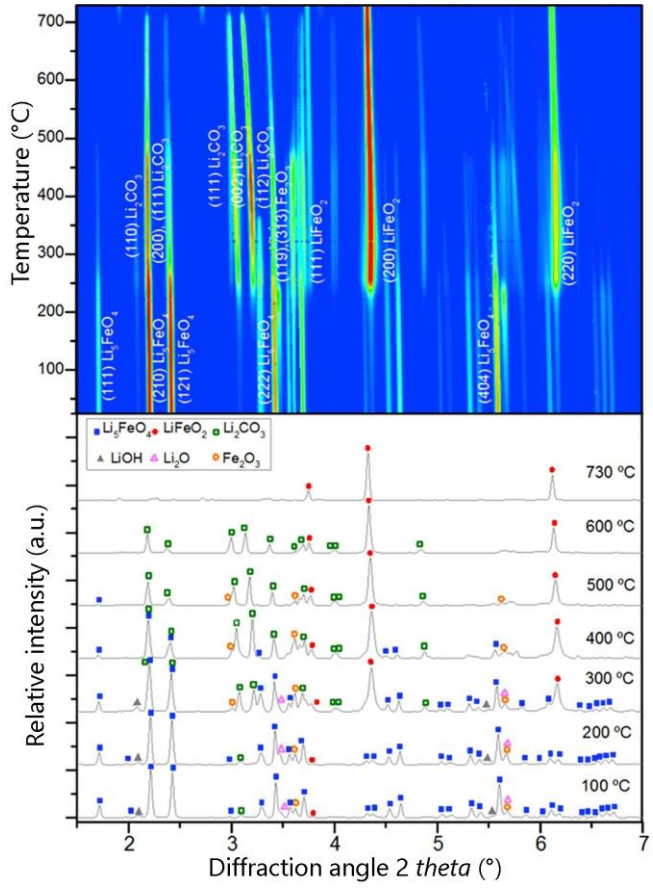

Figure 14. In situ XRD diffractograms tracking phase changes during the carbonation of Li_5FeO_4. Data was acquired using a wavelength of 0.15895 Å. The use high resolution synchrotron XRD data enables phase fractions to be tracked continuously in real time, even with several competing phases. Figure reproduced with permission from [472]*, copyright (2018) Elsevier.*

Molinder et al. [515] utilized in situ XRD in the temperature range 25 – 800 °C to analyze the effect of steam on the carbonation of CaO, $Ca(OH)_2$ and partially hydrated CaO. Firstly, it was shown that $Ca(OH)_2$ carbonates directly to $CaCO_3$ without any oxide intermediate, and transforms more readily to $CaCO_3$ than CaO. Using synchrotron radiation, it was possible to measure accurately the microstrain present in $CaO/Ca(OH)_2$ mixtures from an analysis of peak broadening. Partially hydrated CaO was found to experience strain that is an order of magnitude larger than for pure $Ca(OH)_2$. This increased strain was postulated to be the main driver for the

increased reactivity towards carbonation under steam, with the interfacial stress between the CaO and $Ca(OH)_2$ phases possibly lowering the activation energy for carbonation. Further in situ synchrotron studies on the CaO system by Dunstan et al. [516] analysed the formed phases as a function of depth from the surface of a CaO pellet exposed to the reactant gas stream, showing that the addition of steam led to the formation of $CaCO_3$ that was more evenly dispersed throughout the particle. This finding supported earlier results of Molinder et al. [515] in showing incomplete carbonation for CaO under dry atmospheres in the same time frame (see Section 2.4.2 for more details on the effects of steam on the carbonation of CaO).

In situ XRD can also give insight to specific structural evolution during carbonation. Lundvall et al. [517] employed the technique to monitor CO_2 absorption by dawsonite, $NaAl(OH)_2CO_3$, which forms a poorly crystalline intermediate phase upon carbonation at ~ 280 °C. Monitoring of key Bragg reflections revealed reversible shifts in peak position upon absorption and subsequent desorption, related to swelling and shrinking of the interlayer spacing in the crystal structure, their evolution corresponding to mass changes observed by TGA. These studies demonstrate that in situ XRD can provide complementary information to that of more commonly used techniques such as TGA, and provide insights that would not be possible without its use.

Rietveld refinement of XRD data allows for not only a precise determination of particle size, but in situ XRD also enables tracking of the crystallite size during the carbonation reaction, a key concept that underpins the transition from a rapid surface reaction to a slower diffusion-controlled process with increasing reaction time. Biasin et al. [97] used in situ synchrotron XRD to track the evolution of the $CaCO_3$ crystallite size during carbonation, finding that a local maxima in particle size correlated with the change in the rate of carbonation. Furthermore, by conducting experiments under different conditions and with different starting CaO crystallite sizes, they were able to show that this critical crystallite size correlates directly with temperature (ranging from 12 – 282 nm for different carbonation temperatures between 450 – 750 °C), and inversely with the starting particle size of CaO.

Small-angle X-ray scattering is particularly well suited to analyze microstructural properties of materials such as particle size and strain, and was recently applied for the first time to $CaCO_3$-based sorbents under carbonation and calcination conditions. Benedetti and co-workers [512] utilized small and ultra-small X-ray scattering (SAXS/USAXS) coupled with wide-angle X-ray scattering (WAXS) to observe changes in pore size distribution and surface area of a number of CaO-based samples calcined under vacuum at different temperatures and times, as well as observing the changes produced upon subsequent carbonation. Their results agreed well with

observations from more commonly used N_2 sorption measurements, as well as showing that the coalescence of micropores is the primary process occurring during sintering of $CaCO_3$ through measurement of pore correlation lengths as a function of calcination time and temperature. Their results show the power of this technique to extract microstructural information in situ, and it is hoped that these techniques will be applied more frequently to further materials in the future.

5.1.2 X-ray photoelectron spectroscopy

X-ray photoelectron spectroscopy (XPS) is a surface sensitive technique, compared to the information about bulk phases obtained from XRD. It is able to identify both the identity and oxidation state of elements present, as well as giving further information about those elements' bonding environments, making it perfectly suited to in situ observation of surface species formation during carbonation. It is also useful for materials with secondary metal oxides present that have catalytic activity, being able to track the change in oxidation state during reaction.

Sun et al. used XPS to study the formation of oxygen vacancies in dual functional Ru/CeO_2-MgO materials designed for simultaneous regeneration and conversion of CO_2 in a single reactor, finding that increases in Ru loading lead to increased catalytic activity [518]. Another study focused on core-shell materials composed of CaO, NiO and several calcium aluminate phases for use in sorption-enhanced steam methane reforming (SESMR), using XPS to identify which phases were present at the surface of the synthesized particles [519]. XPS was used to track the cause of higher CO_2 absorption of CeO_2-modified CaO/$Ca_{12}Al_{14}O_{33}$ composites for SESMR [520]. The addition of CeO_2 led to changes in the oxygen 1s orbitals, with a shift to the highest O 1s binding energy for the modified particles compared to the unmodified material denoting the connection between stronger oxidation ability at the surface (i.e. a higher binding energy) with increased CO_2 absorption. Further studies of CaO/NiO particles for methane reforming also used XPS to identify two distinct Ni sites, one corresponding to NiO interacting with CaO, and one without interaction [521]. These two phases aligned well with the observed temperature-programmed reduction curves, which all showed the presence of two separate reduction peaks.

5.1.3 Infrared and Raman spectroscopy

Infrared (IR) and Raman spectroscopy can be complementary to XRD in their ability to distinguish between amorphous and crystalline phases, and their ability to identify structurally similar solid polymorphs of the same material, both of which are key to understanding sample composition both before and after carbonation. Both techniques are also sensitive to different surface species that form during reaction. The choice of which technique to use is dependent

on the specific chemical bonds within the species one wishes to observe, and whether the given bonds are IR or Raman active or inactive.

FTIR, CO_2-TPD, and molecular modelling have been applied to describe the interaction between CO_2 and MgO [124], [126], [131], [136]–[138], [522], [523], but have not often been used to investigate CaO-based sorbents during CO_2 sorption owing to the high carbonation temperatures involved (> 600 °C). During carbonation, the acidic CO_2 molecule interacts with the active basic sites, i.e. undercoordinated oxygen atoms, on the MgO surface [31], [51], [127], [129]. Gregg et al. [124] studied adsorption capacities between -98 °C and 500 °C and measurements below room temperature revealed a fast initial uptake due to physisorption (assigned to the appearance of bands in the IR spectrum between 2300 – 2400 cm^{-1}) followed by a slow uptake owing to chemisorption (corresponding to bands in the 1200 – 1700 cm^{-1} region). At higher temperatures, physisorption decreased and a higher fraction of the uptake resulted from chemisorption. Several researchers have proposed that CO_2 adsorption at room temperature was associated with the formation of a unidentate surface coverage on the sorbent, limiting further CO_2 capture at low temperatures [31], [124], [524]. Meixner et al. [525] utilized laser-induced thermal desorption of a MgO single crystal to measure the CO_2 surface area coverage on MgO(100) at temperatures between -173 °C and -140 °C to probe the validity of this theory. Their results showed that the coverage of MgO with CO_2 did not increase further after a fast, initial uptake, owing to an equilibrium surface coverage. Their investigation confirmed further that the CO_2 coverage decreased with temperature. FTIR has also been used routinely to characterize the formation of carbonates in alkali-promoted MgO [160], [436], [526], and in situ transmission FTIR was used to compare the relative formation of different species (bicarbonate or bidentate carbonate) on the surface of mesoporous MgO versus commercial MgO; whereby the mesoporous MgO sample was characterized by a higher number of acidic surface sites (determined from the comparison of the relative intensity of bands at 1510 and 1410 cm^{-1} assigned to the interaction of gaseous CO_2 with basic surface oxygen sites) [428]. In situ FTIR showed that the formed bicarbonate is stable up to 150 °C, while bidentate carbonate is removed at 300 °C. On the other hand, unidentate carbonate is more stable and is only removed at 500 °C [126]. An example of the use of ex situ Raman is the work by Fricker et al [527], who used Raman, XRD and TGA to study the effect of H_2O on the carbonation of $Mg(OH)_2$. While the XRD patterns showed an increasing disorder in the formed carbonates with increasing p_{H2O} during carbonation, Raman spectroscopy of the same samples was used to quantify the ratio of the different magnesium carbonate polymorphs that formed. The disorder

was attributed to the formation of a mixture of magnesite and nesquehonite, while at the highest p_{H2O} used only pure magnesite was observed.

In situ Raman spectroscopy of various modified lithium zirconates [528] was able to directly observe the formation of molten carbonates during carbonation at 500 °C through the observation of a shift in wavenumbers for the CO_3^{2-} stretching band. In the case of K-doped lithium zirconate the co-existence of a molten Li-K carbonate eutectic, alongside Li_2CO_3 in the solid phase was observed. The formation of a molten phase had been hypothesized to lead to an enhanced ionic mobility and in turn a higher CO_2 absorption [450]. Very similar observations were made in (Li,Na)ZrO_3 [529], and in K-doped Li_4SiO_4 [530]. A further study utilized in situ Raman spectroscopy to probe the crystallization of a range of relevant carbonate phases including calcite and magnesite. It was observed that both amorphous and crystalline phases can act as precursors for nucleation. In particular magnesite only appeared after the prior formation of other crystalline precursors such as hydromagnesite [531].

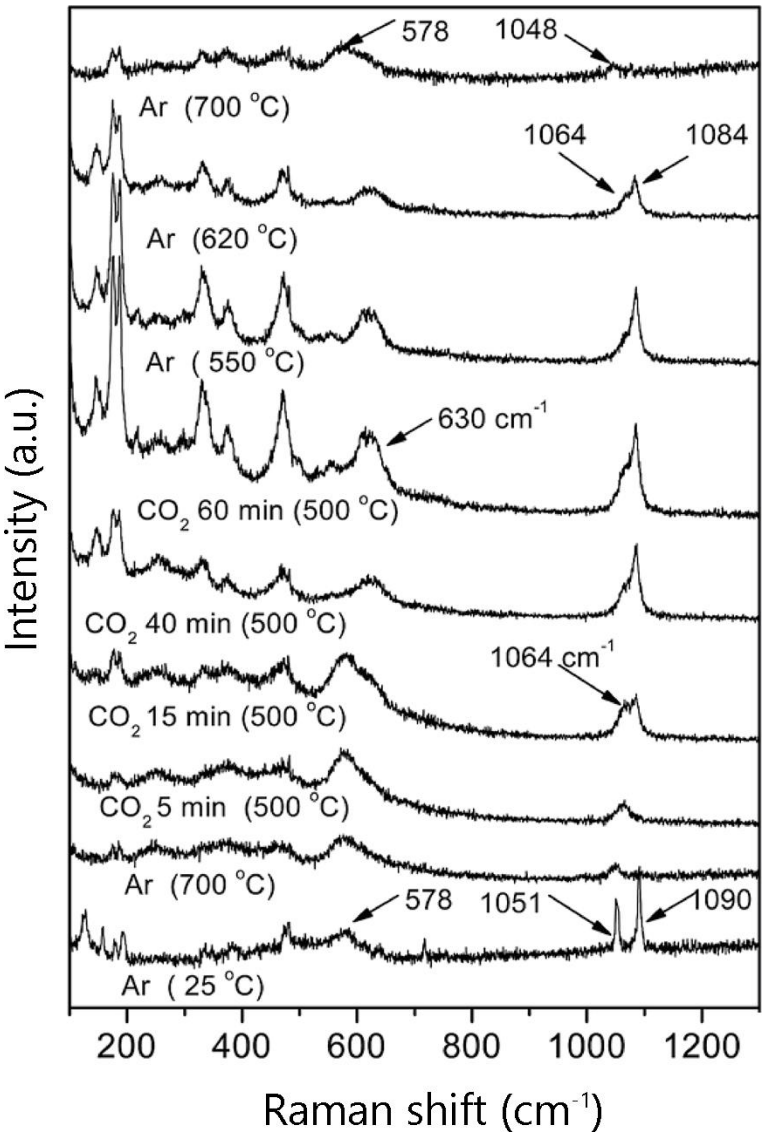

Figure 15. Operando Raman spectroscopy of K-doped Li_2ZrO_3 during a complete carbonation and regeneration cycle. The unique advantage of Raman spectroscopy, its ability to distinguish between solid and molten phases, is clearly displayed in the data: The two peaks at 1064 and 1084 cm^{-1} that appear during carbonation indicate the formation of a molten K_2CO_3-Li_2CO_3 mixture and solid Li_2CO_3, respectively. Figure reproduced with permission from [528]*, copyright (2016) The Royal Society of Chemistry.*

5.1.4 Solid state nuclear magnetic resonance (ssNMR)

One technique that is particularly well suited to study the connection between atomic structure and ionic mobility of specific atomic species is solid-state nuclear magnetic resonance (ssNMR) spectroscopy [532]. The development of probes that are able to operate over the temperature range of interest for CO_2 capture has meant that gleaning specific mechanistic information at realistic temperatures is possible [533], [534]. There have been a number of studies using ^{7}Li ssNMR to elucidate mechanisms of Li ion mobility in different materials. Indris et al. [535] studied $LiAlO_2$ using variable temperature ssNMR to probe Li^+ ionic motion over a wide range of correlation times, validating earlier DFT calculations of rates of Li ion diffusion and activation energies (found to be ~ 1 eV in this case). These techniques were then applied to CO_2

capture by Dunstan et al. [536] to study the lithium and oxygen ion dynamics in Li_2CO_3, a common component formed in all Li-based CO_2 capture materials. Understanding Li ion dynamics in this phase is crucial, given that it forms on the surface of sorbent particles during initial carbonation and determines the rate of reaction during the slower diffusion-controlled stage. Enhanced Li ion mobility at high temperatures (550 – 650 °C) appeared to correlate with the onset of a more rapid CO_2 absorption in the diffusion-controlled stage, and furthermore that this enhanced Li ion mobility relied on the activation of cooperative CO_3^{2-} rotational motion at lower temperatures (100 – 200 °C).

Later studies by the same authors sought to investigate the effect of aliovalent doping on the structure, ionic mobility and CO_2 absorption, as discussed in the previous section. Samples of Li_2ZrO_3 were doped with 5 % Nb, Ta and Y and analyzed with both ssNMR and TGA [482]; doping with higher charge cations (Nb, Ta) led to the formation of Li ion vacancies and a comparable rate of Li ion hopping as evidenced by measurements of NMR linewidths and relaxation rates, while doping with lower charge cations (Y) saw an increase in activation energies for lithium ionic motion following the formation of Li ion interstitials, or O vacancies. However, all doped samples showed a reduced CO_2 uptake capacity compared to pristine Li_2ZrO_3, underlining the importance of optimizing CO_2 capture materials beyond only the single parameter of ionic mobility.

For CaO- and MgO-based sorbents, (solid state) NMR has not been used very often, although it can be very helpful in identifying the nature of phases that are amorphous or exist in small quantities such that XRD techniques cannot be used. To understand the deactivation of their CaO-based sorbents, Kim et al. [385] used ^{27}Al NMR and observed the dynamic transformation of the calcium aluminate phases during cycling (see also section 3.1.2.2). ^{23}Na NMR helped to reveal the Na environment of Na_2CO_3-doped CaO when only very small amounts of dopant (i.e. 0.15 mol%) were used [329]. For AMS-promoted sorbents, Kwak et al. [422] used ^{23}Na, ^{25}Mg, and ^{39}K NMR to probe the state of the respective atoms in alkali metal carbonate-promoted MgO sorbents and compared them with reference double carbonates. The formation of different Mg-double carbonates at the beginning of the carbonation reaction and their stability were found to play an important role in the two-step absorption of CO_2.

We thus expect NMR techniques to become increasingly important to probe the influence of dopants or promoters on CO_2 sorbents where conventional characterization techniques fail to yield conclusive results.

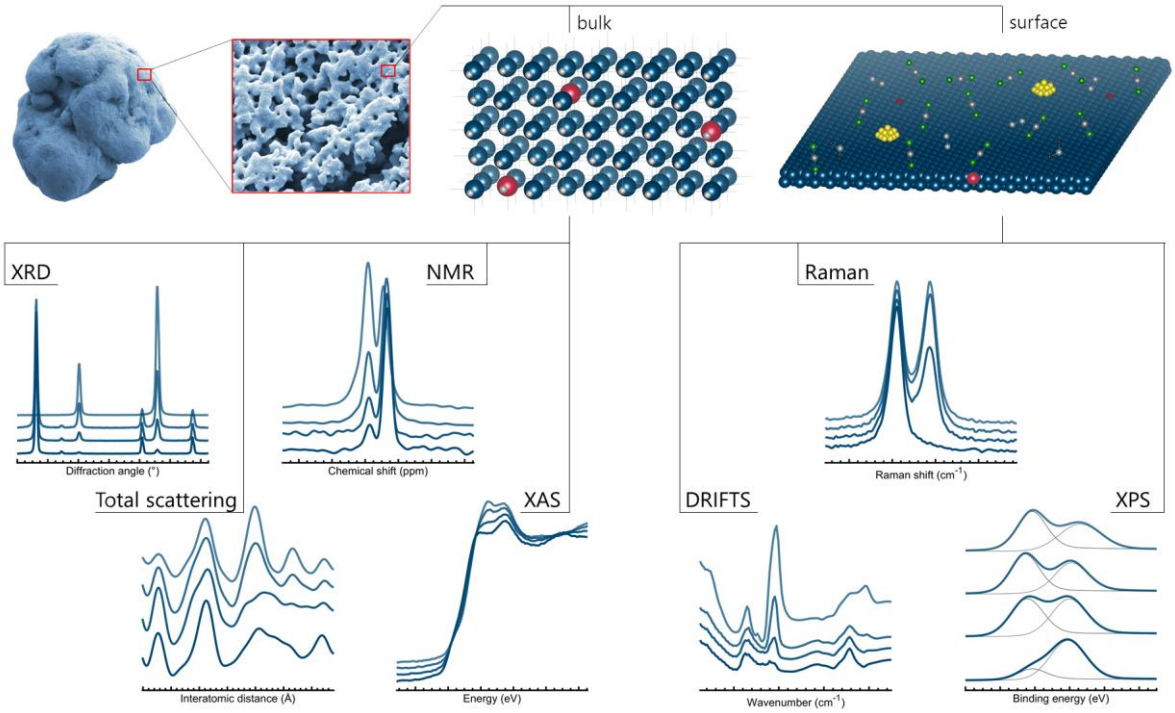

Figure 16: Overview of some advanced experimental techniques for the characterization of CO_2 sorbents.

5.2 Effect of crystallite size, orientation and morphology

The initial crystallite size and exposed facets play an important role on the carbonation of metal oxides. In the following, we review how modifications to crystallite size, orientation, exposed facets and overall morphology affects the CO_2 capture.

As noted in Section 2.2, several experimental works have reported an inverse proportionality between the crystallite size of CaO and its CO_2 uptake [97], [101], [277], [281], [537]–[539]. For example, Valverde et al. [537] determined that modifications to the crystallite size of CaO, achieved by exposing CaO to pretreatment steps, lead to differences in its CO_2 capture performance. Benchmarking with natural limestone, the authors found that ball-milled samples with a reduced crystallite size had a higher CO_2 uptake compared to raw limestone and pre-annealed samples with a large crystallite size. Further CO_2 uptake measurements of ball-milled samples have also been performed under harsh calcination conditions of 900 °C, 70 % CO_2/ 30 % air (v/v) [539]. The ball-milled samples were observed to enhance the rate of calcination, but smaller crystallites also sinter faster ("melting-point depression"), leading to a worse performance over multiple cycles when the regeneration is performed in a CO_2 atmosphere (Figure 17). It was concluded that overall obtaining small crystallites is beneficial, but new methods are required to modify CaO such that its nano-crystallinity is retained (e.g. through the addition of structural stabilizers [540], as is described in detail in Section 3.1.2, or regeneration steps [541]).

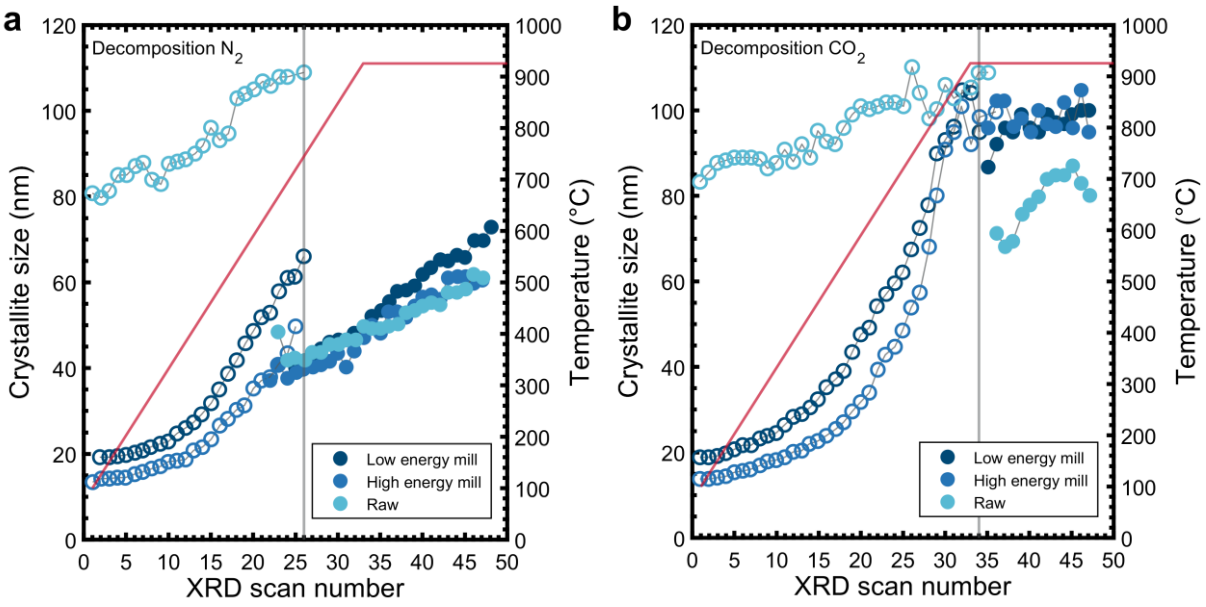

Figure 17. Crystallite size evolution estimated from in situ X-ray diffraction measurements of $CaCO_3$ and CaO during regeneration in an atmosphere of (a) N_2 or (b) CO_2. A heating rate of 10 °C/min was used up to the isotherm at 925 °C. The raw untreated limestone is compared to milled limestone at high and low energy milling intensities. The grey vertical lines highlight the $CaCO_3$ decomposition temperature in each case. Empty circles (○) indicate $CaCO_3$ and filled circles (●) indicate CaO. Figures (a) and (b) were reproduced with permission from [539]*, copyright (2016) American Chemical Society.*

Different to that, thermal pretreatment of CaO has often been employed to improve the cyclic stability of the sorbents [268], [282], [542]; the principal idea behind this approach is that the morphology of the sorbent and the pore network obtained upon an extended initial calcination step at high temperature are largely maintained through cycling ("hard skeleton"), similar to metamorphic rocks such as marble [543], [544]. Thus, although the initial CO_2 uptake is lower after the thermal pretreatment owing to the larger crystallites of the sintered CaO, the CO_2 uptake capacity after a large number of cycles may be improved [545]. The optimum conditions of the thermal pretreatment step depend on the chemical composition of the sorbent [546].

Considering the influence of surface orientation on the CO_2 capture, MgO(111) has shown to have a higher CO_2 uptake than MgO(100) and even nanosized (high surface area) MgO [547]–[550]. In fact, the type of the exposed facet appears to overrule the effects of surface area. By controlling the orientation of the exposed facets, Mutch et al. [547] found a 65 % increase in CO_2 uptake, which is surprising considering that the surface area of the better CO_2 sorbent was 30 % lower. The actual uptake was 56 mg g^{-1} for synthetic MgO(111) with a surface area of 154 m^2 g^{-1} compared to 34 mg g^{-1} for nanosized MgO with a surface area of 227 m^2 g^{-1}. It is worth noting that the highest uptake of 56 mg g^{-1} obtained at 35 °C by MgO(111) is significantly lower than the CO_2 uptakes achieved by promoted MgO, e.g. ~ 650 mg g^{-1} at 350 °C [427]. Nonetheless, the results confirm that the exposed facet plays an important role for the interaction between the CO_2 molecule and the Mg and O atoms at the surface. The MgO(111) facet has alternating layers of O and Mg atoms at the surface, where acidic CO_2 can react

favorably with the basic O^{2-} [547]. On the other hand, CO_2 shows little interaction with terraces of the MgO(100) facet, and reacts only favorably at edge or corner sites [137], [138]. These findings obtained for MgO model surfaces are worth considering when aiming to elucidate the promoting mechanism of molten salts on MgO. The ionic (charged) molten salts will have different electrostatic interactions with the MgO surface depending on the exposed facets [547], [551]. For this reason, new efforts utilizing molecular dynamics simulations that consider the interaction between MgO, CO_2 and molten salts would be valuable to understand the promoting effect of molten salts of MgO-based CO_2 sorbents.

Specific crystal structures can impact directly ionic transport and hence the overall CO_2 uptake rate. One such design is that of pseudo-one-dimensional materials, such as nanowires, which maximize the specific surface area. For example, Akram et al. [464] synthesized Li_6WO_6 nanowires to yield a high surface area material and to reduce the limitations of the formation of a bulk layer of Li_2CO_3. The Li_6WO_6, nanowires showed a very rapid CO_2 uptake at low temperatures (7.6 wt% at 30 – 40 °C in 1 min). Similarly, solvo-plasma techniques have been employed to synthesize Li_4SiO_4 nanowires that equally demonstrated very fast rates of CO_2 uptake reaching 0.22 g g^{-1} min^{-1} in the temperature range 650 – 700 °C [552]. Further studies utilizing a molten-shell and tailored microspheres in Li_4SiO_4 nanoparticles further showed how morphology can influence carbonation kinetics [553], [554].

Another approach to yield different morphologies of the sorbent particles is to use different precursors and precursor treatments. Early on, the CO_2 uptake of CaO derived from different calcium-based precursors, including calcium hydroxide ($Ca(OH)_2$), calcium propanoate ($Ca(C_2H_5COO)_2$), calcium acetylacetonate hydrate ($Ca(C_5H_7O_2)_2$), calcium acetate ($Ca(CH_3COO)_2$), calcium d-gluconate monohydrate ($Ca(C_6H_{11}O_7)_2 \cdot H_2O$), calcium L-lactate hydrate ($Ca(C_2H_5O_3)_2 \cdot H_2O$), calcium citrate tetrahydrate ($Ca_3(C_6H_5O_7)_2 \cdot 4H_2O$), calcium nitrate tetrahydrate ($Ca(NO_3)_2 \cdot 4H_2O$), calcium formate ($Ca(HCOO)_2$), calcium oxalate (CaC_2O_4), and calcium 2-ethylhexanoate, has been compared [286], [361], [555]–[559]. Depending on the type of precursor used, the transition to CaO occurs in several steps; the transition route affects the morphology of the sorbent (including surface area and pore volume distribution) and the crystallite size of the CaO, which all influence the CO_2 uptake performance of the resulting CaO. The combination of different precursors and pretreatment conditions (i.e. temperature, heating rate, p_{CO2} and p_{H2O}) provide rich opportunities to tune the physical properties of the CaO. Another popular approach to enhance the cyclic CO_2 uptake of CaO-based sorbents was to treat them with organic acids, e.g. citric acid or formid acid, which resulted in increased surface areas and pore volumes [560]–[564]. However, no significant long-term stabilization of

the morphology was achieved in most of these studies, and owing to the high cost of the acids this approach has not been followed up recently [565].

A peculiar, yet underexplored precursor for CaO is amorphous calcium carbonate (ACC), despite its high surface area (> 350 m^2 g^{-1}) and porosity [566]–[568]. Amorphous calcium carbonate (ACC) has been synthesized through different approaches, including mechanochemical methods (i.e. ball milling and stabilization by Na_2CO_3 [511] or MgO [569]) or solvochemical approaches [568].

Given the most technologically advanced CO_2 capture system in use today is the liquid amine system [570], finding new CO_2 capture sorbent materials that function as liquids during capture is particularly desirable as existing reactors can potentially be used. Typically, oxides stay as solids during carbonation and calcination, but there are some oxide-based systems that behave differently. The alkali metal borate system $A_xB_{1-x}O_{1.5-x}$ (where A is an alkali metal) presents an interesting example to understand the difference between solid to solid, liquid to solid and liquid to liquid carbon dioxide capture. Hatton and co-workers explored the effect of the choice of the alkali metal and the alkali:borate ratio on CO_2 absorption [571]–[573]. A number of sodium borates such as $Na_{0.75}B_{0.25}O_{0.75}$ that are liquid at ~ 650 °C were identified. The sodium borates were able to capture CO_2 forming $NaBO_2$ and Na_2CO_3, independent of reaction temperature or CO_2 concentration. Adding an equimolar amount of lithium ($(Li_{0.5}Na_{0.5})_{0.75}B_{0.25}O_{0.75}$) to the sodium borate resulted in both the oxide and the resulting carbonate to be in the liquid state; yielding a sorbent with moderate kinetics (10 min for complete conversion) and high capacity (0.35 g CO_2 g^{-1}).

5.3 Connection between ionic conduction and CO_2 absorption in lithium-based oxides

Atomic structure is of fundamental importance when considering rates of ionic conduction in a given material and designing materials with improved kinetics can result in improved CO_2 absorption. The earliest work in this respect was by Nair et al. [574], who compared the relative rates of CO_2 absorption for monoclinic and tetragonal phases of Li_2ZrO_3, the latter being stable only at temperatures below ~ 900 °C. They observed faster absorption rates for the tetragonal phase, citing its higher ionic conductivity, although they were unable to distinguish between the effects of crystallite size and atomic structure. Gomez-Garcia et al. [575] synthesized $LiFeO_2$ and $NaFeO_2$ (along with the Li-Na solid solution) in cubic ($LiFeO_2$), orthorhombic ($NaFeO_2$) and rhombohedral ($LiFeO_2$ and $NaFeO_2$) polymorphs, finding that the rhombohedral phases display the fastest carbonation rates at 750 °C. This corresponds to the structures where the alkali ions were in an octahedral coordination, whereas the phases with alkali ions in a

tetrahedral coordination displayed a stronger temperature dependence for carbonation, taking into account differences in composition.

One of the earliest papers outlining the direct connection between the rate of carbonation and the rate of ionic mobility was for Li_2ZrO_3 by Ida and Lin [576], who proposed a double-shell model for the absorption of CO_2. Firstly, a rapid surface reaction creates a solid layer of Li_2CO_3 covering the original Li_2ZrO_3 particles before a slower absorption step occurs, which depends on Li^+ and O^{2-} ions moving through the carbonate layer to continue reacting with CO_2. This model was used to extrapolate rates of O^{2-} conductivity based on experimental CO_2 absorption curves for K-doped Li_2ZrO_3, finding values in line with literature values in the region of $5 \cdot 10^{-6}$ – $5 \cdot 10^{-8}$ Ω^{-1} m^{-1} [450].

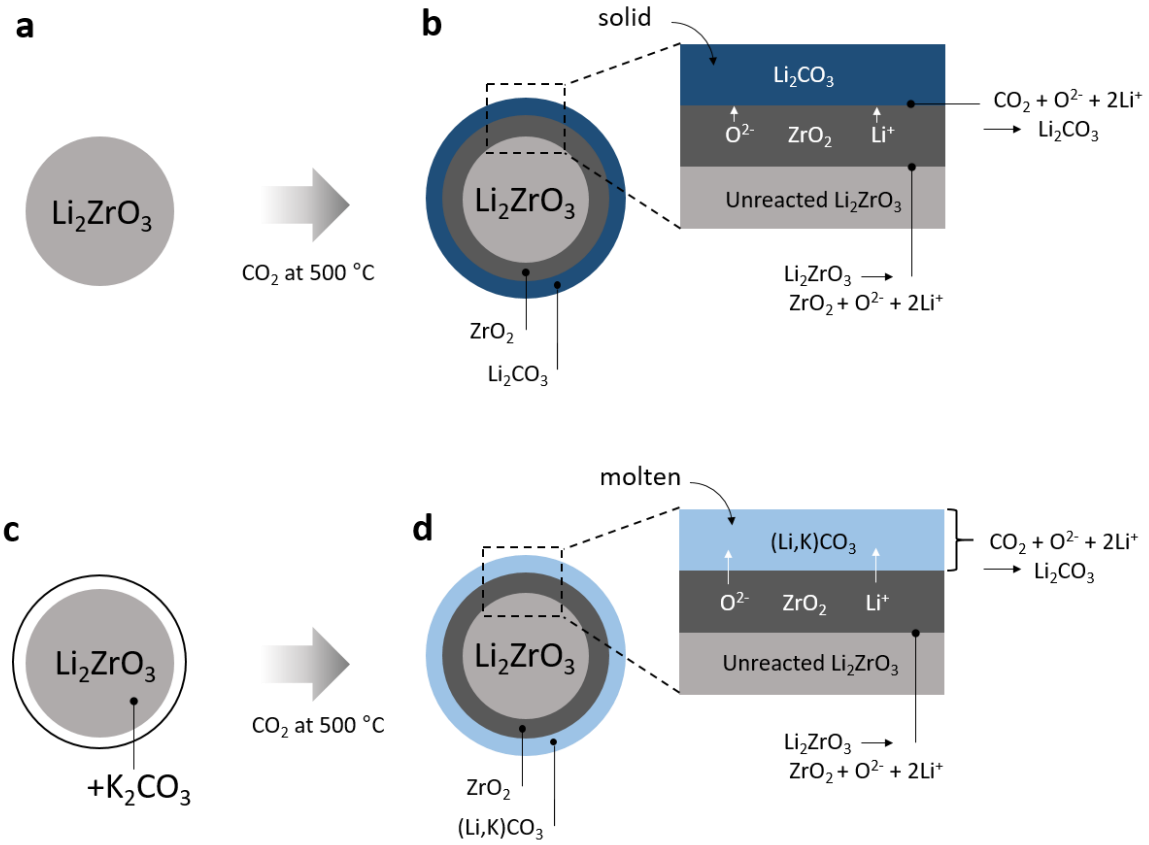

Figure 18. Double shell model of CO_2 absorption on Li_2ZrO_3 as described by Ida et al. After the initial carbonation of Li_2ZrO_3 (a), layers of Li_2CO_3 and ZrO_2 form around an unreacted core of Li_2ZrO_3 (a 'double shell') (b). Further reaction of the core material requires the transport of Li^+ ions from Li_2ZrO_3 through the outer layers, and subsequent O^{2-} or CO_3^{2-} transport from the atmosphere into the outer layer. Thus, the rate of reaction is limited by the rate of ionic conduction of the various ions through the component phases. The addition of a K_2CO_3 coating on Li_2ZrO_3 (c), after carbonation leads to the formation of a molten outer layer formed of a mixed potassium and lithium carbonate, enhancing CO_2 transport through dissolution into the molten layer (d). Figure was reproduced with permission from [576], *copyright (2003) American Chemical Society.*

Atomic substitution, either with other alkali ions or other elements, can produce a material with different thermodynamics of carbonation, lowering the operating temperature compared to the pristine material. Kwon et al. [577] synthesized samples of Li_4SiO_4 with Na substitution,

forming Li_3NaSiO_4 that was able to carbonate and regenerate at lower temperatures than unmodified Li_4SiO_4. Another study of doping of the Si site with Ge also found enhanced CO_2 absorption at temperatures < 450 °C, which was ascribed to lower barriers for Li ion diffusion caused by lattice expansion upon doping [478]. Similar effects have been seen for small amounts of alkali doping of the CaO-$CaCO_3$ system leading to changes in the sintering behavior, with ionic mobility being enhanced through the creation of defects in the crystal lattice (Section 3.1.1). Coating with other active materials can also enhance reactivity and capacity retention, as seen in Li_4SiO_4 sorbent particles coated with Li_2ZrO_3 [578].

Rather than doping existing materials to increase ionic conductivity, some studies have specifically targeted materials with unique atomic structural features that allow high intrinsic conductivity. Galven et al. [579] reported a novel material, Na_2TeO_4, which has a one-dimensional structure in which the Na atoms are located between $[TeO_4]_n^{2n}$ columns allowing for fast Na diffusion during carbonation in which the first step is Na^+/H^+ exchange. Structures that allow atomic extrusion (i.e. the movement of ions out of a single crystalline phase to form a secondary phase) also extend to three-dimensional systems, such as the Ba-containing garnet $Li_6BaLa_2B_2O_{12}$ that subsequently reacts with CO_2 to form $BaCO_3$ and a secondary perovskite phase. Unlike other CO_2 absorption materials that operate through Ba extrusion, such as $Ba_2Fe_2O_5$ [580] and $Ba_4Sb_2O_9$ [581], the garnet's transformation is not reversible; however the work shows that novel structural types can be an approach to generate optimal conduction properties without the need for further modifications such as aliovalent doping. In contrast, the excellent carbonation capacity retention observed for $Ba_4Sb_2O_9$ over 100 cycles [581] is in part attributed to a good O^{2-} ionic conductivity facilitating fast and reversible movement of Ba and O within a network of [SbO_x] polyhedra, which remains a stable framework throughout the entire reaction cycle.

In contrast to the lack of an effect of the presence of unburnt oxygen in the flue gas environment on the CO_2 uptake capacity of Ca and Mg-based sorbents (Section 2.4), many studies have observed improvements in the CO_2 absorption in Li-based sorbents linked to the addition of O_2 into the reactant gas stream – a phenomenon that also supports the role of ionic transport in the process. The common finding is that as diffusion of O^{2-} from the bulk sorbent to the surface is the main kinetic limiting factor for the formation of a carbonate phase, the addition of O_2 to the gas phase improves the availability of O_2 for carbonation, increasing the absorption rate and overall capacity. This effect was observed for a range of materials including Li_6WO_6 nanowires [464], Li_5FeO_4 [473] and Li_5AlO_4 [582], [583], with activation energies for O^{2-} diffusion derived from CO_2 absorption measurements again in line with experimental values of 1 – 2 eV.

Aliovalent doping can also be used to improve the oxygen ionic conductivity through the formation of oxygen vacancies and additional oxide ions. Iron is the most common dopant, with the reduction of Fe^{3+} to Fe^{2+} having the twin effect of creating oxygen vacancies and producing extra electrons to oxidize available oxygen in the gas phase to oxide ions:

$2\ Fe^{3+} \rightarrow 2\ Fe^{2+} + V_O$ (R16)

$Fe^{3+} \rightarrow Fe^{2+} + e^-$ (R17)

$O_2 + 2\ e^- \leftrightarrow 2\ O^-$ (R18)

The net effect of this is an improvement of the oxide ionic conductivity and improvement of the overall rate of CO_2 absorption. This has been observed in practice for Fe-doped Li_4SiO_4 [584], Fe-doped Li_2ZrO_3 [585], [586], Fe-doped Li_5AlO_4 [583] and Fe-doped $NaCoO_2$ [587].

There have been a number of studies that aimed at elucidating the effect of dopant on ionic conductivity. Zhan et al. [586] studied the connection between aliovalent doping of Li_2ZrO_3 leading to the creation of oxygen vacancies, and the resulting change in Li ionic conductivity. Through considering a range of dopants with different valences (from $Fe^{2+/3+}$ to Nb^{5+}) they observed the formation of oxygen vacancies as a result of doping. In turn this led to an increased lithium loss in the materials owing to charge compensation, with this loss resulting in increased numbers of lithium vacancies. Furthermore, the formation of oxygen vacancies also leads to changes in the overall crystal structure, often reducing barriers for Li ion diffusion, further compounding the overall increase in Li ion mobility.

Following this work, a number of further studies have tried to purposely influence the rate of the ionic transport through structural modification to improve CO_2 sorption properties. Subha and co-workers [478] synthesized a range of samples of the $Li_4Si_xGe_{1-x}O_4$ solid solution, with x up to ~ 0.30. Samples with a Si:Ge ratio of 1:0.183 showed the most enhanced absorption capacity (324 mg g^{-1}) and kinetics at both low and high absorption temperatures. According to XRD, the sample remained single phase with the original Li_4SiO_4 monoclinic structure, albeit with an expansion in the lattice parameters due to the substitution of the larger Ge atom on the Si site. This lattice expansion was given as the cause to the lower barriers for Li ionic transport in the material and therefore the improved CO_2 capture performance.

Finally it should be noted that concepts of ionic conduction are still relevant for the CaO-$CaCO_3$ and MgO-$MgCO_3$ systems, albeit more consideration is given to carbonate ion mobility. Ionic conduction in this context is explored in earlier sections which focus on modification of CaO- and MgO-based sorbents with molten alkali metal salt promoters (Section 3.1.1 on alkali doping in CaO and Section 3.2 where the promoter is proposed to facilitate the dissolution of MgO).

5.4 Multiple Carbonation Pathways

There are some studies of Li-based materials which suggest that the availability of multiple carbonation reaction pathways with similar energies can lead to a stabilization of the CO_2 uptake capacity over multiple cycles, as changes in morphology and surface area are compensated by a shift between competing reaction pathways. A new lithium-rich lithium borate, Li_3BO_3, was shown to have an excellent conversion rate, and at different temperatures could undergo a series of different carbonation reactions resulting in the formation of different product borates [477] (R19 – R21). The accessibility of these additional pathways results in a higher experimental gravimetric CO_2 uptake capacity than what would be achieved if the reaction went through R21 alone.

$4\ Li_3BO_3 + 3\ CO_2 \rightarrow 3\ Li_2CO_3 + Li_6B_4O_9 \quad T = 580\ °C$ (R19)

$4\ Li_3BO_3 + 5\ CO_2 \rightarrow 5\ Li_2CO_3 + Li_2B_4O_7 \quad T = 580\ °C$ (R20)

$Li_3BO_3 + CO_2 \rightarrow Li_2CO_3 + LiBO_2 \quad T = 520\ °C$ (R21)

Another recently reported material, Li_5SbO_5, was observed to maintain a relatively stable CO_2 uptake of 80 wt% over multiple cycles [499]. Further analysis of the product formation as a function of cycle number by XRD revealed that initially the reaction proceeded as predicted, forming Li_2CO_3 and the lower-lithium content antimonate Li_3SbO_4 (R22). However, on further carbonation and calcination cycles, a significant phase fraction of another product, Li_7SbO_6, was observed to form and persist after calcination, most likely from a competing calcination reaction (R23). This higher lithium content phase lead to the maintenance of a high gravimetric capacity for the material, again higher than what would be expected if only a single reaction pathway was active in this system.

$Li_5SbO_5 + CO_2 \rightarrow Li_2CO_3 + Li_3SbO_4$ (R22)

$2\ Li_2CO_3 + Li_3SbO_4 \rightarrow Li_7SbO_6 + 2\ CO_2$ (R23)

6 Remaining challenges and future direction for solid sorbents for CO_2 capture

Solid sorbents composed of the oxides of calcium, magnesium and lithium react with CO_2 in different temperature regimes ranging from 200 °C to 1000 °C, and research into these materials has branched into separate fields. Despite the rather simple reaction, there are many factors to consider in the development of new, more effective CO_2 sorbents. Research activities on CO_2 capture by solid sorbents at high temperature can broadly be divided into three categories: (i) Understanding CO_2 capture at the atomic level, which includes CO_2 transport within the sorbent, carbonate product layer formation, structural transformations, crystal growth and sintering, and other surface-related aspects, (ii) the synthesis and manufacture of sorbents on a lab scale, and (iii) enabling CO_2 capture from industrial installations at large scale in the context of climate change. Here, we describe the most pressing questions at each level of development. We formulate some open research questions in each field, but also aim to bridge the gap between the separate fields by identifying fabrication methods or techniques that have not been used equally in all fields. We note that research into CaO-based materials and processes is very advanced and probably a few years ahead of research activities into MgO or Li-based materials; this is also reflected by the existence of large pilot units operating at the MW scale [285], [588]–[592]. Furthermore, the calcium looping process is part of industrial direct air capture systems [71].

6.1 Advancing fundamental understanding

One course of research that requires more attention is the interaction between the active sorbent and structural stabilizers to mitigate sintering. Structural stabilizers are often chosen for their higher melting temperature, but the stabilizing effect does not necessarily correlate directly with the melting temperature (Section 3.1.2). Providing fundamental understanding that can explain why some stabilizers are better suited than others is key to the development of improved sorbents that possess a high cyclic stability. This could include investigations of the mobility of the stabilizing phase in the active phase, the segregation of the active and stabilizing phases, the tendency of the stabilizing phase to form ternary phases with the active phase under certain combinations of T and p_{CO2}, and the kinetics of such phase transformations. Understanding these transformations requires complementary use of in situ XRD and XAS, NMR and microscopy techniques that permit observing cross diffusion at the interface between the active and stabilizing phase under operating conditions and reveal the chemical nature of the species involved. External influences, e.g. the gas environment or the reaction temperature, are well understood such that the observed cyclic CO_2 uptake capacity can relatively accurately be anticipated.

There is general agreement that alkali metal salts (AMS) promote the conversion of MgO and further that there is an optimum ratio of salt to MgO between 20 – 30 wt% that allows for the highest CO_2 uptake [133], [415], [423]. However, there is no consensus on why this optimum exists. Some of the possible explanations have included an optimum surface coverage of the promoter or an optimum thickness. To address this critical question, unequivocal experimental evidence for the location of formation and growth of $MgCO_3$ is required, e.g. inside the promoter, the interface of MgO|AMS or at the triple phase boundary MgO|AMS|CO_2. Furthermore, the highest CO_2 uptakes and uptake rates have been observed when the AMS promoter consisted of a combination of different species, including nitrates and carbonates [593], [594]. Mixtures thereof possess different melting points, viscosities [595] and solubilities for MgO and CO_2 – parameters that have been studied only sparsely thus far and that require more experimental investigations.

Another pressing issue to address for AMS-promoted MgO is the reduced CO_2 uptake for low p_{CO2}. Standard thermodynamic data (Figure 1) predicts that carbonation is unfavorable above 300 °C at 1 bar CO_2, which is in clear contradiction to experimental results showing that the optimum temperature for the highest rates of CO_2 uptake is ~ 330 °C. The study by Hu et al. [596] demonstrated that a highly optimized AMS-promoted MgO sorbent required $p_{CO2} > 1$ atm at 300 °C to reach CO_2 capture efficiencies > 80 %, whereas $p_{CO2} > 8$ atm was required for near-complete (> 99 %) capture of the CO_2. The re-assessment of the thermodynamic equilibrium of the MgO/$MgCO_3$ system is needed to define the application space of MgO sorbents. Currently, MgO-based sorbents appear to have limited potential for post-combustion CO_2 capture, but may be more suitable for pre-combustion CO_2 capture that involves much higher p_{CO2} which offer kinetic and thermodynamic advantages.

Finally, our fundamental understanding of MgO-based sorbents would also profit substantially when applying the characterization methods at the relevant operating conditions, viz. operando characterization. Advanced techniques such as X-ray tomography, atomic force microscopy (AFM) and neutron reflectometry are increasingly able to be utilized at both high temperatures and variable gas atmospheres, making it possible to gain real-time morphological information at reactive surfaces, and at the interface between phases. Pair distribution function (PDF) analysis provides structural information of not only crystalline phases but also amorphous phases which is of interest to understand the transformation of the AMS under operating conditions [177]. Structural methods such as X-ray diffraction and NMR provide only information of the evolution of the bulk phase of the sorbents under reactive conditions, yet experimental techniques that can obtain selective information of surface features, such as AFM,

XPS and Raman/FTIR, will be critical to elucidate the effect of alkali promoters on the CO_2 absorption of MgO.

6.2 Future development of sorbents on the lab scale

The dominant reason for the decay in the CO_2 uptake of MgO-based sorbents over repeated carbonation-calcination cycles is sintering analogous to CaO. In pure MgO, the uptake at low temperature (25 – 200 °C) scales with the surface area, making it critical to stabilize the nanostructured morphology. Here, we may learn from the considerable efforts to stabilize the morphology of CaO. The use of structural stabilizers, both reactive and inert, may allow substantial advancements in MgO-based sorbents for CO_2 capture at temperatures < 200 °C. Considering that the calcination of MgO-based sorbents is typically performed at temperatures close to 500 °C for thermodynamic reasons, a larger set of stabilizers is possible when compared to CaO. The higher temperatures required for the calcination of Li_2O-based CO_2 sorbents reduce the number of materials that are suitable for a potential structural stabilization; however, Li_2O-based sorbents usually exist in mixed oxide environments and are thus inherently stabilized provided that the bulk phase transitions upon CO_2 sorption and release are fully reversible (see also Section 4.1). Furthermore, we note that the decay of the CO_2 capture capacity of MgO-based sorbents promoted with alkali metal salts does not appear to be related only to sintering, but also to a redistribution of the promoter at the surface and/or the loss of the promoter from the sorbent. Further, the transformation of the salt-containing phases during cycling affects the CO_2 sorption properties. These observations impose additional requirements to any new structural stabilizer, i.e. it should not only stabilize the morphology of the MgO backbone but also reduce the mobility of the promoter on the surface. Triviño et al. [597] showed that the immobilization of eutectic salts within the sorbent can be achieved through core-shell MgO fibers. Valuable lessons may be learned also from high temperature CO_2-conducting membranes, where the molten carbonate needs to be retained within the porous solid matrix [333], [598]–[601].

The reactivity of solid CO_2 sorbents is usually assessed using powdery materials. However, fine powders cannot be used in packed or fluidized bed reactors, requiring additional processing steps (e.g. granulation, palletization or spray-drying) to convert the powder into (mechanically stable) particles > 100 μm, which will inevitably result in the densification of the sorbent. For reference, limestone used in large pilot plants ranged from 100 – 850 μm in size [590], [591]. Since both CaO- and MgO-based sorbents require high pore volumes and surface areas for fast CO_2 uptake, sorbent particles will perform worse than a sorbent powder. Thus far, there has only been limited research on how the performance of the sorbent is affected when it is

converted from a powder into a particle [561], [602]–[607], particularly how such processing affects the effectiveness of stabilizers or other components of the sorbent that were initially added to improve its cyclic CO_2 uptake capacity. These considerations extend to lithium sorbents that have rarely been studied in relevant reactor setups, and preparing suitable and durable particles for cycling is an area of priority for future research. Further, basic performance testing, especially longer-term cycling beyond 100 cycles, is also lacking for these sorbents.

6.3 Enabling CO_2 capture on an industrial scale

If the objective is to capture CO_2 at the large scale, sorbents and potential candidates need to be investigated under relevant reaction conditions. Different from direct air capture processes, CO_2 capture from concentrated gas streams needs to occur at high efficiencies. Thus far, only CaO-based sorbents have shown to be practical in post-combustion CO_2 capture for the removal of CO_2 from a gas stream and have been investigated at the large pilot scale. Thermodynamics in Figure 1 dictate that for typical CO_2 concentrations in the off-gas from industrial installations (3 – 15 vol.%) the maximum practical carbonation temperature is ~ 700 °C, whereas the calcination reaction requires temperatures > 900 °C (in case that no large quantities of steam are present) such that the CO_2 can be released from the sorbent at atmospheric pressure. As discussed above, the partial pressure of CO_2 during the actual calcination reaction affects the long-term reactivity of the sorbent for CO_2 capture because it enhances crystal growth and sintering. Any experimental investigation on the suitability of sorbents for large-scale CO_2 capture employing reaction conditions that deviate from the framework mentioned above will thus not be relevant in advancing the calcium looping process towards its industrial implementation.

Further, there has been consensus that large-scale CO_2 capture requires fluidized beds for efficient heat and mass transfer and to handle large gas streams [608], [609]. This involves the movement of sorbent particles, possibly between spatially separated reactors. The mechanical stability of the sorbent particles is thus important from an operational point of view, as loss of material and replacement would increase the operational costs and complicate process design. If the sorbent particle size falls below a certain threshold due to abrasion and/or particle breakage (see Section 2.5), the sorbent will be entrained from the fluidized bed and removed from the CO_2 capture process via cyclones and filters. Sorbent testing protocols should thus employ what is considered as “realistic reaction conditions” and also use reactor systems in which mechanical stress on sorbent particles is significant, e.g. fluidized beds, or employ designated test equipment such as jet cups or rotating drums [610]. We note that such

engineering-related investigations might be considered to be of lower impact than fundamental, chemistry-related investigations, yet they are essential for advancing the technology.

Most previous studies have indeed used TGAs, where mechanical stress on particles is eliminated. Such instruments are helpful in assessing the inherent ability of the sorbents to capture CO_2, e.g. when modifying them with structural stabilizers, promoters or dopants (Section 3), as the measured changes in sample mass correlate with the amount of CO_2 absorbed by the sorbent. However, care must be taken in the interpretation of the results when screening for sorbents, since extrapolating the results from a TGA-based study to a CO_2 capture process at the industrial scale is usually not possible owing to the instrument's inherent limitation in reflecting actual process conditions [93], [611].

Several works have dealt with techno-economic aspects of the calcium looping process, and very early it was anticipated that it could have significant advantages over the amine-based process with regards to the price per ton of CO_2 captured (< 20 USD t_{CO2}^{-1}, which was less than half of the costs for an amine-based CO_2 capture process; note that correcting for inflation this is ~ 26 USD t_{CO2}^{-1} in 2021) [612]–[614]. The sensitivity towards the cost of the sorbent for CO_2 and its rate of deactivation was relatively high in these early analyses, and indeed synthetic sorbents were predicted not to be competitive with natural limestone unless their long-term stability is significantly better under realistic process conditions [615], [616]. Interestingly, although most of the literature has dealt with the development of novel, synthetic sorbents, estimates of the production costs are scarce and thus make it difficult to assess their suitability for a large-scale CO_2 capture process on economic grounds. Often sorbent costs have been estimated based on values published decades ago [617], [618]. Recently, many studies have utilized industrial waste products rich in species that are typically used to stabilize the CaO in a sorbent, e.g. Mg, Al, or Si [544], [619]–[625], or bioderived materials [380], [626]–[629] to reduce the costs of sorbent production. Questions related to the recycling and reuse of spent sorbents or their processing (e.g. the separation of the inert phases and the Ca phase) have not been addressed and thus offer potential for research (as e.g. in [630], [631] in the context of chemical looping).

The calcium looping process can be run most efficiently if integrated in power plants (e.g. coal-fired), resulting in net efficiency penalties < 8 % [30], [632]–[636]. In Europe and other parts of the world, reliance on coal for power generation is expected to decrease significantly in the next decades as per governmental decisions, so it remains doubtful whether efforts will be made to retrofit existing power plants with a calcium looping process for CO_2 capture. However, there exists many CO_2-intensive industries for which an integration with the calcium looping process

is considered beneficial, e.g. the cement industry [40], [637]–[643], even though current prices of CO_2 are low [644]. The calcium looping process can be designed flexibly such that it is suitable for the CO_2 capture from power plants with large load fluctuations [645], [646]. The economic attractiveness of the calcium looping process increases further if (besides CO_2 capture) products are generated that have a certain value, e.g. hydrogen (sorption-enhanced reforming or water-gas shift) [399], [596], [647]–[656] or thermal energy (thermochemical energy storage) [657]–[668], and may therefore accelerate the implementation at the industrial scale. What is certainly missing currently are demonstration units that prove that the different processes employing metal oxide sorbents for CO_2 work reliably at the industrial scale. A promising example for the industrial application of the calcium looping process at small, distributed scale is where CaO-based sorbents capture the CO_2 emitted from a biomass combustion/gasification process, and then release that CO_2 through an air stream into greenhouses [669], [670].

We note that the sorbent development (incl. CaO, MgO and Li-mixed oxides) for the sorption-enhanced reforming still offers enormous potential for optimization and goes beyond what has been covered in Section 3; this comprises fundamental aspects but also understanding at the process level. The complexity arises from the ability of the materials to enable several sub-reactions, i.e. to catalyze the actual reforming reaction through the activation of the fuel (e.g. CH_4 [671]–[674], biomass [413], glycerol [448], [675]–[678] or ethanol [679]–[682]), to capture CO_2 at a high efficiency for a long time, and possibly to enable redox-reactions simultaneously for a better heat integration [683]–[686]. Combining these functionalities in a single particle (bi-functional or tri-functional catalyst-sorbent [687]) would maximize the heat integration of the different sub-reactions, but the design of such multifunctional materials is challenging so that typically separated particle systems (i.e. catalyst, sorbent and oxygen carrier) have been used [443], [688].

Lastly, even the most basic techno-economic assessments still remain to be performed for sorbents based on lithium, sodium and magnesium, and such works need to be undertaken to understand in which capacity these sorbents would be best suited. The relatively high cost of lithium, considering high demand from the battery industry, may well limit the use of such sorbents to more niche applications that require their specific thermodynamic properties.

7 Conclusions

CCUS remains a vital technology platform both to reduce CO_2 emissions to combat climate change, and to generate a supply of CO_2 as feedstock towards the production of chemicals or synthetic fuels. Recently, the IPCC raised concerns about the limited pace of the current deployment of CCUS technologies and it is hoped that government or market incentives can compensate for the incremental costs of CO_2 capture, and the development of transport and storage infrastructures [1]. Solid oxides are a promising alternative – to be understood as supplement rather than replacement – to the widely used liquid amines for CO_2 capture at mid- to high temperature in terms of reduced energy penalties and potential for application to a wide range of CCUS contexts, but there remain significant challenges to overcome to enable their widespread use, including large-scale demonstration projects.

This review has sought to outline the current state of the field, focusing on the materials used, and the fundamental understanding of the key parameters controlling their CO_2 absorption properties. Innovation is needed both in materials design, preparation and optimization, as well as in the analytical methods used to assess their performance and factors leading to degradation over time. This requires a multidisciplinary effort from chemists, materials scientists, chemical and process engineers, and this work aims to bring research from these sometimes disparate fields together in order to learn the most from their combined insights. Through this cooperation a new generation of CCUS processes might be implemented, and through them provide new opportunities for environmental protection and economic opportunity.

8 Biographies

Matthew T. Dunstan is currently a postdoctoral research associate at the Department of Chemistry, University of Cambridge. He received a B.Sc. (Hons) (Adv) degree from the University of Sydney in 2011, and a PhD from the University of Cambridge in 2015 under the supervision of Prof Clare Grey. He stayed in Cambridge with a Research Fellowship from Clare College from 2016-2019 and is currently a part of the Faraday Institution investigating mechanisms of degradation in electrochemical devices. His research focuses on harnessing big data approaches to the study of structure-property relationships in energy materials.

Felix Donat obtained a Diploma in Business Administration and Engineering from the TU Bergakademie Freiberg in 2011, which included a research stay at Imperial College in London. He received a PhD in Chemical Engineering from the University of Cambridge in 2016 under the supervision of Prof. John Dennis. Since 2016, he works as a postdoctoral researcher in the group of Prof. Christoph R. Müller at ETH Zürich, where he is also a lecturer. His research focuses on materials for gas-solid reactions for energy applications and solid looping concepts in the context of CO_2 capture.

Alexander H. Bork obtained a M.Sc. in Sustainable Energy from the Technical University of Denmark in 2013 in the Honors Program Fuel Cells and Hydrogen. He earned his PhD in Materials Science from ETH Zürich in 2017 for his work on perovskites for thermochemical CO_2 and H_2O conversion. Following his PhD, he worked as a postdoctoral researcher at the Massachusetts Institute of Technology, MIT, where he focused on the development of composite metal oxides for solar thermochemical cycles. His current research is focused on advancing the fundamental understanding of solid sorbents for CO_2 capture as a postdoctoral researcher in the Laboratory of Energy Science and Engineering at ETH Zürich.

Clare P. Grey, FRS is the Geoffrey Moorhouse-Gibson Professor of Chemistry at the University of Cambridge, a Royal Society Professsor and a Fellow of Pembroke College Cambridge. She received a BA and D. Phil. (1991) in Chemistry from the University of Oxford. After post-doctoral fellowships in the Netherlands and at DuPont CR&D in Wilmington, DE, she joined the faculty at Stony Brook University (SBU) as an Assistant (1994), Associate (1997) and then Full Professor (2001-2015). She moved to Cambridge in 2009, maintaining an adjunct position at SBU. She was Director of the Northeastern Chemical Energy Storage Center, a Department of Energy, Energy Frontier Research Center (2009-2010) and Associate Director (2011-2014). She is currently Director of the EPSRC Centre for Advanced Materials for Integrated Energy Systems (CAM-IES) and a member of the Expert Panel of the Faraday Institution. Recent honours and awards include the Royal Society Davy Award (2014), the

Arfvedson-Schlenk-Preis from the German Chemical Society (2015), the Société Chimique de France, French-British Prize (2017), the Solid State Ionics Galvani-Nernst-Wagner Mid-Career Award (2017), the Eastern Analytical Symposium Award for Outstanding Achievements in Magnetic Resonance (2018), the Sacconi Medal from the Italian Chemical Society (2018), the Charles Hatchett Award, Institute of Materials, Minerals and Mining (2019), the RSC John Goodenough Award (2019), the Richard R. Ernst Prize in Magnetic Resonance (2020) and the Hughes Medal, Royal Society (2020). She is a foreign member of the American Academy of Arts and Sciences, and a Fellow of the Electrochemical Society and the International Society of Magnetic Resonance. Her current research interests include the use of solid-state NMR and diffraction-based methods to determine structure-function relationships in materials for energy storage (batteries and supercapacitors), conversion (fuel cells) and carbon capture.

Christoph R. Müller obtained a Diploma in Mechanical/Process Engineering from TU Munich in 2004 and a PhD in Chemical Engineering from the University of Cambridge in 2008 under the supervision of Prof. John Dennis. In 2010, he became an assistant professor at the Department of Mechanical and Process Engineering at ETH Zürich. Since 2018, he is a full professor at the same institution. His research group is active in the development of solid CO_2 sorbents, heterogeneous catalysts with a particular focus on operando characterization, and the studying of single- and multiphase granular flows.

Acknowledgements

M.T.D acknowledges support from Clare College, Cambridge via a Junior Research Fellowship. C.P.G acknowledges support from the Royal Society via a Research Professorship (RP\R1\180147). F.D. acknowledges financial support by the Swiss Federal Office of Energy (SI/501550-01) and the European Commission (“GaSTech” project under the Horizon 2020 programme, ACT Grant Agreement No. 691712). A.H.B and C.R.M. acknowledge funding from the European Research Council (ERC) under the European Union's Horizon 2020 research and innovation program grant agreement No. 819573. C.R.M. also acknowledges funding from the Swiss National Science Foundation (SNSF, 200020_156015).

9 References

[1] IPCC, “Global Warming of 1.5°C. An IPCC Special Report on the impacts of global warming of 1.5°C above pre-industrial levels and related global greenhouse gas emission pathways, in the context of strengthening the global response to the threat of climate change,” 2018.

[2] M. Bui *et al.*, “Carbon capture and storage (CCS): the way forward,” *Energy Environ. Sci.*, vol. 11, no. 5, pp. 1062–1176, 2018.

[3] D. Reiner, M. Bui, and N. Mac Dowell, *Carbon Capture and Storage*. The Royal Society of Chemistry, 2020.

[4] M. E. Boot-Handford *et al.*, “Carbon capture and storage update,” *Energy Environ. Sci.*, vol. 7, no. 1, pp. 130–189, 2014.

[5] V. Becattini, P. Gabrielli, and M. Mazzotti, “Role of Carbon Capture, Storage, and Utilization to Enable a Net-Zero-CO2-Emissions Aviation Sector,” *Ind. Eng. Chem. Res.*, Jan. 2021.

[6] T. Wilberforce, A. G. Olabi, E. T. Sayed, K. Elsaid, and M. A. Abdelkareem, “Progress in carbon capture technologies,” *Sci. Total Environ.*, p. 143203, 2020.

[7] E. I. Koytsoumpa, C. Bergins, and E. Kakaras, “The CO2 economy: Review of CO2 capture and reuse technologies,” *J. Supercrit. Fluids*, vol. 132, no. July 2017, pp. 3–16, 2018.

[8] T. P. Senftle and E. A. Carter, “The Holy Grail: Chemistry Enabling an Economically Viable CO2 Capture, Utilization, and Storage Strategy,” *Acc. Chem. Res.*, vol. 50, no. 3, pp. 472–475, Mar. 2017.

[9] T. Kober *et al.*, “Perspectives of Power-to-X technologies in Switzerland,” 2019.

[10] Ministry of Foreign Affairs of Denmark, “Hydrogen and PtX Opportunities in Denmark.” [Online]. Available: https://investindk.com/-/media/invest-in-denmark/publications/cleantech/hydrogen-and-ptx-opportunities_2.ashx. [Accessed: 26-Jul-2020].

[11] V. Pflug, E. Zindel, G. Zimmermann, O. R. Olvera, I. Pyc, and C. Trulley, “Power-to-X: The crucial business on the way to a carbon-free world,” *Technial Paper Siemens AG*, 2019. [Online]. Available: https://new.siemens.com/global/en/products/energy/technical-papers/download-power-to-x.html. [Accessed: 26-Jul-2020].

[12] Z. Chehade, C. Mansilla, P. Lucchese, S. Hilliard, and J. Proost, “Review and analysis of demonstration projects on power-to-X pathways in the world,” *Int. J. Hydrogen Energy*, vol. 44, no. 51, pp. 27637–27655, 2019.

[13] J. C. Koj, C. Wulf, and P. Zapp, “Environmental impacts of power-to-X systems - A review of technological and methodological choices in Life Cycle Assessments,” *Renew. Sustain. Energy Rev.*, vol. 112, pp. 865–879, 2019.

[14] A. Otto, T. Grube, S. Schiebahn, and D. Stolten, “Closing the loop: captured CO2 as a feedstock in the chemical industry,” *Energy Environ. Sci.*, vol. 8, no. 11, pp. 3283–3297, 2015.

[15] B. Castellani, S. Rinaldi, E. Morini, B. Nastasi, and F. Rossi, “Flue gas treatment by power-to-gas integration for methane and ammonia synthesis – Energy and environmental analysis,” *Energy Convers. Manag.*, vol. 171, pp. 626–634, 2018.

[16] Z. Zhang *et al.*, “Recent advances in carbon dioxide utilization,” *Renew. Sustain. Energy Rev.*, vol. 125, p. 109799, 2020.

[17] H. Ostovari, A. Sternberg, and A. Bardow, “Rock ‘n’ use of CO2: carbon footprint of carbon capture and utilization by mineralization,” *Sustain. Energy Fuels*, vol. 4, no. 9, pp. 4482–4496, 2020.

[18] W. Gao *et al.*, “Industrial carbon dioxide capture and utilization: state of the art and future challenges,” *Chem. Soc. Rev.*, vol. 49, no. 23, pp. 8584–8686, 2020.
[19] L. Tao, T. S. Choksi, W. Liu, and J. Pérez-Ramírez, “Synthesizing High-Volume Chemicals from CO2 without Direct H2 Input,” *ChemSusChem*, vol. 13, no. 23, pp. 6066–6089, Dec. 2020.
[20] M. Aresta and A. Dibenedetto, “Utilisation of CO2 as a chemical feedstock: opportunities and challenges,” *Dalt. Trans.*, no. 28, pp. 2975–2992, 2007.
[21] A. M. Varghese and G. N. Karanikolos, “CO2 capture adsorbents functionalized by amine – bearing polymers: A review,” *Int. J. Greenh. Gas Control*, vol. 96, p. 103005, 2020.
[22] P. H. M. Feron, A. Cousins, K. Jiang, R. Zhai, and M. Garcia, “An update of the benchmark post-combustion CO2-capture technology,” *Fuel*, vol. 273, p. 117776, 2020.
[23] R. Idem *et al.*, “Practical experience in post-combustion CO2 capture using reactive solvents in large pilot and demonstration plants,” *Int. J. Greenh. Gas Control*, vol. 40, pp. 6–25, 2015.
[24] X. Chen, G. Huang, C. An, Y. Yao, and S. Zhao, “Emerging N-nitrosamines and N-nitramines from amine-based post-combustion CO2 capture – A review,” *Chem. Eng. J.*, vol. 335, pp. 921–935, 2018.
[25] C. M. Tessie du Motay and C. R. Marechal, “A New Process for Producing Hydrogen,” British Patent No. 2548, 1867.
[26] A. Silaban and D. P. Harrison, “High temperature capture of carbon dioxide: Characteristics of the reversible reaction between CaO(s) and CO2(g),” *Chem. Eng. Commun.*, vol. 137, pp. 177–190, 1995.
[27] T. Shimizu, T. Hirama, H. Hosoda, K. Kitano, M. Inagaki, and K. Tejima, “A twin fluid-bed reactor for removal of CO2 from combustion processes,” *Chem. Eng. Res. Des.*, vol. 77, no. 1, pp. 62–68, 1999.
[28] R. T. J. Porter, M. Fairweather, M. Pourkashanian, and R. M. Woolley, “The range and level of impurities in CO2 streams from different carbon capture sources,” *Int. J. Greenh. Gas Control*, vol. 36, pp. 161–174, 2015.
[29] M. Haaf, R. Anantharaman, S. Roussanaly, J. Ströhle, and B. Epple, “CO2 capture from waste-to-energy plants: Techno-economic assessment of novel integration concepts of calcium looping technology,” *Resour. Conserv. Recycl.*, vol. 162, p. 104973, 2020.
[30] D. P. Hanak, S. Michalski, and V. Manovic, “From post-combustion carbon capture to sorption-enhanced hydrogen production: A state-of-the-art review of carbonate looping process feasibility,” *Energy Convers. Manag.*, vol. 177, no. April, pp. 428–452, 2018.
[31] S. Choi, J. H. Drese, and C. W. Jones, “Adsorbent materials for carbon dioxide capture from large anthropogenic point sources,” *ChemSusChem*, vol. 2, no. 9, pp. 796–854, 2009.
[32] A. Samanta, A. Zhao, G. K. H. Shimizu, P. Sarkar, and R. Gupta, “Post-combustion CO 2 capture using solid sorbents: A review,” *Ind. Eng. Chem. Res.*, vol. 51, no. 4, pp. 1438–1463, 2012.
[33] M. Ding, R. W. Flaig, H.-L. Jiang, and O. M. Yaghi, “Carbon capture and conversion using metal–organic frameworks and MOF-based materials,” *Chem. Soc. Rev.*, vol. 48, no. 10, pp. 2783–2828, 2019.
[34] X. Zhu, S. Li, Y. Shi, and N. Cai, “Recent advances in elevated-temperature pressure swing adsorption for carbon capture and hydrogen production,” *Prog. Energy Combust. Sci.*, vol. 75, p. 100784, 2019.
[35] J. Wang *et al.*, “Recent advances in solid sorbents for CO2 capture and new development trends,” *Energy Environ. Sci.*, vol. 7, no. 11, pp. 3478–3518, 2014.

[36] A. Sharma, J. Jindal, A. Mittal, K. Kumari, S. Maken, and N. Kumar, “Carbon materials as CO2 adsorbents: a review,” *Environ. Chem. Lett.*, 2021.
[37] L. K. G. Bhatta, S. Subramanyam, M. D. Chengala, S. Olivera, and K. Venkatesh, “Progress in hydrotalcite like compounds and metal-based oxides for CO2 capture: a review,” *J. Clean. Prod.*, vol. 103, pp. 171–196, Sep. 2015.
[38] A. Mukherjee, J. A. Okolie, A. Abdelrasoul, C. Niu, and A. K. Dalai, “Review of post-combustion carbon dioxide capture technologies using activated carbon,” *J. Environ. Sci.*, vol. 83, pp. 46–63, 2019.
[39] J. C. Abanades *et al.*, “Emerging CO2 capture systems,” *Int. J. Greenh. Gas Control*, vol. 40, pp. 126–166, Sep. 2015.
[40] C. C. Dean, J. Blamey, N. H. Florin, M. J. Al-Jeboori, and P. S. Fennell, “The calcium looping cycle for CO2 capture from power generation, cement manufacture and hydrogen production,” *Chem. Eng. Res. Des.*, vol. In Press, 2011.
[41] J. Blamey, E. J. Anthony, J. Wang, and P. S. Fennell, “The calcium looping cycle for large-scale CO2 capture,” *Prog. Energy Combust. Sci.*, vol. 36, no. 2, pp. 260–279, Apr. 2010.
[42] Q. Wang, J. Luo, Z. Zhong, and A. Borgna, “CO2 capture by solid adsorbents and their applications: current status and new trends,” *Energy Environ. Sci.*, vol. 4, no. 1, pp. 42–55, 2011.
[43] A. M. Kierzkowska, R. Pacciani, and C. R. Müller, “CaO-Based CO2 Sorbents: From Fundamentals to the Development of New, Highly Effective Materials,” *ChemSusChem*, vol. 6, no. 7, pp. 1130–1148, Jul. 2013.
[44] S. A. Salaudeen, B. Acharya, and A. Dutta, “CaO-based CO2 sorbents: A review on screening, enhancement, cyclic stability, regeneration and kinetics modelling,” *J. CO2 Util.*, vol. 23, no. July 2017, pp. 179–199, 2018.
[45] Y. Hu, H. Lu, W. Liu, Y. Yang, and H. Li, “Incorporation of CaO into inert supports for enhanced CO2 capture: A review,” *Chem. Eng. J.*, vol. 396, p. 125253, 2020.
[46] J. Chen, L. Duan, and Z. Sun, “Review on the Development of Sorbents for Calcium Looping,” *Energy & Fuels*, vol. 34, no. 7, pp. 7806–7836, Jul. 2020.
[47] W. Liu *et al.*, “Performance enhancement of calcium oxide sorbents for cyclic CO 2 capture-a review,” *Energy and Fuels*, vol. 26, no. 5, pp. 2751–2767, 2012.
[48] M. Erans, V. Manovic, and E. J. Anthony, “Calcium looping sorbents for CO2 capture,” *Appl. Energy*, vol. 180, pp. 722–742, 2016.
[49] G. Ji *et al.*, “Recent advances on kinetics of carbon dioxide capture using solid sorbents at elevated temperatures,” *Appl. Energy*, vol. 267, p. 114874, 2020.
[50] S. Kumar and S. K. Saxena, “A comparative study of CO2 sorption properties for different oxides,” *Mater. Renew. Sustain. Energy*, vol. 3, no. 3, 2014.
[51] Y. Hu, Y. Guo, J. Sun, H. Li, and W. Liu, “Progress in MgO sorbents for cyclic CO2 capture: A comprehensive review,” *J. Mater. Chem. A*, vol. 7, no. 35, pp. 20103–20120, 2019.
[52] A. H. Ruhaimi, M. A. A. Aziz, and A. A. Jalil, “Magnesium oxide-based adsorbents for carbon dioxide capture: Current progress and future opportunities,” *J. CO2 Util.*, vol. 43, p. 101357, 2021.
[53] Y. Hu, W. Liu, Y. Yang, M. Qu, and H. Li, “CO2 capture by Li4SiO4 sorbents and their applications: Current developments and new trends,” *Chem. Eng. J.*, vol. 359, no. October 2018, pp. 604–625, 2019.
[54] Y. Zhang *et al.*, “Recent advances in lithium containing ceramic based sorbents for high-temperature CO2 capture,” *J. Mater. Chem. A*, vol. 7, no. 14, pp. 7962–8005, 2019.
[55] M. C. Romano *et al.*, “Application of Advanced Technologies for CO2 Capture From Industrial Sources,” *Energy Procedia*, vol. 37, pp. 7176–7185, 2013.

[56] M. Songolzadeh, M. Soleimani, M. Takht Ravanchi, and R. Songolzadeh, “Carbon Dioxide Separation from Flue Gases: A Technological Review Emphasizing Reduction in Greenhouse Gas Emissions,” *Sci. World J.*, vol. 2014, p. 828131, 2014.
[57] B. Metz, O. Davidson, H. de Coninck, M. Loos, and L. Meyer, *IPCC Special Report on Carbon dioxide Capture and Storage*. Cambridge University Press, 2005.
[58] P. Bains, P. Psarras, and J. Wilcox, “CO2 capture from the industry sector,” *Prog. Energy Combust. Sci.*, vol. 63, pp. 146–172, 2017.
[59] S. Zarghami *et al.*, “Effect of Steam on the Reactivity of MgO-Based Sorbents in Precombustion CO2 Capture Processes,” *Ind. Eng. Chem. Res.*, vol. 54, no. 36, pp. 8860–8866, May 2015.
[60] H. Zhai and E. S. Rubin, “Systems Analysis of Physical Absorption of CO2 in Ionic Liquids for Pre-Combustion Carbon Capture,” *Environ. Sci. Technol.*, vol. 52, no. 8, pp. 4996–5004, Apr. 2018.
[61] A. A. Olajire, “CO2 capture and separation technologies for end-of-pipe applications – A review,” *Energy*, vol. 35, no. 6, pp. 2610–2628, Jun. 2010.
[62] B. J. McBride, M. J. Zehe, and S. Gordon, “NASA Glenn coefficients for calculating thermodynamic properties of individual species Technical Paper 2002-211556,” 2002.
[63] R. Zevenhoven, S. Teir, and S. Eloneva, “Heat optimisation of a staged gas-solid mineral carbonation process for long-term CO2 storage,” *Energy*, vol. 33, no. 2, pp. 362–370, 2008.
[64] J. Fagerlund, J. Highfield, and R. Zevenhoven, “Kinetics studies on wet and dry gas-solid carbonation of MgO and Mg(OH) 2 for CO 2 sequestration,” *RSC Adv.*, vol. 2, no. 27, pp. 10380–10393, 2012.
[65] V. Nikulshina and A. Steinfeld, “CO2 capture from air via CaO-carbonation using a solar-driven fluidized bed reactor—Effect of temperature and water vapor concentration,” *Chem. Eng. J.*, vol. 155, no. 3, pp. 867–873, 2009.
[66] V. Nikulshina, C. Gebald, and A. Steinfeld, “CO2 capture from atmospheric air via consecutive CaO-carbonation and CaCO3-calcination cycles in a fluidized-bed solar reactor,” *Chem. Eng. J.*, vol. 146, no. 2, pp. 244–248, 2009.
[67] M. Erans, S. A. Nabavi, and V. Manović, “Carbonation of lime-based materials under ambient conditions for direct air capture,” *J. Clean. Prod.*, vol. 242, p. 118330, 2020.
[68] B. J. McBride, M. J. Zehe, and S. Gordon, “NASA Glenn Coefficients for Calculating Thermodynamic Properties of Individual Species.” Cleveland, Ohio, 2002.
[69] M. Gigantino, D. Kiwic, and A. Steinfeld, “Thermochemical energy storage via isothermal carbonation-calcination cycles of MgO-stabilized SrO in the range of 1000–1100 °C,” *Sol. Energy*, vol. 188, no. May, pp. 720–729, 2019.
[70] L. André and S. Abanades, “Recent Advances in Thermochemical Energy Storage via Solid–Gas Reversible Reactions at High Temperature,” *Energies*, vol. 13, no. 22, p. 5859, Nov. 2020.
[71] D. W. Keith, G. Holmes, D. St. Angelo, and K. Heidel, “A Process for Capturing CO2 from the Atmosphere,” *Joule*, vol. 2, no. 8, pp. 1573–1594, 2018.
[72] R. Sen, A. Goeppert, S. Kar, and G. K. S. Prakash, “Hydroxide Based Integrated CO 2 Capture from Air and Conversion to Methanol,” *J. Am. Chem. Soc.*, p. jacs.9b12711, 2020.
[73] E. S. Sanz-Pérez, C. R. Murdock, S. A. Didas, and C. W. Jones, “Direct Capture of CO2 from Ambient Air,” *Chem. Rev.*, vol. 116, no. 19, pp. 11840–11876, Oct. 2016.
[74] A. Gambhir and M. Tavoni, “Direct Air Carbon Capture and Sequestration: How It Works and How It Could Contribute to Climate-Change Mitigation,” *One Earth*, vol. 1, no. 4, pp. 405–409, 2019.
[75] C. M. Matty, “Overview of Long-Term Lithium Hydroxide Storage aboard the International Space Station.” SAE International , 2008.

[76] C. M. Matty, “Overview of Carbon Dioxide Control Issues During International Space Station/Space Shuttle Joint Docked Operations,” in *40th International Conference on Environmental Systems*, American Institute of Aeronautics and Astronautics, 2010.
[77] B. Feng, H. An, and E. Tan, “Screening of CO2 adsorbing materials for zero emission power generation systems,” *Energy and Fuels*, vol. 21, no. 2, pp. 426–434, 2007.
[78] Y. Duan, B. Zhang, D. C. Sorescu, and J. K. Johnson, “{CO2} capture properties of {M--C--O--H} {(M=Li}, Na, K) systems: A combined density functional theory and lattice phonon dynamics study,” *J. Solid State Chem.*, vol. 184, no. 2, pp. 304–311, Feb. 2011.
[79] Y. C. Park *et al.*, “Test operation results of the 10 MWe-scale dry-sorbent CO2 capture process integrated with a real coal-fired power plant in Korea,” *Energy Procedia*, vol. 63, pp. 2261–2265, 2014.
[80] S. Bin Jo *et al.*, “Regenerable potassium-based alumina sorbents prepared by CO2 thermal treatment for post-combustion carbon dioxide capture,” *Korean J. Chem. Eng.*, vol. 33, no. 11, pp. 3207–3215, 2016.
[81] C.-K. Yi, S.-H. Jo, Y. Seo, J.-B. Lee, and C.-K. Ryu, “Continuous operation of the potassium-based dry sorbent CO2 capture process with two fluidized-bed reactors,” *Int. J. Greenh. Gas Control*, vol. 1, no. 1, pp. 31–36, 2007.
[82] Y. Liang, D. P. Harrison, R. P. Gupta, D. A. Green, and W. J. McMichael, “Carbon Dioxide Capture Using Dry Sodium-Based Sorbents,” *Energy & Fuels*, vol. 18, no. 2, pp. 569–575, Mar. 2004.
[83] S. C. Lee, B. Y. Choi, S. J. Lee, S. Y. Jung, C. K. Ryu, and J. C. Kim, “CO2 Absorption and Regeneration using Na and K Based Sorbents,” in *Carbon Dioxide Utilization for Global Sustainability*, vol. 153, S.-E. Park, J.-S. Chang, and K.-W. B. T.-S. in S. S. and C. Lee, Eds. Elsevier, 2004, pp. 527–530.
[84] C. Qin, J. Yin, J. Ran, L. Zhang, and B. Feng, “Effect of support material on the performance of K2CO3-based pellets for cyclic CO2 capture,” *Appl. Energy*, vol. 136, pp. 280–288, 2014.
[85] S. Sengupta *et al.*, “Circulating Fluid-Bed Studies for CO2 Capture from Flue Gas using K2CO3/Al2O3 Adsorbent,” *Energy and Fuels*, vol. 32, no. 8, pp. 8594–8604, 2018.
[86] C. Zhao *et al.*, “Capturing CO2 in flue gas from fossil fuel-fired power plants using dry regenerable alkali metal-based sorbent,” *Prog. Energy Combust. Sci.*, vol. 39, no. 6, pp. 515–534, 2013.
[87] R. D. Shannon, “Revised effective ionic radii in halides and chalcogenides,” *Acta Crystallogr.*, no. A32, p. 751, 1976.
[88] R. Besson and L. Favergeon, “Atomic-scale study of calcite nucleation in calcium oxide,” *J. Phys. Chem. C*, vol. 117, no. 17, pp. 8813–8821, 2013.
[89] M. Zhang, J. Li, J. Zhao, Y. Cui, and X. Luo, “Comparison of CH4 and CO2 Adsorptions onto Calcite(10.4), Aragonite(011)Ca, and Vaterite(010)CO3 Surfaces: An MD and DFT Investigation,” *ACS Omega*, vol. 5, no. 20, pp. 11369–11377, May 2020.
[90] M. Maciejewski and A. Reller, “Formation of Amorphous Caco3 during the Reaction of Co2 with Cao,” *Thermochim. Acta*, vol. 142, no. 1, pp. 175–188, 1989.
[91] P. Sun, J. R. Grace, C. J. Lim, and E. J. Anthony, “Determination of intrinsic rate constants of the CaO-CO2 reaction,” *Chem. Eng. Sci.*, vol. 63, no. 1, pp. 47–56, 2008.
[92] F. C. Yu and L. S. Fan, “Kinetic study of high-pressure carbonation reaction of calcium-based sorbents in the calcium looping process (CLP),” *Ind. Eng. Chem. Res.*, vol. 50, no. 20, pp. 11528–11536, 2011.
[93] M. Alonso, Y. A. Criado, J. C. Abanades, and G. Grasa, “Undesired effects in the determination of CO2 carrying capacities of CaO during TG testing,” *Fuel*, vol. 127, pp. 52–61, 2014.

[94] L. Rouchon, L. Favergeon, and M. Pijolat, “Analysis of the kinetic slowing down during carbonation of CaO by CO2,” *J. Therm. Anal. Calorim.*, vol. 113, no. 3, pp. 1145–1155, 2013.
[95] L. Rouchon, L. Favergeon, and M. Pijolat, “New kinetic model for the rapid step of calcium oxide carbonation by carbon dioxide,” *J. Therm. Anal. Calorim.*, vol. 116, no. 3, pp. 1181–1188, 2014.
[96] L. Fedunik-Hofman, A. Bayon, and S. W. Donne, “Kinetics of solid-gas reactions and their application to carbonate looping systems,” *Energies*, vol. 12, no. 15, 2019.
[97] A. Biasin, C. U. Segre, and M. Strumendo, “CaCO3 Crystallite Evolution during CaO Carbonation: Critical Crystallite Size and Rate Constant Measurement by In-Situ Synchrotron Radiation X-ray Powder Diffraction,” *Cryst. Growth Des.*, vol. 15, no. 11, pp. 5188–5201, 2015.
[98] M. Ramezani, P. Tremain, E. Doroodchi, and B. Moghtaderi, “Determination of Carbonation/Calcination Reaction Kinetics of a Limestone Sorbent in low CO2 Partial Pressures Using TGA Experiments,” *Energy Procedia*, vol. 114, pp. 259–270, 2017.
[99] Y. Li, Z. Li, H. Wang, and N. Cai, “CaO carbonation kinetics determined using micro-fluidized bed thermogravimetric analysis,” *Fuel*, vol. 264, no. May 2019, 2020.
[100] A. Scaltsoyiannes, A. Antzaras, G. Koilaridis, and A. Lemonidou, “Towards a generalized carbonation kinetic model for CaO-based materials using a modified random pore model,” *Chem. Eng. J.*, vol. 407, p. 127207, 2021.
[101] R. Barker, “The reversibility of the reaction CaCO3 ⇄ CaO+CO2,” *J. Appl. Chem. Biotechnol.*, vol. 23, no. 10, pp. 733–742, Oct. 1973.
[102] D. Alvarez and J. Carlos Abanades, “Determination of the critical product layer thickness in the reaction of CaO with CO2,” *Ind. Eng. Chem. Res.*, vol. 44, no. 15, pp. 5608–5615, 2005.
[103] G. Grasa, R. Murillo, M. Alonso, and J. C. Abanades, “Application of the Random Pore Model to the Carbonation Cyclic Reaction,” *Aiche J.*, vol. 55, no. 5, pp. 1246–1255, 2009.
[104] H. Sun *et al.*, “Fundamental studies of carbon capture using CaO-based materials,” *J. Mater. Chem. A*, vol. 7, no. 16, pp. 9977–9987, 2019.
[105] A. Biasin, C. U. Segre, G. Salviulo, F. Zorzi, and M. Strumendo, “Investigation of CaO-CO2 reaction kinetics by in-situ XRD using synchrotron radiation,” *Chem. Eng. Sci.*, vol. 127, pp. 13–24, 2015.
[106] Z. Li, F. Fang, X. Tang, and N. Cai, “Effect of Temperature on the Carbonation Reaction of CaO with CO2,” *Energy & Fuels*, vol. 26, no. 4, pp. 2473–2482, Apr. 2012.
[107] D. Mess, A. F. Sarofim, and J. P. Longwell, “Product layer diffusion during the reaction of calcium oxide with carbon dioxide,” *Energy {&} Fuels*, vol. 13, no. 5, pp. 999–1005, 1999.
[108] Z. Li, H. Sun, and N. Cai, “Rate Equation Theory for the Carbonation Reaction of CaO with CO2,” *Energy & Fuels*, vol. 26, no. 7, pp. 4607–4616, Jul. 2012.
[109] Z. Sun, S. Luo, P. Qi, and L.-S. Fan, “Ionic diffusion through Calcite (CaCO3) layer during the reaction of CaO and CO2,” *Chem. Eng. Sci.*, vol. 81, pp. 164–168, Oct. 2012.
[110] S. K. Bhatia and D. D. Perlmutter, “Effect of the Product Layer on the Kinetics of the Co2-Lime Reaction,” *Aiche J.*, vol. 29, no. 1, pp. 79–86, 1983.
[111] T. C. Labotka, D. R. Cole, L. R. Riciputi, and M. Fayek, “Diffusion of C and O in calcite from 0.1 to 200 MPa,” *Am. Mineral.*, vol. 89, no. 5–6, pp. 799–806, May 2004.
[112] R. Besson and L. Favergeon, “Understanding the mechanisms of CaO carbonation: Role of point defects in CaCO3 by atomic-scale simulations,” *J. Phys. Chem. C*, vol. 118, no. 39, pp. 22583–22591, 2014.

[113] E. L. Cussler, “Values of Diffusion Coefficients,” in *Diffusion: Mass Transfer in Fluid Systems*, 3rd ed., E. L. Cussler, Ed. Cambridge: Cambridge University Press, 2009, pp. 117–160.
[114] E. L. Cussler, “Diffusion of Interacting Species,” in *Diffusion: Mass Transfer in Fluid Systems*, 3rd ed., E. L. Cussler, Ed. Cambridge: Cambridge University Press, 2009, pp. 161–210.
[115] H. Wang, Z. Li, and N. Cai, “Multiscale model for steam enhancement effect on the carbonation of CaO particle,” *Chem. Eng. J.*, vol. 394, p. 124892, 2020.
[116] Z. Li, “General rate equation theory for gas–solid reaction kinetics and its application to CaO carbonation,” *Chem. Eng. Sci.*, vol. 227, p. 115902, 2020.
[117] M. Krödel, A. Landuyt, P. M. Abdala, and C. R. Müller, “Mechanistic Understanding of CaO-Based Sorbents for High-Temperature CO2 Capture: Advanced Characterization and Prospects,” *ChemSusChem*, vol. 13, no. 23, pp. 6259–6272, Dec. 2020.
[118] G. S. Grasa and J. C. Abanades, “CO2 capture capacity of CaO in long series of carbonation/calcination cycles,” *Ind. Eng. Chem. Res.*, vol. 45, no. 26, pp. 8846–8851, 2006.
[119] M. A. Naeem *et al.*, “Optimization of the structural characteristics of CaO and its effective stabilization yield high-capacity CO2 sorbents,” *Nat. Commun.*, vol. 9, no. 1, p. 2408, 2018.
[120] A. Kurlov, A. Armutlulu, F. Donat, A. R. Studart, and C. R. Müller, “CaO-Based CO2 Sorbents with a Hierarchical Porous Structure Made via Microfluidic Droplet Templating,” *Ind. Eng. Chem. Res.*, 2020.
[121] C. Chen, S. T. Yang, and W. S. Ahn, “Calcium oxide as high temperature CO 2 sorbent: Effect of textural properties,” *Mater. Lett.*, vol. 75, pp. 140–142, 2012.
[122] J. Chen *et al.*, “Metal-oxide stabilized CaO/CuO Composites for the Integrated Ca/Cu Looping Process,” *Chem. Eng. J.*, vol. 403, p. 126330, 2021.
[123] C. Su, L. Duan, F. Donat, and E. J. Anthony, “From waste to high value utilization of spent bleaching clay in synthesizing high-performance calcium-based sorbent for CO2 capture,” *Appl. Energy*, vol. 210, pp. 117–126, 2018.
[124] S. J. Gregg and J. D. Ramsay, “Adsorption of Carbon Dioxide by Magnesia studied by Use of Infrared and Isotherm Measurements,” *J. Chem. Soc. A Inorganic, Phys. Theor.*, vol. 1, no. 2784, pp. 2784–2787, 1970.
[125] C. L. Soo *et al.*, “Development of Regenerable MgO-Based Sorbent Promoted with K2CO3 for CO2 Capture at Low Temperatures,” *Environ. Sci. Technol.*, vol. 42, no. 8, pp. 2736–2741, 2008.
[126] L. Li *et al.*, “MgO/Al2O3 sorbent for CO2 capture,” *Energy and Fuels*, vol. 24, no. 10, pp. 5773–5780, 2010.
[127] M. Bhagiyalakshmi, J. Y. Lee, and H. T. Jang, “Synthesis of mesoporous magnesium oxide: Its application to CO2 chemisorption,” *Int. J. Greenh. Gas Control*, vol. 4, no. 1, pp. 51–56, 2010.
[128] K. K. Han, Y. Zhou, W. G. Lin, and J. H. Zhu, “One-pot synthesis of foam-like magnesia and its performance in CO2 adsorption,” *Microporous Mesoporous Mater.*, 2013.
[129] W. Gao, T. Zhou, and Q. Wang, “Controlled synthesis of MgO with diverse basic sites and its CO2 capture mechanism under different adsorption conditions,” *Chem. Eng. J.*, vol. 336, no. October 2017, pp. 710–720, 2018.
[130] W. J. Liu, H. Jiang, K. Tian, Y. W. Ding, and H. Q. Yu, “Mesoporous carbon stabilized MgO nanoparticles synthesized by pyrolysis of MgCl2 preloaded waste biomass for highly efficient CO2 capture,” *Environ. Sci. Technol.*, vol. 47, no. 16, pp. 9397–9403, 2013.

[131] R. Philipp and K. Fujimoto, “FTIR spectroscopic study of carbon dioxide adsorption/desorption on magnesia/calcium oxide catalysts,” *J. Phys. Chem.*, vol. 96, no. 22, pp. 9035–9038, 1992.
[132] G. Pacchioni, J. M. Ricart, and F. Illas, “Ab Initio Cluster Model Calculations on the Chemisorption of CO2 and SO2 Probe Molecules on MgO and CaO (100) Surfaces. A Theoretical Measure of Oxide Basicity,” *J. Am. Chem. Soc.*, vol. 116, no. 22, pp. 10152–10158, Nov. 1994.
[133] T. Harada, F. Simeon, E. Z. Hamad, and T. A. Hatton, “Alkali metal nitrate-promoted high-capacity MgO adsorbents for regenerable CO2 capture at moderate temperatures,” *Chem. Mater.*, vol. 27, no. 6, pp. 1943–1949, Mar. 2015.
[134] K. Zhang *et al.*, “Phase Transfer-Catalyzed Fast CO2 Absorption by MgO-Based Absorbents with High Cycling Capacity,” *Adv. Mater. Interfaces*, vol. 1, no. 3, pp. 1–6, 2014.
[135] K. Tanabe and Y. Fukuda, “Basic properties of alkaline earth metal oxides and their catalytic activity in the decomposition of diacetone alcohol,” *React. Kinet. Catal. Lett.*, vol. 1, no. 1, pp. 21–24, 1974.
[136] N. N. A. H. Meis, J. H. Bitter, and K. P. De Jong, “On the influence and role of alkali metals on supported and unsupported activated hydrotalcites for CO2 sorption,” *Ind. Eng. Chem. Res.*, vol. 49, no. 17, pp. 8086–8093, 2010.
[137] M. B. Jensen, L. G. M. Pettersson, O. Swang, and U. Olsbye, “CO2 sorption on MgO and CaO surfaces: A comparative quantum chemical cluster study,” *J. Phys. Chem. B*, vol. 109, no. 35, pp. 16774–16781, 2005.
[138] E. J. Karlsen, M. A. Nygren, and L. G. M. Pettersson, “Comparative study on structures and energetics of NOx, SO x, and COx adsorption on alkaline-earth-metal oxides,” *J. Phys. Chem. B*, vol. 107, no. 31, pp. 7795–7802, 2003.
[139] G. Pacchioni and H. Freund, “Electron Transfer at Oxide Surfaces. The MgO Paradigm: from Defects to Ultrathin Films,” *Chem. Rev.*, vol. 113, no. 6, pp. 4035–4072, Jun. 2013.
[140] A. M. Ruminski, K. J. Jeon, and J. J. Urban, “Size-dependent CO2 capture in chemically synthesized magnesium oxide nanocrystals,” *J. Mater. Chem.*, vol. 21, no. 31, pp. 11486–11491, 2011.
[141] K. K. Han, Y. Zhou, Y. Chun, and J. H. Zhu, “Efficient MgO-based mesoporous CO 2 trapper and its performance at high temperature,” *J. Hazard. Mater.*, vol. 203–204, pp. 341–347, 2012.
[142] S. Jin, K. J. Ko, and C. H. Lee, “Direct formation of hierarchically porous MgO-based sorbent bead for enhanced CO2 capture at intermediate temperatures,” *Chem. Eng. J.*, vol. 371, no. February, pp. 64–77, 2019.
[143] Y. and Z. Duan Keling and Li, Xiaohong S. and King, David L. and Li, Bingyun and Zhao, Lifeng and Xiao, Yunhan, “ab initio Thermodynamic Study of the CO2 Capture Properties of M2CO3 (M = Na, K)- and CaCO3-Promoted MgO Sorbents Towards Forming Double Salts,” *Aerosol Air Qual. Res.*, vol. 14, no. 2, pp. 470–479, 2014.
[144] J. S. Dennis and A. N. Hayhurst, “The effect of CO2 on the kinetics and extent of calcination of limestone and dolomite particles in fluidised beds,” *Chem. Eng. Sci.*, vol. 42, no. 10, pp. 2361–2372, 1987.
[145] C. Song *et al.*, “Decomposition kinetics analysis of doped calcium carbonate nanoparticles with high solar absorptance and cycle stability,” *Chem. Eng. J.*, p. 126282, 2020.
[146] D. T. Beruto, A. W. Searcy, and M. G. Kim, “Microstructure, kinetic, structure, thermodynamic analysis for calcite decomposition: free-surface and powder bed experiments,” *Thermochim. Acta*, vol. 424, no. 1–2, pp. 99–109, 2004.

[147] C. Rodriguez-Navarro, E. Ruiz-Agudo, A. Luque, A. B. Rodriguez-Navarro, and M. Ortega-Huertas, “Thermal decomposition of calcite: Mechanisms of formation and textural evolution of CaO nanocrystals,” *Am. Mineral.*, vol. 94, no. 4, pp. 578–593, 2009.
[148] J. M. Valverde and S. Medina, “Crystallographic transformation of limestone during calcination under CO2,” *Phys. Chem. Chem. Phys.*, vol. 17, no. 34, pp. 21912–21926, 2015.
[149] J. M. Valverde, P. E. Sanchez-Jimenez, and L. A. Perez-Maqueda, “Limestone Calcination Nearby Equilibrium: Kinetics, CaO Crystal Structure, Sintering and Reactivity,” *J. Phys. Chem. C*, vol. 119, no. 4, pp. 1623–1641, Jan. 2015.
[150] J. M. Valverde, “On the negative activation energy for limestone calcination at high temperatures nearby equilibrium,” *Chem. Eng. Sci.*, vol. 132, pp. 169–177, 2015.
[151] S. Dash, M. Kamruddin, P. K. Ajikumar, A. K. Tyagi, and B. Raj, “Nanocrystalline and metastable phase formation in vacuum thermal decomposition of calcium carbonate,” *Thermochim. Acta*, vol. 363, no. 1, pp. 129–135, 2000.
[152] F. Donat and C. R. Müller, “A critical assessment of the testing conditions of CaO-based CO2 sorbents,” *Chem. Eng. J.*, vol. 336, no. November 2017, pp. 544–549, 2018.
[153] J. C. Maya, F. Chejne, and S. K. Bhatia, “On the modeling of the co2-catalyzed sintering of calcium oxide,” *AIChE J.*, vol. 63, no. 8, pp. 3286–3296, Aug. 2017.
[154] J. C. Maya, F. Chejne, C. A. Gómez, and S. K. Bhatia, “Effect of the CaO sintering on the calcination rate of CaCO3 under atmospheres containing CO2,” *AIChE J.*, vol. 64, no. 10, pp. 3638–3648, Oct. 2018.
[155] B. Arias, M. E. Diego, A. Méndez, M. Alonso, and J. C. Abanades, “Calcium looping performance under extreme oxy-fuel combustion conditions in the calciner,” *Fuel*, vol. 222, no. January, pp. 711–717, 2018.
[156] L. M. Romeo *et al.*, “Oxyfuel carbonation/calcination cycle for low Cost CO2 capture in existing power plants,” *Energy Convers. Manag.*, vol. 49, no. 10, pp. 2809–2814, 2008.
[157] J. Parkkinen, K. Myöhänen, J. C. Abanades, B. Arias, and T. Hyppänen, “Modelling a Calciner with High Inlet Oxygen Concentration for a Calcium Looping Process,” *Energy Procedia*, vol. 114, pp. 242–249, 2017.
[158] L. A. Hollingbery and T. R. Hull, “The thermal decomposition of huntite and hydromagnesite—A review,” *Thermochim. Acta*, vol. 509, no. 1, pp. 1–11, 2010.
[159] S. I. Jo *et al.*, “Mechanisms of absorption and desorption of CO2 by molten NaNO3-promoted MgO,” *Phys. Chem. Chem. Phys.*, vol. 19, no. 8, pp. 6224–6232, 2017.
[160] A. Dal Pozzo, A. Armutlulu, M. Rekhtina, P. M. Abdala, and C. R. Müller, “ CO 2 Uptake and Cyclic Stability of MgO-Based CO 2 Sorbents Promoted with Alkali Metal Nitrates and Their Eutectic Mixtures ,” *ACS Appl. Energy Mater.*, vol. 2, no. 2, pp. 1295–1307, Jan. 2019.
[161] J. E. Readman and R. Blom, “The use of in situ powder X-ray diffraction in the investigation of dolomite as a potential reversible high-temperature CO2 sorbent,” *Phys. Chem. Chem. Phys.*, vol. 7, no. 6, pp. 1214–1219, 2005.
[162] T. D. Humphries *et al.*, “Dolomite: A low cost thermochemical energy storage material,” *J. Mater. Chem. A*, vol. 7, no. 3, pp. 1206–1215, 2019.
[163] R. Filitz, A. M. Kierzkowska, M. Broda, and C. R. Müller, “Highly efficient CO 2 sorbents: Development of synthetic, calcium-rich dolomites,” *Environ. Sci. Technol.*, vol. 46, no. 1, pp. 559–565, 2012.
[164] B. Arstad, A. Lind, K. A. Andreassen, J. Pierchala, K. Thorshaug, and R. Blom, “In-situ XRD studies of dolomite based CO2 sorbents,” *Energy Procedia*, vol. 63, no. 1876, pp. 2082–2091, 2014.
[165] J. M. Valverde, P. E. Sanchez-Jimenez, and L. A. Perez-Maqueda, “Ca-looping for

postcombustion CO2 capture: A comparative analysis on the performances of dolomite and limestone," *Appl. Energy*, vol. 138, pp. 202–215, 2015.
[166] A. Coppola, F. Scala, P. Salatino, and F. Montagnaro, "Fluidized bed calcium looping cycles for CO2 capture under oxy-firing calcination conditions: Part 1. Assessment of six limestones," *Chem. Eng. J.*, vol. 231, pp. 537–543, Sep. 2013.
[167] C. Rodriguez-Navarro, K. Kudlacz, and E. Ruiz-Agudo, "The mechanism of thermal decomposition of dolomite: New insights from 2D-XRD and TEM analyses," *Am. Mineral.*, vol. 97, no. 1, pp. 38–51, 2012.
[168] G. Spinolo and U. A. Tamburini, "Dolomite Decomposition to (Ca,Mg)O Solid Solutions: An X-Ray Diffraction Study.Part II.," *Zeitschrift für Naturforsch. A*, vol. 39, no. 10, pp. 981–985, 1984.
[169] G. Spinolo and U. Anselmi-Tamburini, "Nonequilibrium calcium oxide-magnesium oxide solid solutions produced by chemical decomposition," *J. Phys. Chem.*, vol. 93, no. 18, pp. 6837–6843, Sep. 1989.
[170] T. T. Dai, "Decomposition of Group II Carbonates: An Investigation by Transmission Electron Microscopy," University of California, 1981.
[171] T. Takamori and J. J. Boland, "Thermal decomposition mechanism of triple carbonate (Ba,Sr,Ca)CO3," *J. Appl. Phys.*, vol. 64, no. 4, pp. 2130–2133, Aug. 1988.
[172] M. G. KIM, U. DAHMEN, and A. W. SEARCY, "Structural Transformations in the Decomposition of Mg(OH)2 and MgCO3," *J. Am. Ceram. Soc.*, vol. 70, no. 3, pp. 146–154, Mar. 1987.
[173] D. R. Dasgupta, "Oriented Transformation of Magnesite," *Indian J. Phys.*, vol. 38, pp. 623–626, 1964.
[174] D. R. Glasson, "Reactivity of lime and related oxides. VIII. Production of activated lime and magnesia," *J. Appl. Chem.*, vol. 13, no. 3, pp. 111–119, 2007.
[175] D. Beruto, R. Botter, and A. W. Searcy, "Thermodynamics of two, two-dimensional phases formed by carbon dioxide chemisorption on magnesium oxide," *J. Phys. Chem.*, vol. 91, no. 13, pp. 3578–3581, Jun. 1987.
[176] N. Khan, D. Dollimore, K. Alexander, and F. W. Wilburn, "The origin of the exothermic peak in the thermal decomposition of basic magnesium carbonate," *Thermochim. Acta*, vol. 367–368, pp. 321–333, 2001.
[177] M. Rekhtina *et al.*, "Effect of Molten Sodium Nitrate on the Decomposition Pathways of Hydrated Magnesium Hydroxycarbonate to Magnesium Oxide Probed by in Situ Total Scattering," *Nanoscale*, 2020.
[178] M. Samtani, E. Skrzypczak-Janktun, D. Dollimore, and K. Alexander, "Thermal analysis of ground dolomite, confirmation of results using an X-ray powder diffraction methodology," *Thermochim. Acta*, vol. 367–368, pp. 297–309, 2001.
[179] K. Wieczorek-ciurowa, J. Paulik, and F. Paulik, "Influence of foreign materials upon the thermal decomposition of dolomite, calcite and magnesite part I. Influence of sodium chloride," *Thermochim. Acta*, vol. 38, no. 2, pp. 157–164, 1980.
[180] R. M. Mcintosh, J. H. Sharp, and F. W. Wilburn, "The Thermal-Decomposition of Dolomite," *Thermochim. Acta*, vol. 165, no. 2, pp. 281–296, 1990.
[181] E. E. Berger, "Effect of Steam on the Decomposition of Limestone," *Ind. Eng. Chem.*, vol. 19, no. 5, pp. 594–596, 1927.
[182] J. M. Valverde and S. Medina, "Reduction of Calcination Temperature in the Calcium Looping Process for CO2 Capture by Using Helium: In Situ XRD Analysis," *ACS Sustain. Chem. Eng.*, vol. 4, no. 12, pp. 7090–7097, 2016.
[183] K. Dam-Johansen and K. Østergaard, "High-temperature reaction between sulphur dioxide and limestone—I. Comparison of limestones in two laboratory reactors and a pilot plant," *Chem. Eng. Sci.*, vol. 46, no. 3, pp. 827–837, 1991.
[184] E. J. Anthony and D. L. Granatstein, "Sulfation phenomena in fluidized bed

combustion systems," *Prog. Energy Combust. Sci.*, vol. 27, no. 2, pp. 215–236, 2001.
[185] B. R. Stanmore and P. Gilot, "Review--calcination and carbonation of limestone during thermal cycling for CO2 sequestration," *Fuel Process. Technol.*, vol. 86, no. 16, pp. 1707–1743, 2005.
[186] V. Manovic and E. J. Anthony, "Competition of Sulphation and Carbonation Reactions during Looping Cycles for CO, Capture by CaO-Based Sorbents," *J. Phys. Chem. A*, vol. 114, no. 11, pp. 3997–4002, 2010.
[187] S. Chen, C. Qin, T. Deng, J. Yin, and J. Ran, "Particle-scale modeling of the simultaneous carbonation and sulfation in calcium looping for CO2 capture," *Sep. Purif. Technol.*, vol. 252, p. 117439, 2020.
[188] V. Manovic and E. J. Anthony, "Sulfation Performance of CaO-Based Pellets Supported by Calcium Aluminate Cements Designed for High-Temperature CO2 Capture," *Energy {&} Fuels*, vol. 24, pp. 1414–1420, 2010.
[189] M. V Iyer, H. Gupta, B. B. Sakadjian, and L. S. Fan, "Multicyclic study on the simultaneous carbonation and sulfation of high-reactivity CaO," *Ind. {&} Eng. Chem. Res.*, vol. 43, no. 14, pp. 3939–3947, 2004.
[190] J. C. Abanades, G. S. Grasa, and M. Alonso, "Sulfation of CaO particles in a carbonation/calcination loop to capture CO2," *Ind. {&} Eng. Chem. Res.*, vol. 47, no. 5, pp. 1630–1635, 2008.
[191] V. Manovic, E. J. Anthony, and D. Loncarevic, "SO2 Retention by CaO-Based Sorbent Spent in CO2 Looping Cycles," *Ind. Eng. Chem. Res.*, vol. 48, no. 14, pp. 6627–6632, Jul. 2009.
[192] D. He, Y. Shao, C. Qin, G. Pu, J. Ran, and L. Zhang, "Understanding the Sulfation Pattern of CaO-Based Sorbents in a Novel Process for Sequential CO2 and SO2 Capture," *Ind. Eng. Chem. Res.*, vol. 55, no. 39, pp. 10251–10262, 2016.
[193] F. Donat, N. H. Florin, E. J. Anthony, and P. S. Fennell, "Influence of high-temperature steam on the reactivity of CaO sorbent for CO2 capture," *Environ. Sci. Technol.*, vol. 46, no. 2, pp. 1262–1269, 2012.
[194] A. N. Antzara, A. Arregi, E. Heracleous, and A. A. Lemonidou, "In-depth evaluation of a ZrO2 promoted CaO-based CO2 sorbent in fluidized bed reactor tests," *Chem. Eng. J.*, vol. 333, no. October 2017, pp. 697–711, 2018.
[195] H. Dieter, A. R. Bidwe, G. Varela-Duelli, A. Charitos, C. Hawthorne, and G. Scheffknecht, "Development of the calcium looping CO2 capture technology from lab to pilot scale at IFK, University of Stuttgart," *Fuel*, vol. 127, pp. 23–37, 2014.
[196] V. Manovic, P. S. Fennell, M. J. Al-Jeboori, and E. J. Anthony, "Steam-Enhanced Calcium Looping Cycles with Calcium Aluminate Pellets Doped with Bromides," *Ind. Eng. Chem. Res.*, vol. 52, no. 23, pp. 7677–7683, Jun. 2013.
[197] N. Rong, Q. Wang, M. Fang, L. Cheng, Z. Luo, and K. Cen, "Steam Hydration Reactivation of CaO-Based Sorbent in Cyclic Carbonation/Calcination for CO2 Capture," *Energy & Fuels*, vol. 27, no. 9, pp. 5332–5340, Sep. 2013.
[198] A. Coppola, M. Allocca, F. Montagnaro, F. Scala, and P. Salatino, "The effect of steam on CO2 uptake and sorbent attrition in fluidised bed calcium looping: The influence of process conditions and sorbent properties," *Sep. Purif. Technol.*, vol. 189, no. July, pp. 101–107, 2017.
[199] W. Zhang, Y. Li, Z. He, X. Ma, and H. Song, "CO2 capture by carbide slag calcined under high-concentration steam and energy requirement in calcium looping conditions," *Appl. Energy*, vol. 206, pp. 869–878, Nov. 2017.
[200] H. Chen, P. Zhang, Y. Duan, and C. Zhao, "CO2 capture of calcium based sorbents developed by sol–gel technique in the presence of steam," *Chem. Eng. J.*, vol. 295, pp. 218–226, Jul. 2016.
[201] Z. He, Y. Li, W. Zhang, X. Ma, L. Duan, and H. Song, "Effect of re-carbonation on

CO2 capture by carbide slag and energy consumption in the calciner," *Energy Convers. Manag.*, vol. 148, no. Supplement C, pp. 1468–1477, 2017.
[202] A. Recio, S. Liew, D. Lu, R. Rahman, A. Macchi, and J. Hill, "The Effects of Thermal Treatment and Steam Addition on Integrated CuO/CaO Chemical Looping Combustion for CO2 Capture," *Technologies*, vol. 4, no. 2, p. 11, Apr. 2016.
[203] H. Dieter, C. Hawthorne, M. Zieba, and G. Scheffknecht, "Progress in Calcium Looping Post Combustion CO2 Capture: Successful Pilot Scale Demonstration," *Energy Procedia*, vol. 37, pp. 48–56, Jan. 2013.
[204] H. Pawlak-Kruczek, M. Baranowski, and M. Tkaczuk-Serafin, "Impact of SO2 in the Presence of Steam on Carbonation and Sulfation of Calcium Sorbents," *Chem. Eng. Technol.*, vol. 36, no. 9, pp. 1511–1517, Sep. 2013.
[205] M. Shokrollahi Yancheshmeh, H. R. Radfarnia, and M. C. Iliuta, "Influence of steam addition during carbonation or calcination on the CO2 capture performance of Ca9Al6O18[sbnd]CaO sorbent," *J. Nat. Gas Sci. Eng.*, vol. 36, pp. 1062–1069, 2016.
[206] M. Erans *et al.*, "Effect of SO2 and steam on CO2 capture performance of biomass-templated calcium aluminate pellets," *Faraday Discuss.*, vol. 192, no. 0, pp. 97–111, 2016.
[207] P. Sun, J. R. Grace, C. J. Lim, and E. J. Anthony, "Investigation of attempts to improve cyclic CO2 capture by sorbent hydration and modification," *Ind. {&} Eng. Chem. Res.*, vol. 47, no. 6, pp. 2024–2032, 2008.
[208] D. Y. Lu, R. T. Symonds, R. W. Hughes, E. J. Anthony, and A. Macchi, "CO(2) Capture from Simulated Syngas via Cyclic Carbonation/Calcination for a Naturally Occurring Limestone: Pilot-Plant Testing," *Ind. {&} Eng. Chem. Res.*, vol. 48, no. 18, pp. 8431–8440, 2009.
[209] A. Coppola, E. Gais, G. Mancino, F. Montagnaro, F. Scala, and P. Salatino, "Effect of steam on the performance of Ca-based sorbents in calcium looping processes," *Powder Technol.*, vol. 316, pp. 578–584, Jul. 2017.
[210] L. Chen and N. Qian, "The effects of water vapor and coal ash on the carbonation behavior of CaO-sorbent supported by Γ-Al2O3 for CO2 capture," *Fuel Process. Technol.*, vol. 177, no. April, pp. 200–209, 2018.
[211] Y. Liu, X. Yang, L. Zhao, F. Lei, and Y. Xiao, "Effects of steam on CO2 absorption ability of calcium-based sorbent modified by peanut husk ash," *Sci. China Technol. Sci.*, vol. 60, no. 6, pp. 953–962, 2017.
[212] Y.-C. Chou, J.-Y. Cheng, W.-H. Liu, and H.-W. Hsu, "Effects of Steam Addition during Calcination on Carbonation Behavior in a Calcination/Carbonation Loop," *Chem. Eng. Technol.*, vol. 41, no. 10, pp. 1921–1927, Oct. 2018.
[213] Z. He, Y. Li, X. Ma, W. Zhang, C. Chi, and Z. Wang, "Influence of steam in carbonation stage on CO2 capture by Ca-based industrial waste during calcium looping cycles," *Int. J. Hydrogen Energy*, vol. 41, no. 7, pp. 4296–4304, Feb. 2016.
[214] S. Dobner, L. Sterns, R. A. Graff, and A. M. Squires, "Cyclic Calcination and Recarbonation of Calcined Dolomite," *Ind. Eng. Chem. Process Des. Dev.*, vol. 16, no. 4, pp. 479–486, Oct. 1977.
[215] M. Kavosh, K. Patchigolla, E. J. Anthony, and J. E. Oakey, "Carbonation performance of lime for cyclic CO2 capture following limestone calcination in steam/CO2 atmosphere," *Appl. Energy*, vol. 131, pp. 499–507, Oct. 2014.
[216] B. González, J. Blamey, M. J. Al-Jeboori, N. H. Florin, P. T. Clough, and P. S. Fennell, "Additive effects of steam addition and HBr doping for CaO-based sorbents for CO2 capture," *Chem. Eng. Process. Process Intensif.*, vol. 103, pp. 21–26, May 2016.
[217] B. Arias, M. Alonso, and C. Abanades, "CO2 Capture by Calcium Looping at Relevant Conditions for Cement Plants: Experimental Testing in a 30 kWth Pilot Plant," *Ind. Eng. Chem. Res.*, vol. 56, no. 10, pp. 2634–2640, Mar. 2017.

[218] R. T. Symonds, D. Y. Lu, V. Manovic, and E. J. Anthony, “Pilot-Scale Study of CO2 Capture by CaO-Based Sorbents in the Presence of Steam and SO2,” *Ind. Eng. Chem. Res.*, vol. 51, no. 21, pp. 7177–7184, May 2012.
[219] G. Duelli (Varela), A. Charitos, M. E. Diego, E. Stavroulakis, H. Dieter, and G. Scheffknecht, “Investigations at a 10 kWth calcium looping dual fluidized bed facility: Limestone calcination and CO2 capture under high CO2 and water vapor atmosphere,” *Int. J. Greenh. Gas Control*, vol. 33, pp. 103–112, Feb. 2015.
[220] C. Wang and L. Chen, “The effect of steam on simultaneous calcination and sulfation of limestone in CFBB,” *Fuel*, vol. 175, pp. 164–171, Jul. 2016.
[221] W. H. Maclntire and T. B. Stansel, “Steam Catalysis in Calcinations of Dolomite and Limestone Fines,” *Ind. {&} Eng. Chem.*, vol. 45, no. 7, pp. 1548–1555, 1953.
[222] S. Zarghami, E. Ghadirian, H. Arastoopour, and J. Abbasian, “Effect of Steam on Partial Decomposition of Dolomite,” *Ind. Eng. Chem. Res.*, vol. 54, no. 20, pp. 5398–5406, May 2015.
[223] Y. Wang and W. J. Thomson, “The effects of steam and carbon dioxide on calcite decomposition using dynamic X-ray diffraction,” *Chem. Eng. Sci.*, vol. 50, no. 9, pp. 1373–1382, May 1995.
[224] Z. Li *et al.*, “Limestone Decomposition in an O2/CO2/Steam Atmosphere Integrated with Coal Combustion,” *Energy & Fuels*, vol. 30, no. 6, pp. 5092–5100, Jun. 2016.
[225] J. M. Valverde and S. Medina, “Limestone calcination under calcium-looping conditions for CO2 capture and thermochemical energy storage in the presence of H2O: An in situ XRD analysis,” *Phys. Chem. Chem. Phys.*, vol. 19, no. 11, pp. 7587–7596, 2017.
[226] A. Coppola, A. Esposito, F. Montagnaro, M. Iuliano, F. Scala, and P. Salatino, “The combined effect of H2O and SO2 on CO2 uptake and sorbent attrition during fluidised bed calcium looping,” *Proc. Combust. Inst.*, vol. 37, no. 4, pp. 4379–4387, 2019.
[227] S. Champagne, D. Y. Lu, A. MacChi, R. T. Symonds, and E. J. Anthony, “Influence of steam injection during calcination on the reactivity of CaO-based sorbent for carbon capture,” *Ind. Eng. Chem. Res.*, vol. 52, no. 6, pp. 2241–2246, 2013.
[228] S. Champagne, D. Y. Lu, R. T. Symonds, A. Macchi, and E. J. Anthony, “The effect of steam addition to the calciner in a calcium looping pilot plant,” *Powder Technol.*, vol. 290, pp. 114–123, Mar. 2016.
[229] L. Zhang, B. Zhang, Z. Yang, and M. Guo, “The Role of Water on the Performance of Calcium Oxide-Based Sorbents for Carbon Dioxide Capture: A Review,” *Energy Technol.*, vol. 3, no. 1, pp. 10–19, 2015.
[230] B. Arias, G. Grasa, J. C. Abanades, V. Manovic, and E. J. Anthony, “The Effect of Steam on the Fast Carbonation Reaction Rates of CaO,” *Ind. Eng. Chem. Res.*, vol. 51, no. 5, pp. 2478–2482, Feb. 2012.
[231] M. Broda, V. Manovic, E. J. Anthony, and C. R. Müller, “Effect of Pelletization and Addition of Steam on the Cyclic Performance of Carbon-Templated, CaO-Based CO2 Sorbents,” *Environ. Sci. Technol.*, vol. 48, no. 9, pp. 5322–5328, May 2014.
[232] V. Manovic and E. J. Anthony, “Carbonation of CaO-Based Sorbents Enhanced by Steam Addition,” *Ind. {&} Eng. Chem. Res.*, vol. 49, no. 19, pp. 9105–9110, 2010.
[233] B. González, W. Liu, D. S. Sultan, and J. S. Dennis, “The effect of steam on a synthetic Ca-based sorbent for carbon capture,” *Chem. Eng. J.*, vol. 285, pp. 378–383, Feb. 2016.
[234] J. Blamey, M. J. Al-Jeboori, V. Manovic, P. S. Fennell, and E. J. Anthony, “CO2 capture by calcium aluminate pellets in a small fluidized bed,” *Fuel Process. Technol.*, vol. 142, pp. 100–106, 2016.
[235] C. Wang, X. Zhou, L. Jia, and Y. Tan, “Sintering of Limestone in Calcination/Carbonation Cycles,” *Ind. Eng. Chem. Res.*, vol. 53, no. 42, pp. 16235–16244, Oct. 2014.

[236] J. Dong, Y. Tang, A. Nzihou, and E. Weiss-Hortala, “Effect of steam addition during carbonation, calcination or hydration on re-activation of CaO sorbent for CO2 capture,” *J. CO2 Util.*, vol. 39, p. 101167, 2020.
[237] S. J. Yang and Y. H. Xiao, “Steam catalysis in CaO carbonation under low steam partial pressure,” *Ind. {&} Eng. Chem. Res.*, vol. 47, no. 12, pp. 4043–4048, 2008.
[238] G. Giammaria and L. Lefferts, “Catalytic effect of water on calcium carbonate decomposition,” *J. CO2 Util.*, vol. 33, pp. 341–356, Oct. 2019.
[239] J. Yin, X. Kang, C. Qin, B. Feng, A. Veeraragavan, and D. Saulov, “Modeling of CaCO3 decomposition under CO2/H2O atmosphere in calcium looping processes,” *Fuel Process. Technol.*, vol. 125, pp. 125–138, Sep. 2014.
[240] D. He, Z. Ou, C. Qin, T. Deng, J. Yin, and G. Pu, “Understanding the catalytic acceleration effect of steam on CaCO3 decomposition by density function theory,” *Chem. Eng. J.*, vol. 379, no. July 2019, 2020.
[241] Y. Fan *et al.*, “Pressurized calcium looping in the presence of steam in a spout-fluidized-bed reactor with DFT analysis,” *Fuel Process. Technol.*, vol. 169, no. July 2017, pp. 24–41, 2018.
[242] Z. Li, Y. Liu, and N. Cai, “Understanding the enhancement effect of high-temperature steam on the carbonation reaction of CaO with CO2,” *Fuel*, vol. 127, pp. 88–93, Jul. 2014.
[243] Z.-H. Li, Y. Wang, K. Xu, J.-Z. Yang, S.-B. Niu, and H. Yao, “Effect of steam on CaO regeneration, carbonation and hydration reactions for CO2 capture,” *Fuel Process. Technol.*, vol. 151, pp. 101–106, Oct. 2016.
[244] B. Dou, Y. Song, Y. Liu, and C. Feng, “High temperature CO2 capture using calcium oxide sorbent in a fixed-bed reactor,” *J. Hazard. Mater.*, vol. 183, no. 1–3, pp. 759–765, Nov. 2010.
[245] V. Materić, B. Ingham, and R. Holt, “In situ synchrotron XRD investigation of the dehydration and high temperature carbonation of Ca(OH)2,” *CrystEngComm*, vol. 17, no. 38, pp. 7306–7315, 2015.
[246] I. Lindén, P. Backman, A. Brink, and M. Hupa, “Influence of water vapor on carbonation of CaO in the temperature range 400-550 °c,” *Ind. Eng. Chem. Res.*, vol. 50, no. 24, pp. 14115–14120, 2011.
[247] J. Blamey, V. Manovic, E. J. Anthony, D. R. Dugwell, and P. S. Fennell, “On steam hydration of CaO-based sorbent cycled for CO2 capture,” *Fuel*, vol. 150, pp. 269–277, 2015.
[248] A. Coppola, L. Palladino, F. Montagnaro, F. Scala, and P. Salatino, “Reactivation by steam hydration of sorbents for fluidized-bed calcium looping,” *Energy and Fuels*, vol. 29, no. 7, pp. 4436–4446, 2015.
[249] C. C. Li, J. Y. Cheng, W. H. Liu, C. M. Huang, H. W. Hsu, and H. P. Lin, “Enhancement in cyclic stability of the CO2 adsorption capacity of CaO-based sorbents by hydration for the calcium looping cycle,” *J. Taiwan Inst. Chem. Eng.*, vol. 45, no. 1, pp. 227–232, 2014.
[250] V. Manovic and E. J. Anthony, “Steam reactivation of spent CaO-based sorbent for multiple CO2 capture cycles,” *Environ. Sci. Technol.*, vol. 41, no. 4, pp. 1420–1425, 2007.
[251] J. Blamey, N. P. M. Paterson, D. R. Dugwell, P. Stevenson, and P. S. Fennell, “Reactivation of a CaO-based sorbent for CO2 capture from stationary sources,” *Proc. Combust. Inst.*, vol. 33, no. 2, pp. 2673–2681, 2011.
[252] R. W. Hughes, D. Lu, E. J. Anthony, and Y. H. Wu, “Improved long-term conversion of limestone-derived sorbents for in situ capture of CO2 in a fluidized bed combustor,” *Ind. {&} Eng. Chem. Res.*, vol. 43, no. 18, pp. 5529–5539, 2004.
[253] J. Blamey, N. P. M. Paterson, D. R. Dugwell, and P. S. Fennell, “Mechanism of

Particle Breakage during Reactivation of CaO-Based Sorbents for CO2 Capture," *Energy & Fuels*, vol. 24, no. 8, pp. 4605–4616, Aug. 2010.
[254] S. Jin, K. Ho, A. T. Vu, and C. H. Lee, "Salt-Composition-Controlled Precipitation of Triple-Salt-Promoted MgO with Enhanced CO2 Sorption Rate and Working Capacity," *Energy and Fuels*, vol. 31, no. 9, pp. 9725–9735, 2017.
[255] A. T. Vu, K. Ho, S. Jin, and C. H. Lee, "Double sodium salt-promoted mesoporous MgO sorbent with high CO2 sorption capacity at intermediate temperatures under dry and wet conditions," *Chem. Eng. J.*, vol. 291, pp. 161–173, 2016.
[256] X. Yang, L. Zhao, Y. Liu, Z. Sun, and Y. Xiao, "Carbonation performance of NaNO3 modified MgO sorbents," *Ind. Eng. Chem. Res.*, vol. 56, no. 1, pp. 342–350, 2017.
[257] M. K. Ram Reddy, Z. P. Xu, G. Q. Lu, and J. C. Diniz Da Costa, "Influence of water on high-temperature CO2 capture using layered double hydroxide derivatives," *Ind. Eng. Chem. Res.*, vol. 47, no. 8, pp. 2630–2635, 2008.
[258] H. Béarat, M. J. McKelvy, A. V. G. Chizmeshya, R. Sharma, and R. W. Carpenter, "Magnesium Hydroxide Dehydroxylation/Carbonation Reaction Processes: Implications for Carbon Dioxide Mineral Sequestration," *J. Am. Ceram. Soc.*, vol. 85, no. 4, pp. 742–748, 2004.
[259] D. P. Butt *et al.*, "Kinetics of thermal dehydroxylation and carbonation of magnesium hydroxide," *Journal of the American Ceramic Society*, vol. 79, no. 7. pp. 1892–1898, 1996.
[260] M. J. McKelvy, R. Sharma, A. V. G. Chizmeshya, R. W. Carpenter, and K. Streib, "Magnesium hydroxide dehydroxylation: In situ nanoscale observations of lamellar nucleation and growth," *Chem. Mater.*, vol. 13, no. 3, pp. 921–926, 2001.
[261] D. Alvarez and J. C. Abanades, "Pore-size and shape effects on the recarbonation performance of calcium oxide submitted to repeated calcination/recarbonation cycles," *Energy {&} Fuels*, vol. 19, no. 1, pp. 270–278, 2005.
[262] P. Sun, J. R. Grace, C. J. Lim, and E. J. Anthony, "The effect of CaO sintering on cyclic CO2 capture in energy systems," *Aiche J.*, vol. 53, no. 9, pp. 2432–2442, 2007.
[263] J. C. Abanades, "The maximum capture efficiency of CO2 using a carbonation/calcination cycle of CaO/CaCO3," *Chem. Eng. J.*, vol. 90, no. 3, pp. 303–306, 2002.
[264] J. C. Abanades and D. Alvarez, "Conversion Limits in the Reaction of CO2 with Lime," *Energy & Fuels*, vol. 17, no. 2, pp. 308–315, Mar. 2003.
[265] J. S. Wang and E. J. Anthony, "On the decay behavior of the CO2 absorption capacity of CaO-based sorbents," *Ind. {&} Eng. Chem. Res.*, vol. 44, no. 3, pp. 627–629, 2005.
[266] R. M. GERMAN and Z. A. MUNIR, "Surface Area Reduction During Isothermal Sintering," *J. Am. Ceram. Soc.*, vol. 59, no. 9–10, pp. 379–383, 1976.
[267] M. C. Mai and T. F. Edgar, "Surface-Area Evolution of Calcium Hydroxide during Calcination and Sintering," *Aiche J.*, vol. 35, no. 1, pp. 30–36, 1989.
[268] Z. Chen, H. S. Song, M. Portillo, C. J. Lim, J. R. Grace, and E. J. Anthony, "Long-term calcination/carbonation cycling and thermal pretreatment for CO2 capture by limestone and dolomite," *Energy and Fuels*, vol. 23, no. 3, pp. 1437–1444, 2009.
[269] M. Krödel, D. Spescha, F. Donat, and C. R. Müller, "Understanding the fundamental interplay of morphological and structural changes during the carbonation of limestone via quenched CO2 capture experiments in a fluidized bed," *Prep.*, 2021.
[270] D. R. Glasson, "Reactivity of lime and related oxides. VII crystal size variations in calcium oxide produced from limestone," *J. Appl. Chem.*, vol. 11, no. 6, pp. 201–206, 2007.
[271] D. R. Glasson, "Reactivity of lime and related oxides. XVI. Sintering of lime," *J. Appl. Chem.*, vol. 17, no. 4, pp. 91–96, 2007.
[272] C. C. Furnas, "The Rate of Calcination of Limestone," *Ind. Eng. Chem.*, vol. 23, no. 5,

pp. 534–538, May 1931.
[273] E. P. Hyatt, I. B. Cutler, and M. E. Wadsworth, “Carbon Dioxide Atmosphere,” *J. Am. Ceram. Soc.*, vol. 61, no. 1943, pp. 70–74, 1955.
[274] Y. Zhu, S. Wu, and X. Wang, “Nano CaO grain characteristics and growth model under calcination,” *Chem. Eng. J.*, vol. 175, pp. 512–518, 2011.
[275] R. H. Borgwardt, “Sintering of nascent calcium oxide,” *Chem. Eng. Sci.*, vol. 44, no. 1, pp. 53–60, 1989.
[276] R. H. Borgwardt, “Calcium-Oxide Sintering in Atmospheres Containing Water and Carbon-Dioxide,” *Ind. {&} Eng. Chem. Res.*, vol. 28, no. 4, pp. 493–500, 1989.
[277] H. Liu, F. Pan, and S. Wu, “The grain growth mechanism of nano-CaO regenerated by nano-CaCO3 in calcium looping,” *RSC Adv.*, vol. 9, no. 46, pp. 26949–26955, 2019.
[278] Y. Deutsch and L. Heller-Kallai, “Decarbonation and recarbonation of calcites heated m CO2. Part 1. Effect of the thermal regime,” *Thermochim. Acta*, vol. 182, no. 1, pp. 77–89, 1991.
[279] B. Arias, J. C. Abanades, and G. S. Grasa, “An analysis of the effect of carbonation conditions on CaO deactivation curves,” *Chem. Eng. J.*, vol. 167, no. 1, pp. 255–261, 2011.
[280] Y. A. Criado, B. Arias, and J. C. Abanades, “Effect of the Carbonation Temperature on the CO2 Carrying Capacity of CaO,” *Ind. Eng. Chem. Res.*, vol. 57, no. 37, pp. 12595–12599, 2018.
[281] N. H. Florin and A. T. Harris, “Reactivity of CaO derived from nano-sized CaCO3 particles through multiple CO2 capture-and-release cycles,” *Chem. Eng. Sci.*, vol. 64, no. 2, pp. 187–191, 2009.
[282] V. Manovic, E. J. Anthony, G. Grasa, and J. C. Abanades, “CO2 looping cycle performance of a high-purity limestone after thermal activation/doping,” *Energy {&} Fuels*, vol. 22, no. 5, pp. 3258–3264, 2008.
[283] P. Lan and S. Wu, “Mechanism for self-reactivation of nano-CaO-based CO2 sorbent in calcium looping,” *Fuel*, vol. 143, pp. 9–15, 2015.
[284] M. E. Diego, B. Arias, and J. C. Abanades, “Investigation of the dynamic evolution of the CO2 carrying capacity of solids with time in La Pereda 1.7 MWth calcium looping pilot plant,” *Int. J. Greenh. Gas Control*, vol. 92, no. October 2019, p. 102856, 2020.
[285] J. Ströhle, J. Hilz, and B. Epple, “Performance of the carbonator and calciner during long-term carbonate looping tests in a 1 MWth pilot plant,” *J. Environ. Chem. Eng.*, vol. 8, no. 1, p. 103578, 2020.
[286] M. Broda, A. M. Kierzkowska, and C. R. Müller, “Application of the sol-gel technique to develop synthetic calcium-based sorbents with excellent carbon dioxide capture characteristics,” *ChemSusChem*, vol. 5, no. 2, pp. 411–418, 2012.
[287] C. S. Martavaltzi and A. A. Lemonidou, “Development of new CaO based sorbent materials for CO2 removal at high temperature,” *Microporous Mesoporous Mater.*, 2008.
[288] M. Wang, C. G. Lee, and C. K. Ryu, “CO2 sorption and desorption efficiency of Ca2SiO 4,” *Int. J. Hydrogen Energy*, 2008.
[289] L. Hong, A. Khan, S. E. Pratsinis, and P. G. Smirniotis, “Flame-made durable doped-CaO nanosorbents for CO capture,” *Energy and Fuels*, vol. 23, no. 2, pp. 1093–1100, 2009.
[290] V. S. Derevschikov, A. I. Lysikov, and A. G. Okunev, “High temperature CaO/Y2O3 carbon dioxide absorbent with enhanced stability for sorption-enhanced reforming applications,” *Ind. Eng. Chem. Res.*, vol. 50, no. 22, pp. 12741–12749, 2011.
[291] L. Li, D. L. King, Z. Nie, and C. Howard, “Magnesia-stabilized calcium oxide absorbents with improved durability for high temperature CO2 capture,” *Ind. Eng. Chem. Res.*, vol. 48, no. 23, pp. 10604–10613, 2009.

[292] C. Luo, Y. Zheng, N. Ding, and C. Zheng, “Enhanced cyclic stability of CO_2 adsorption capacity of CaO-based sorbents using La_2O_3 or $Ca_{12}Al_{14}O_{33}$ as additives,” *Korean J. Chem. Eng.*, vol. 28, no. 4, pp. 1042–1046, 2011.
[293] N. H. Florin, J. Blamey, and P. S. Fennell, “Synthetic CaO-based sorbent for CO2 capture from large-point sources,” *Energy and Fuels*, vol. 24, no. 8, pp. 4598–4604, 2010.
[294] F. Zeman, “Effect of steam hydration on performance of lime sorbent for CO2 capture,” *Int. J. Greenh. Gas Control*, vol. 2, no. 2, pp. 203–209, 2008.
[295] B. Arias, G. S. Grasa, and J. C. Abanades, “Effect of sorbent hydration on the average activity of CaO in a Ca-looping system,” *Chem. Eng. J.*, vol. 163, no. 3, pp. 324–330, 2010.
[296] R. K. Lyon and J. A. Cole, “Unmixed combustion: an alternative to fire,” *Combust. Flame*, vol. 121, no. 1–2, pp. 249–261, Apr. 2000.
[297] V. Manovic and E. J. Anthony, “Integration of Calcium and Chemical Looping Combustion using Composite CaO / CuO-Based Materials,” pp. 10750–10756, 2011.
[298] V. Manovic and E. J. Anthony, “CaO-based pellets with oxygen carriers and catalysts,” *Energy and Fuels*, vol. 25, no. 10, pp. 4846–4853, 2011.
[299] B. Sarrión *et al.*, “Calcination under low CO2 pressure enhances the calcium Looping performance of limestone for thermochemical energy storage,” *Chem. Eng. J.*, p. 127922, 2020.
[300] C. Ortiz, M. C. Romano, J. M. Valverde, M. Binotti, and R. Chacartegui, “Process integration of Calcium-Looping thermochemical energy storage system in concentrating solar power plants,” *Energy*, vol. 155, pp. 535–551, 2018.
[301] R. Chacartegui, A. Alovisio, C. Ortiz, J. M. Valverde, V. Verda, and J. A. Becerra, “Thermochemical energy storage of concentrated solar power by integration of the calcium looping process and a CO2 power cycle,” *Appl. Energy*, vol. 173, pp. 589–605, 2016.
[302] B. Sarrión, A. Perejón, P. E. Sánchez-Jiménez, L. A. Pérez-Maqueda, and J. M. Valverde, “Role of calcium looping conditions on the performance of natural and synthetic Ca-based materials for energy storage,” *J. CO2 Util.*, vol. 28, no. June, pp. 374–384, 2018.
[303] E. P. Reddy and P. G. Smirniotis, “High-temperature sorbents for CO2 made of alkali metals doped on CaO supports,” *J. Phys. Chem. B*, vol. 108, no. 23, pp. 7794–7800, 2004.
[304] N. H. Florin and A. T. Harris, “Screening CaO-Based sorbents for Co-2 capture in biomass gasifiers,” *Energy {&} Fuels*, vol. 22, no. 4, pp. 2734–2742, 2008.
[305] V. S. Derevschikov, A. I. Lysikov, and A. G. Okunev, “Sorption properties of lithium carbonate doped CaO and its performance in sorption enhanced methane reforming,” *Chem. Eng. Sci.*, vol. 66, no. 13, pp. 3030–3038, Jul. 2011.
[306] C. Salvador, D. Lu, E. J. Anthony, and J. C. Abanades, “Enhancement of CaO for CO2 capture in an FBC environment,” *Chem. Eng. J.*, vol. 96, no. 1–3, pp. 187–195, 2003.
[307] Y. Xu *et al.*, “NaBr-Enhanced CaO-Based Sorbents with a Macropore-Stabilized Microstructure for CO2 Capture,” *Energy and Fuels*, vol. 32, no. 8, pp. 8571–8578, 2018.
[308] Y. Xu *et al.*, “Potential Synergy of Chlorine and Potassium and Sodium Elements in Carbonation Enhancement of CaO-Based Sorbents,” *ACS Sustain. Chem. Eng.*, vol. 6, no. 9, pp. 11677–11684, 2018.
[309] L. Morona, M. Erans, and D. P. Hanak, “Effect of Seawater, Aluminate Cement, and Alumina-Rich Spinel on Pelletized CaO-Based Sorbents for Calcium Looping,” *Ind. Eng. Chem. Res.*, vol. 58, no. 27, pp. 11910–11919, 2019.
[310] C. Chi, Y. Li, R. Sun, X. Ma, L. Duan, and Z. Wang, “HCl removal performance of

Mg-stabilized carbide slag from carbonation/calcination cycles for CO2 capture," *RSC Adv.*, vol. 6, no. 106, pp. 104303–104310, 2016.
[311] Y. Xu, C. Luo, Y. Zheng, H. Ding, and L. Zhang, "Macropore-Stabilized Limestone Sorbents Prepared by the Simultaneous Hydration-Impregnation Method for High-Temperature CO2 Capture," *Energy and Fuels*, vol. 30, no. 4, pp. 3219–3226, 2016.
[312] Y. Xu, C. Luo, Y. Zheng, H. Ding, D. Zhou, and L. Zhang, "Natural Calcium-Based Sorbents Doped with Sea Salt for Cyclic CO2 Capture," *Chem. Eng. Technol.*, vol. 40, no. 3, pp. 522–528, Mar. 2017.
[313] B. González, J. Kokot-Blamey, and P. Fennell, "Enhancement of CaO-based sorbent for CO2 capture through doping with seawater," *Greenh. Gases Sci. Technol.*, vol. n/a, no. n/a, Jun. 2020.
[314] J.-W. Kim and H.-G. Lee, "Thermal and carbothermic decomposition of Na2CO3 and Li2CO3," *Metall. Mater. Trans. B*, vol. 32, no. 1, pp. 17–24, 2001.
[315] R. L. Lehman, J. S. Gentry, and N. G. Glumac, "Thermal stability of potassium carbonate near its melting point," *Thermochim. Acta*, vol. 316, no. 1, pp. 1–9, 1998.
[316] X. Jiang, J. Zhu, Z. Liu, S. Guo, and W. Jin, "CO2-Tolerant SrFe0.8Nb0.2O3−δ–Carbonate Dual-Phase Multichannel Hollow Fiber Membrane for CO2 Capture," *Ind. Eng. Chem. Res.*, vol. 55, no. 12, pp. 3300–3307, Mar. 2016.
[317] C. Chen, T. Tran, R. Olivares, S. Wright, and S. Sun, "Coupled Experimental Study and Thermodynamic Modeling of Melting Point and Thermal Stability of Li2CO3-Na2CO3-K2CO3 Based Salts," *J. Sol. Energy Eng.*, vol. 136, no. 3, May 2014.
[318] R. I. Olivares, C. Chen, and S. Wright, "The Thermal Stability of Molten Lithium–Sodium–Potassium Carbonate and the Influence of Additives on the Melting Point," *J. Sol. Energy Eng.*, vol. 134, no. 4, Jun. 2012.
[319] C. Winbo, E. Rosén, and M. Heim, "Thermal Analytical Study of the Decomposition of K2Ca2(CO3)3," *Acta Chem. Scand.*, vol. 52, pp. 431–434, 1998.
[320] A. Navrotsky, R. L. Putnam, C. Winbo, and E. Rosén, "Thermochemistry of double carbonates in the K2CO3-CaCO3 system," *Am. Mineral.*, vol. 82, no. 5–6, pp. 546–548, 1997.
[321] C. H. Lee *et al.*, "Na2CO3-doped CaO-based high-temperature CO2 sorbent and its sorption kinetics," *Chem. Eng. J.*, vol. 352, no. April, pp. 103–109, 2018.
[322] C. H. Lee, S. Mun, and K. B. Lee, "Characteristics of Na-Mg double salt for high-temperature CO2 sorption," *Chem. Eng. J.*, vol. 258, pp. 367–373, 2014.
[323] K. Zhang, X. S. Li, H. Chen, P. Singh, and D. L. King, "Molten Salt Promoting Effect in Double Salt CO2 Absorbents," *J. Phys. Chem. C*, vol. 120, no. 2, pp. 1089–1096, Jan. 2016.
[324] J.-S. Kwak, K.-R. Oh, K.-Y. Kim, J.-M. Lee, and Y.-U. Kwon, "CO2 absorption and desorption characteristics of MgO-based absorbent promoted by triple eutectic alkali carbonate," *Phys. Chem. Chem. Phys.*, vol. 21, no. 37, pp. 20805–20813, 2019.
[325] C. H. Lee, H. J. Kwon, H. C. Lee, S. Kwon, S. G. Jeon, and K. B. Lee, "Effect of pH-controlled synthesis on the physical properties and intermediate-temperature CO2 sorption behaviors of K–Mg double salt-based sorbents," *Chem. Eng. J.*, vol. 294, pp. 439–446, 2016.
[326] A. Al-Mamoori, H. Thakkar, X. Li, A. A. Rownaghi, and F. Rezaei, "Development of Potassium- and Sodium-Promoted CaO Adsorbents for CO2 Capture at High Temperatures," *Ind. Eng. Chem. Res.*, vol. 56, no. 29, pp. 8292–8300, 2017.
[327] L. Huang *et al.*, "Alkali Carbonate Molten Salt Coated Calcium Oxide with Highly Improved Carbon Dioxide Capture Capacity," *Energy Technol.*, vol. 5, no. 8, pp. 1328–1336, Aug. 2017.
[328] L. Huang *et al.*, "Revealing how molten salts promote CO 2 capture on CaO: Via an impedance study and sorption kinetics simulation," *Sustain. Energy Fuels*, vol. 2, no. 1,

pp. 68–72, 2018.
[329] M. Krödel *et al.*, “Na K-edge XANES combined with 23Na-NMR and in-situ XRD unravel structure-property relationships in Na2CO3-promoted CaO-based sorbents for CO2 capture,” *submitted*, 2021.
[330] A. Kurlov, A. M. Kierzkowska, T. Huthwelker, P. M. Abdala, and C. R. Müller, “Na2CO3-modified CaO-based CO2 sorbents: the effects of structure and morphology on CO2 uptake,” *Phys. Chem. Chem. Phys.*, vol. 22, no. 42, pp. 24697–24703, 2020.
[331] C. M. C. Soares, S. G. Patrício, F. M. L. Figueiredo, and F. M. B. Marques, “Relevance of the ceramic content on dual oxide and carbonate-ion transport in composite membranes,” *Int. J. Hydrogen Energy*, vol. 39, no. 10, pp. 5424–5432, 2014.
[332] A. T. Ward and G. J. Janz, “Molten carbonate electrolytes: Electrical conductance, density and surface tension of binary and ternary mixtures,” *Electrochim. Acta*, vol. 10, no. 8, pp. 849–857, 1965.
[333] G. A. Mutch, L. Qu, G. Triantafyllou, W. Xing, M. L. Fontaine, and I. S. Metcalfe, “Supported molten-salt membranes for carbon dioxide permeation,” *J. Mater. Chem. A*, vol. 7, no. 21, pp. 12951–12973, 2019.
[334] J. Fang, N. Xu, T. Yang, P. Zhang, J. Tong, and K. Huang, “CO2 capture performance of silver-carbonate membrane with electrochemically dealloyed porous silver matrix,” *J. Memb. Sci.*, vol. 523, pp. 439–445, 2017.
[335] K. Laursen, J. R. Grace, and C. J. Lim, “Enhancement of the Sulfur Capture Capacity of Limestones by the Addition of Na2CO3 and NaCl,” *Environ. Sci. Technol.*, vol. 35, no. 21, pp. 4384–4389, Nov. 2001.
[336] K. Laursen, A. A. Kern, J. R. Grace, and C. J. Lim, “Characterization of the Enhancement Effect of Na2CO3 on the Sulfur Capture Capacity of Limestones,” *Environ. Sci. Technol.*, vol. 37, no. 16, pp. 3709–3715, Aug. 2003.
[337] R. Han, F. Sun, J. Gao, S. Wei, Y. Su, and Y. Qin, “Trace Na2CO3 Addition to Limestone Inducing High-Capacity SO2 Capture,” *Environ. Sci. Technol.*, vol. 51, no. 21, pp. 12692–12698, 2017.
[338] P. S. Fennell, R. Pacciani, J. S. Dennis, J. F. Davidson, and A. N. Hayhurst, “The Effects of Repeated Cycles of Calcination and Carbonation on a Variety of Different Limestones, as Measured in a Hot Fluidized Bed of Sand,” *Energy & Fuels*, vol. 21, no. 4, pp. 2072–2081, Jul. 2007.
[339] B. González *et al.*, “Calcium looping for CO2 capture: sorbent enhancement through doping,” *Energy Procedia*, vol. 4, pp. 402–409, 2011.
[340] J. A. Shearer, I. Johnson, and C. B. Turner, “Effects of sodium chloride on limestone calcination and sulfation in fluidized-bed combustion,” *Environ. Sci. Technol.*, vol. 13, no. 9, pp. 1113–1118, Sep. 1979.
[341] C. Shen *et al.*, “Effect of Sodium Bromide on CaO-Based Sorbents Derived from Three Kinds of Sources for CO2 Capture,” *ACS Omega*, vol. 5, no. 29, pp. 17908–17917, Jul. 2020.
[342] M. J. Al-Jeboori, P. S. Fennell, M. Nguyen, and K. Feng, “Effects of different dopants and doping procedures on the reactivity of CaO-based sorbents for CO2 capture,” *Energy and Fuels*, vol. 26, no. 11, pp. 6584–6594, 2012.
[343] M. J. Al-Jeboori, M. Nguyen, C. Dean, and P. S. Fennell, “Improvement of limestone-based CO2 sorbents for Ca looping by HBr and other mineral acids,” *Ind. Eng. Chem. Res.*, vol. 52, no. 4, pp. 1426–1433, 2013.
[344] S. Kyi and B. L. Chadwick, “Screening of potential mineral additives for use as fouling preventatives in Victorian brown coal combustion,” *Fuel*, vol. 78, no. 7, pp. 845–855, 1999.
[345] T. Rizvi, P. Xing, M. Pourkashanian, L. I. Darvell, J. M. Jones, and W. Nimmo, “Prediction of biomass ash fusion behaviour by the use of detailed characterisation

methods coupled with thermodynamic analysis," *Fuel*, vol. 141, pp. 275–284, 2015.
[346] M. Pronobis, "The influence of biomass co-combustion on boiler fouling and efficiency," *Fuel*, vol. 85, no. 4, pp. 474–480, 2006.
[347] M. N. Rahaman, *Ceramic processing and sintering, second edition*, 2nd Editio. CRC Press, 2017.
[348] J. Szekely, *Gas-solid reactions*. Elsevier, 2012.
[349] H. F. W. Taylor, *Cement Chemistry*, 2nd Editio. Thomas Telford, 1997.
[350] Y. Hu *et al.*, "Screening of inert solid supports for CaO-based sorbents for high temperature CO2 capture," *Fuel*, vol. 181, pp. 199–206, 2016.
[351] D. K. Fisler and R. T. Cygan, "Diffusion of Ca and Mg in calcite," *Am. Mineral.*, vol. 84, no. 9, pp. 1392–1399, 1999.
[352] A. Silaban, M. Narcida, and D. P. Harrison, "Characteristics of the reversible reaction between CO2(g) and calcined dolomite," *Chem. Eng. Commun.*, vol. 146, pp. 149–162, 1996.
[353] J. C. Abanades, E. J. Anthony, D. Y. Lu, C. Salvador, and D. Alvarez, "Capture of CO2 from combustion gases in a fluidized bed of CaO," *Aiche J.*, vol. 50, no. 7, pp. 1614–1622, 2004.
[354] Z. Li, N. Cai, Y. Huang, and H. Han, "Synthesis, Experimental Studies, and Analysis of a New Calcium-Based Carbon Dioxide Absorbent," *Energy & Fuels*, vol. 19, no. 4, pp. 1447–1452, Jul. 2005.
[355] M. Aihara, T. Nagai, J. Matsushita, Y. Negishi, and H. Ohya, "Development of porous solid reactant for thermal-energy storage and temperature upgrade using carbonation/decarbonation reaction," *Appl. Energy*, vol. 69, no. 3, pp. 225–238, 2001.
[356] Z. Li, N. Cai, and Y. Huang, "Effect of Preparation Temperature on Cyclic CO2 Capture and Multiple Carbonation−Calcination Cycles for a New Ca-Based CO2 Sorbent," *Ind. Eng. Chem. Res.*, vol. 45, no. 6, pp. 1911–1917, Mar. 2006.
[357] B. Feng, W. Q. Liu, X. Li, and H. An, "Overcoming the problem of loss-in-capacity of calcium oxide in CO2 capture," *Energy {&} Fuels*, vol. 20, no. 6, pp. 2417–2420, 2006.
[358] R. Pacciani, C. R. Muller, J. F. Davidson, J. S. Dennis, and A. N. Hayhurst, "Synthetic Ca-based solid sorbents suitable for capturing CO2 in a fluidized bed," *Can. J. Chem. Eng.*, vol. 86, no. 3, pp. 356–366, 2008.
[359] K. O. Albrecht, K. S. Wagenbach, J. A. Satrio, B. H. Shanks, and T. D. Wheelock, "Development of a CaO-Based CO2 Sorbent with Improved Cyclic Stability," *Ind. {&} Eng. Chem. Res.*, vol. 47, no. 20, pp. 7841–7848, 2008.
[360] H. Sun, C. Wu, B. Shen, X. Zhang, Y. Zhang, and J. Huang, "Progress in the development and application of CaO-based adsorbents for CO2 capture—a review," *Mater. Today Sustain.*, vol. 1–2, pp. 1–27, 2018.
[361] W. Liu, B. Feng, Y. Wu, G. Wang, J. Barry, and J. C. Diniz Da Costa, "Synthesis of sintering-resistant sorbents for CO 2 capture," *Environ. Sci. Technol.*, vol. 44, no. 8, pp. 3093–3097, Apr. 2010.
[362] F. D. M. Daud, K. Vignesh, S. Sreekantan, and A. R. Mohamed, "Improved CO2 adsorption capacity and cyclic stability of CaO sorbents incorporated with MgO," *New J. Chem.*, vol. 40, no. 1, pp. 231–237, 2016.
[363] X. Yan, Y. Li, J. Zhao, and Z. Wang, "Density Functional Theory Study on CO2 Adsorption by Ce-Promoted CaO in the Presence of Steam," *Energy & Fuels*, vol. 34, no. 5, pp. 6197–6208, May 2020.
[364] N. Nityashree, G. V Manohara, M. M. Maroto-Valer, and S. Garcia, "Advanced High-Temperature CO2 Sorbents with Improved Long-Term Cycling Stability," *ACS Appl. Mater. Interfaces*, Jul. 2020.
[365] L. Huang, Q. Zheng, B. Louis, and Q. Wang, "A facile Solvent/Nonsolvent Preparation

of Sintering-Resistant MgO/CaO Composites for High-Temperature CO2 Capture," *Energy Technol.*, vol. 6, no. 12, pp. 2469–2478, Dec. 2018.
[366] C. Luo, Y. Zheng, N. Ding, Q. Wu, G. Bian, and C. Zheng, "Development and performance of CaO/La2O3 sorbents during calcium looping cycles for CO2 capture," *Ind. Eng. Chem. Res.*, vol. 49, no. 22, pp. 11778–11784, 2010.
[367] A. Orera, G. Larraz, and M. L. Sanjuán, "Spectroscopic study of the competition between dehydration and carbonation effects in La2O3-based materials," *J. Eur. Ceram. Soc.*, vol. 33, no. 11, pp. 2103–2110, 2013.
[368] A. N. Shirsat, M. Ali, K. N. G. Kaimal, S. R. Bharadwaj, and D. Das, "Thermochemistry of La2O2CO3 decomposition," *Thermochim. Acta*, vol. 399, no. 1, pp. 167–170, 2003.
[369] H. Guo, X. Kou, Y. Zhao, S. Wang, Q. Sun, and X. Ma, "Effect of synergistic interaction between Ce and Mn on the CO2 capture of calcium-based sorbent: Textural properties, electron donation, and oxygen vacancy," *Chem. Eng. J.*, vol. 334, pp. 237–246, Feb. 2018.
[370] S. Wang, S. Fan, L. Fan, Y. Zhao, and X. Ma, "Effect of cerium oxide doping on the performance of CaO-based sorbents during calcium looping cycles," *Environ. Sci. Technol.*, vol. 49, no. 8, pp. 5021–5027, 2015.
[371] K. Wang, F. Gu, P. T. Clough, P. Zhao, and E. J. Anthony, "CO2 Capture Performance of Gluconic Acid Modified Limestone-Dolomite Mixtures under Realistic Conditions," *Energy and Fuels*, vol. 33, no. 8, pp. 7550–7560, 2019.
[372] F. Donat, W. Hu, S. A. Scott, and J. S. Dennis, "Characteristics of Copper-based Oxygen Carriers Supported on Calcium Aluminates for Chemical-Looping Combustion with Oxygen Uncoupling (CLOU)," *Ind. Eng. Chem. Res.*, vol. 54, no. 26, pp. 6713–6723, 2015.
[373] X. W. (David) Lou, L. A. Archer, and Z. Yang, "Hollow Micro-/Nanostructures: Synthesis and Applications," *Adv. Mater.*, vol. 20, no. 21, pp. 3987–4019, Nov. 2008.
[374] F. Donat, Q. Imtiaz, A. Armutlulu, and C. R. Müller, "Preventing Agglomeration of Cu-Based Oxygen Carriers for High-Temperature Chemical Looping Applications," in *5th International Conference on Chemical Looping*, 2018.
[375] Z. Zhou, Y. Qi, M. Xie, Z. Cheng, and W. Yuan, "Synthesis of CaO-based sorbents through incorporation of alumina/aluminate and their CO 2 capture performance," *Chem. Eng. Sci.*, vol. 74, pp. 172–180, 2012.
[376] P. Xu, M. Xie, Z. Cheng, and Z. Zhou, "CO2 capture performance of CaO-based sorbents prepared by a sol-gel method," *Ind. Eng. Chem. Res.*, vol. 52, no. 34, pp. 12161–12169, 2013.
[377] S. F. Wu, Q. H. Li, J. N. Kim, and K. B. Yi, " Properties of a Nano CaO/Al 2 O 3 CO 2 Sorbent ," *Ind. Eng. Chem. Res.*, vol. 47, no. 1, pp. 180–184, 2007.
[378] M. A. Naeem, A. Armutlulu, M. Broda, D. Lebedev, and C. R. Müller, "The development of effective CaO-based CO2 sorbents: Via a sacrificial templating technique," *Faraday Discuss.*, vol. 192, pp. 85–95, 2016.
[379] C. Luo *et al.*, "Effect of support material on carbonation and sulfation of synthetic CaO-based sorbents in calcium looping cycle," *Energy and Fuels*, vol. 27, no. 8, pp. 4824–4831, 2013.
[380] M. Mohammadi, P. Lahijani, and A. R. Mohamed, "Refractory dopant-incorporated CaO from waste eggshell as sustainable sorbent for CO2 capture: Experimental and kinetic studies," *Chem. Eng. J.*, vol. 243, pp. 455–464, 2014.
[381] Y. Xu *et al.*, "Characteristics and performance of CaO-based high temperature CO2 sorbents derived from a sol-gel process with different supports," *RSC Adv.*, vol. 6, no. 83, pp. 79285–79296, 2016.
[382] R. Pacciani, C. R. Mueller, J. F. Davidson, J. S. Dennis, and A. N. Hayhurst, "How

Does the Concentration of CO2 Affect Its Uptake by a Synthetic Ca-Based Solid Sorbent?," *Aiche J.*, vol. 54, no. 12, pp. 3308–3311, Dec. 2008.
[383] W. Liu, J. S. Dennis, D. S. Sultan, S. A. T. Redfern, and S. A. Scott, "An investigation of the kinetics of CO 2 uptake by a synthetic calcium based sorbent," *Chem. Eng. Sci.*, vol. 69, no. 1, pp. 644–658, 2012.
[384] M. S. Cho, S. C. Lee, H. J. Chae, Y. M. Kwon, J. B. Lee, and J. C. Kim, "Characterization of new potassium-based solid sorbents prepared using metal silicates for post-combustion CO2 capture," *Process Saf. Environ. Prot.*, vol. 117, pp. 296–306, Jul. 2018.
[385] S. M. Kim *et al.*, "In Situ XRD and Dynamic Nuclear Polarization Surface Enhanced NMR Spectroscopy Unravel the Deactivation Mechanism of CaO-Based, Ca3Al2O6-Stabilized CO2 Sorbents," *Chem. Mater.*, vol. 30, no. 4, pp. 1344–1352, 2018.
[386] F. Q. Liu, W. H. Li, B. C. Liu, and R. X. Li, "Synthesis, characterization, and high temperature CO2 capture of new CaO based hollow sphere sorbents," *J. Mater. Chem. A*, vol. 1, no. 27, pp. 8037–8044, 2013.
[387] K. Wang, P. T. Clough, P. Zhao, and E. J. Anthony, "Synthesis of highly effective stabilized CaO sorbents: Via a sacrificial N-doped carbon nanosheet template," *J. Mater. Chem. A*, vol. 7, no. 15, pp. 9173–9182, 2019.
[388] S. Wang, H. Shen, S. Fan, Y. Zhao, X. Ma, and J. Gong, "CaO-based meshed hollow spheres for CO2 capture," *Chem. Eng. Sci.*, vol. 135, pp. 532–539, 2015.
[389] H. Li, M. Qu, Y. Yang, Y. Hu, and W. Liu, "One-step synthesis of spherical CaO pellets via novel graphite-casting method for cyclic CO2 capture," *Chem. Eng. J.*, vol. 374, no. May, pp. 619–625, 2019.
[390] A. Armutlulu *et al.*, "Multishelled CaO Microspheres Stabilized by Atomic Layer Deposition of Al $_2$ O $_3$ for Enhanced CO $_2$ Capture Performance," *Adv. Mater.*, vol. 29, no. 41, p. 1702896, Nov. 2017.
[391] M. Broda and C. R. Müller, "Synthesis of highly efficient, Ca-based, Al 2O 3-stabilized, carbon gel-templated CO 2 sorbents," *Adv. Mater.*, vol. 24, no. 22, pp. 3059–3064, 2012.
[392] J. Chen, L. Duan, and Z. Sun, "Accurate Control of Cage-Like CaO Hollow Microspheres for Enhanced CO 2 Capture in Calcium Looping via a Template-Assisted Synthesis Approach," *Environ. Sci. Technol.*, vol. 53, no. 4, pp. 2249–2259, 2019.
[393] C. Chi, Y. Li, W. Zhang, and Z. Wang, "Synthesis of a hollow microtubular Ca/Al sorbent with high CO2 uptake by hard templating," *Appl. Energy*, vol. 251, no. May, p. 113382, 2019.
[394] J. Feng, H. Guo, S. Wang, Y. Zhao, and X. Ma, "Fabrication of multi-shelled hollow Mg-modified CaCO3 microspheres and their improved CO2 adsorption performance," *Chem. Eng. J.*, vol. 321, pp. 401–411, 2017.
[395] H. Li, Y. Hu, H. Chen, and M. Qu, "Porous spherical calcium aluminate-supported CaO-based pellets manufactured via biomass-templated extrusion–spheronization technique for cyclic CO2 capture," *Environ. Sci. Pollut. Res.*, vol. 26, no. 21, pp. 21972–21982, 2019.
[396] S. Li, J. Feng, X. Kou, Y. Zhao, X. Ma, and S. Wang, "Al-Stabilized Double-Shelled Hollow CaO-Based Microspheres with Superior CO2 Adsorption Performance," *Energy and Fuels*, vol. 32, no. 9, pp. 9692–9700, 2018.
[397] J. Chen *et al.*, "A facile one-pot synthesis of CaO/CuO hollow microspheres featuring highly porous shells for enhanced CO2 capture in a combined Ca-Cu looping process: Via a template-free synthesis approach," *J. Mater. Chem. A*, vol. 7, no. 37, pp. 21096–21105, 2019.
[398] R. Han, J. Gao, S. Wei, Y. Su, and Y. Qin, "Development of highly effective CaO@Al2O3 with hierarchical architecture CO2 sorbents: Via a scalable limited-space

chemical vapor deposition technique," *J. Mater. Chem. A*, vol. 6, no. 8, pp. 3462–3470, 2018.
[399] S. M. Kim, A. Armutlulu, A. M. Kierzkowska, D. Hosseini, F. Donat, and C. Müller, "Development of an effective bi-functional Ni-CaO catalyst-sorbent for the sorption-enhanced water gas shift reaction through structural optimization and the controlled deposition of a stabilizer by atomic layer deposition," *Sustain. Energy Fuels*, vol. 4, no. 2, pp. 713–729, 2020.
[400] W. Peng, Z. Xu, C. Luo, and H. Zhao, " Tailor-Made Core–Shell CaO/TiO 2 –Al 2 O 3 Architecture as a High-Capacity and Long-Life CO 2 Sorbent ," *Environ. Sci. Technol.*, vol. 49, no. 13, pp. 8237–8245, 2015.
[401] M. Zhao *et al.*, "A novel calcium looping absorbent incorporated with polymorphic spacers for hydrogen production and CO2 capture," *Energy Environ. Sci.*, vol. 7, no. 10, pp. 3291–3295, Oct. 2014.
[402] P. T. Clough, M. E. Boot-Handford, M. Zhao, and P. S. Fennell, "Degradation study of a novel polymorphic sorbent under realistic post-combustion conditions," *Fuel*, vol. 186, pp. 708–713, Dec. 2016.
[403] M. Zhao, Y. Song, G. Ji, and X. Zhao, "Demonstration of Polymorphic Spacing Strategy against Sintering: Synthesis of Stabilized Calcium Looping Absorbents for High-Temperature CO2 Sorption," *Energy and Fuels*, vol. 32, no. 4, pp. 5443–5452, 2018.
[404] S. Li, T. Jiang, Z. Xu, Y. Zhao, X. Ma, and S. Wang, "The Mn-promoted double-shelled CaCO3 hollow microspheres as high efficient CO2 adsorbents," *Chem. Eng. J.*, vol. 372, no. February, pp. 53–64, 2019.
[405] Y. Wang, W. Zhang, R. Li, W. Duan, and B. Liu, "Design of Stable Cage-like CaO/CaZrO3 Hollow Spheres for CO2 Capture," *Energy and Fuels*, vol. 30, no. 2, pp. 1248–1255, 2016.
[406] Q. Zhang, W. Wang, J. Goebl, and Y. Yin, "Self-templated synthesis of hollow nanostructures," *Nano Today*, vol. 4, no. 6, pp. 494–507, 2009.
[407] C. Huang, M. Xu, X. Huai, and Z. Liu, "Template-Free Synthesis of Hollow CaO/Ca2SiO4 Nanoparticle as a Cyclically Stable High-Capacity CO2 Sorbent," *ACS Sustain. Chem. Eng.*, Jan. 2021.
[408] Z. Sun *et al.*, "A Facile fabrication of mesoporous core-shell CaO-Based pellets with enhanced reactive stability and resistance to attrition in cyclic CO2 capture," *J. Mater. Chem. A*, vol. 2, no. 39, pp. 16577–16588, 2014.
[409] N. Mahinpey, M. H. Sedghkerdar, A. Aqsha, and A. H. Soleimanisalim, "CO2 Capture Performance of Core/Shell CaO-Based Sorbent Using Mesostructured Silica and Titania in a Multicycle CO2 Capture Process," *Ind. Eng. Chem. Res.*, vol. 55, no. 16, pp. 4532–4538, 2016.
[410] A. Armutlulu *et al.*, "Multishelled CaO Microspheres Stabilized by Atomic Layer Deposition of Al 2 O 3 for Enhanced CO 2 Capture Performance," *Adv. Mater.*, vol. 29, no. 41, pp. 1–9, 2017.
[411] L. Zhang, Y. Lu, and M. Rostam-Abadi, "Sintering of calcium oxide (CaO) during CO2 chemisorption: a reactive molecular dynamics study," *Phys. Chem. Chem. Phys.*, vol. 14, no. 48, pp. 16633–16643, 2012.
[412] S. M. Kim, A. Armutlulu, A. M. Kierzkowska, and C. R. Müller, "Inverse Opal-Like, Ca3Al2O6-Stabilized, CaO-Based CO2 Sorbent: Stabilization of a Highly Porous Structure to Improve Its Cyclic CO2 Uptake," *ACS Appl. Energy Mater.*, vol. 2, no. 9, pp. 6461–6471, 2019.
[413] P. T. Clough, M. E. Boot-Handford, L. Zheng, Z. Zhang, and P. S. Fennell, "Hydrogen production by sorption enhanced steam reforming (SESR) of biomass in a fluidised-bed reactor using combined multifunctional particles," *Materials (Basel).*, vol. 11, no. 5,

2018.
[414] A. K. Prashar *et al.*, “Factors Affecting the Rate of CO 2 Absorption after Partial Desorption in NaNO 3 -Promoted MgO,” *Energy and Fuels*, vol. 30, no. 4, pp. 3298–3305, 2016.
[415] A. T. Vu, Y. Park, P. R. Jeon, and C. H. Lee, “Mesoporous MgO sorbent promoted with KNO3 for CO2 capture at intermediate temperatures,” *Chem. Eng. J.*, vol. 258, pp. 254–264, Dec. 2014.
[416] J. Wang, M. Li, P. Lu, P. Ning, and Q. Wang, “Kinetic study of CO2 capture on ternary nitrates modified MgO with different precursor and morphology,” *Chem. Eng. J.*, vol. 392, p. 123752, 2020.
[417] J. Chen, L. Duan, F. Donat, and C. R. Müller, “Assessment of the effect of process conditions and material characteristics of alkali metal salt-promoted MgO-based sorbents on their CO2 capture performance,” *submitted*, 2021.
[418] L. Wang, Z. Zhou, Y. Hu, Z. Cheng, and X. Fang, “Nanosheet MgO-Based CO2 Sorbent Promoted by Mixed-Alkali-Metal Nitrate and Carbonate: Performance and Mechanism,” *Ind. Eng. Chem. Res.*, vol. 56, no. 20, pp. 5802–5812, May 2017.
[419] R. Singh, M. K. Ram Reddy, S. Wilson, K. Joshi, J. C. Diniz da Costa, and P. Webley, “High temperature materials for CO2capture,” *Energy Procedia*, vol. 1, no. 1, pp. 623–630, 2009.
[420] G. Xiao, R. Singh, A. Chaffee, and P. Webley, “Advanced adsorbents based on MgO and K2CO3 for capture of CO2 at elevated temperatures,” *Int. J. Greenh. Gas Control*, vol. 5, no. 4, pp. 634–639, 2011.
[421] M. Liu, C. Vogt, A. L. Chaffee, and S. L. Y. Chang, “Nanoscale Structural Investigation of Cs2CO3-Doped MgO Sorbent for CO2 Capture at Moderate Temperature,” *J. Phys. Chem. C*, vol. 117, no. 34, pp. 17514–17520, Aug. 2013.
[422] J.-S. Kwak, K.-Y. Kim, J. W. Yoon, K.-R. Oh, and Y.-U. Kwon, “Interfacial Interactions Govern the Mechanisms of CO2 Absorption and Desorption on A2CO3-Promoted MgO (A = Na, K, Rb, and Cs) Absorbents,” *J. Phys. Chem. C*, vol. 122, no. 35, pp. 20289–20300, Sep. 2018.
[423] K. Zhang, X. S. Li, Y. Duan, D. L. King, P. Singh, and L. Li, “Roles of double salt formation and NaNO3 in Na2CO3-promoted MgO absorbent for intermediate temperature CO2 removal,” *Int. J. Greenh. Gas Control*, vol. 12, pp. 351–358, 2013.
[424] H. Jeon *et al.*, “Graft copolymer templated synthesis of mesoporous MgO/TiO 2 mixed oxide nanoparticles and their CO 2 adsorption capacities,” *Colloids Surfaces A Physicochem. Eng. Asp.*, 2012.
[425] H. Yu, X. Wang, Z. Shu, M. Fujii, and C. Song, “Al2O3 and CeO2-promoted MgO sorbents for CO2 capture at moderate temperatures,” *Front. Chem. Sci. Eng.*, vol. 12, no. 1, pp. 83–93, 2018.
[426] Y. Y. Li, X. Y. M. Dong, X. D. Sun, Y. Wang, and J. H. Zhu, “New Solid-Base Cu-MgO for CO2 Capture at 473 K and Removal of Nitrosamine,” *ACS Appl. Mater. Interfaces*, vol. 8, no. 44, pp. 30193–30204, 2016.
[427] H. Cui *et al.*, “Ultrafast and Stable CO 2 Capture Using Alkali Metal Salt-Promoted MgO-CaCO 3 Sorbents,” *ACS Appl. Mater. Interfaces*, vol. 10, no. 24, pp. 20611–20620, 2018.
[428] S. W. Bian, J. Baltrusaitis, P. Galhotra, and V. H. Grassian, “A template-free, thermal decomposition method to synthesize mesoporous MgO with a nanocrystalline framework and its application in carbon dioxide adsorption,” *J. Mater. Chem.*, vol. 20, no. 39, pp. 8705–8710, 2010.
[429] T. K. Kim, K. J. Lee, J. Y. Cheon, J. H. Lee, S. H. Joo, and H. R. Moon, “Nanoporous metal oxides with tunable and nanocrystalline frameworks via conversion of metal-organic frameworks,” *J. Am. Chem. Soc.*, vol. 135, no. 24, pp. 8940–8946, Jun. 2013.

[430] K. Kim, J. W. Han, K. S. Lee, and W. B. Lee, “Promoting alkali and alkaline-earth metals on MgO for enhancing CO2 capture by first-principles calculations,” *Phys. Chem. Chem. Phys.*, vol. 16, no. 45, pp. 24818–24823, 2014.
[431] J. M. Jang and S. G. Kang, “Understanding CO2 Adsorption on a M1 (M2)-Promoted (Doped) MgO-CaO(100) Surface (M1 = Li, Na, K, and Rb, M2 = Sr): A DFT Theoretical Study,” *ACS Sustain. Chem. Eng.*, vol. 7, no. 20, pp. 16979–16984, 2019.
[432] B. W. Hwang *et al.*, “CO2 capture and regeneration properties of MgO-based sorbents promoted with alkali metal nitrates at high pressure for the sorption enhanced water gas shift process,” *Process Saf. Environ. Prot.*, vol. 116, pp. 219–227, May 2018.
[433] R. N. Kust and J. D. Burke, “Thermal decomposition in alkali metal nitrate melts,” *Inorg. Nucl. Chem. Lett.*, vol. 6, no. 3, pp. 333–335, 1970.
[434] R. I. Olivares, “The thermal stability of molten nitrite/nitrates salt for solar thermal energy storage in different atmospheres,” *Sol. Energy*, vol. 86, no. 9, pp. 2576–2583, 2012.
[435] H. Lee *et al.*, “In Situ Observation of Carbon Dioxide Capture on Pseudo-Liquid Eutectic Mixture-Promoted Magnesium Oxide,” *ACS Appl. Mater. Interfaces*, vol. 10, no. 3, pp. 2414–2422, 2018.
[436] Y. Qiao *et al.*, “Alkali Nitrates Molten Salt Modified Commercial MgO for Intermediate-Temperature CO2 Capture: Optimization of the Li/Na/K Ratio,” *Ind. Eng. Chem. Res.*, vol. 56, no. 6, pp. 1509–1517, 2017.
[437] X. Zhao, G. Ji, W. Liu, X. He, E. J. Anthony, and M. Zhao, “Mesoporous MgO promoted with NaNO3/NaNO2 for rapid and high-capacity CO2 capture at moderate temperatures,” *Chem. Eng. J.*, 2018.
[438] Q. Chen, X. Yang, R. Li, N. Dong, Y. Zhang, and Y. Ding, “Influence of rheological behavior of molten sodium sulfate on adherent heterogeneous surface on performance of high-temperature thermochemical energy storage,” *Appl. Surf. Sci.*, vol. 525, p. 146530, 2020.
[439] W. R. Brice and L. L. Y. Chang, “Subsolidus phase relations in aragonite-type carbonates. III. The systems MgCO3-CaCO3-BaCO3, MgCO3-CaCO3-SrCO3, and MgCO3-SrCO3-BaCO3,” *Am. Mineral.*, vol. 58, no. 11–12, pp. 979–985, 1973.
[440] V. Hiremath, M. L. T. Trivino, and J. G. Seo, “Eutectic mixture promoted CO2 sorption on MgO-TiO2 composite at elevated temperature,” *J. Environ. Sci.*, vol. 76, pp. 80–88, 2019.
[441] M. L. T. Triviño, V. Hiremath, and J. G. Seo, “Stabilization of NaNO3-Promoted Magnesium Oxide for High-Temperature CO2 Capture,” *Environ. Sci. Technol.*, vol. 52, no. 20, pp. 11952–11959, 2018.
[442] X. Zhu, K. Li, L. Neal, and F. Li, “Perovskites as Geo-inspired Oxygen Storage Materials for Chemical Looping and Three-Way Catalysis: A Perspective,” *ACS Catal.*, vol. 8, no. 9, pp. 8213–8236, Sep. 2018.
[443] X. Zhu, Q. Imtiaz, F. Donat, C. R. Müller, and F. Li, “Chemical looping beyond combustion – a perspective,” *Energy Environ. Sci.*, vol. 13, no. 3, pp. 772–804, 2020.
[444] F. Donat and C. R. Müller, “CO2-free conversion of CH4 to syngas using chemical looping,” *Appl. Catal. B Environ.*, vol. 278, p. 119328, 2020.
[445] F. Donat, Y. Xu, and C. R. Müller, “Combined partial oxidation of methane to synthesis gas and production of hydrogen or carbon monoxide in a fluidized bed using lattice oxygen,” *Energy Technol.*, 2019.
[446] E. Marek, W. Hu, M. Gaultois, C. P. Grey, and S. A. Scott, “The use of strontium ferrite in chemical looping systems,” *Appl. Energy*, vol. 223, pp. 369–382, Aug. 2018.
[447] D. Hosseini, F. Donat, P. M. Abdala, S. M. Kim, A. M. Kierzkowska, and C. R. Müller, “Reversible Exsolution of Dopant Improves the Performance of Ca2Fe2O5 for Chemical Looping Hydrogen Production,” *ACS Appl. Mater. Interfaces*, vol. 11, no.

20, pp. 18276–18284, May 2019.
[448] C. Dang *et al.*, “Calcium cobaltate: a phase-change catalyst for stable hydrogen production from bio-glycerol,” *Energy Environ. Sci.*, vol. 11, no. 3, pp. 660–668, 2018.
[449] J. Ida, R. T. Xiong, and Y. S. Lin, “Synthesis and CO2 sorption properties of pure and modified lithium zirconate,” *Sep. Purif. Technol.*, vol. 36, no. 1, pp. 41–51, Apr. 2004.
[450] R. Xiong, J. Ida, and Y. S. Lin, “Kinetics of carbon dioxide sorption on potassium-doped lithium zirconate,” *Chem. Eng. Sci.*, vol. 58, no. 19, pp. 4377–4385, 2003.
[451] G. Pannocchia, M. Puccini, M. Seggiani, and S. Vitolo, “Experimental and modeling studies on high-temperature capture of CO2 using lithium zirconate based sorbents,” *Ind. Eng. Chem. Res.*, vol. 46, no. 21, pp. 6696–6706, Oct. 2007.
[452] E. Ochoa-Fernandez, M. Ronning, T. Grande, and D. Chen, “Synthesis and CO2 capture properties of nanocrystalline lithium zirconate,” *Chem. Mater.*, vol. 18, no. 25, pp. 6037–6046, Dec. 2006.
[453] K. B. Yi and D. O. Eriksen, “Low temperature liquid state synthesis of lithium zirconate and its characteristics as a CO2 sorbent,” *Sep. Sci. Technol.*, vol. 41, no. 2, pp. 283–296, Feb. 2006.
[454] B. N. Nair, T. Yamaguchi, H. Kawamura, S. I. Nakao, and K. Nakagawa, “Processing of lithium zirconate for applications in carbon dioxide separation: Structure and properties of the powders,” *J. Am. Ceram. Soc.*, vol. 87, no. 1, pp. 68–74, Jan. 2004.
[455] Y. Duan, “Electronic structural and electrochemical properties of lithium zirconates and their capabilities of CO2 capture: A first-principles density-functional theory and phonon dynamics approach,” *J. Renew. Sustain. Energy*, vol. 3, no. 1, p. 13102, Jan. 2011.
[456] M. Kato *et al.*, “Novel CO2 absorbents using lithium-containing oxide,” *Int. J. Appl. Ceram. Technol.*, vol. 2, no. 6, pp. 467–475, 2005.
[457] K. Nakagawa and T. Ohashi, “A novel method of CO2 capture from high temperature gases,” *J. Electrochem. Soc.*, vol. 145, no. 4, pp. 1344–1346, Apr. 1998.
[458] M. Kato, K. Essaki, K. Nakagawa, Y. Suyama, and K. Terasaka, “CO2 absorption properties of lithium ferrite for application as a high-temperature CO2 absorbent,” *J. Ceram. Soc. Japan*, vol. 113, no. 1322, pp. 684–686, Oct. 2005.
[459] M. J. Venegas, E. Fregoso-Israel, R. Escamilla, and H. Pfeiffer, “Kinetic and reaction mechanism of CO2 sorption on Li4SiO4: Study of the particle size effect,” *Ind. Eng. Chem. Res.*, vol. 46, no. 8, pp. 2407–2412, Apr. 2007.
[460] Y. Yang *et al.*, “High-temperature CO2 adsorption by one-step fabricated Nd-doped Li4SiO4 pellets,” *Chem. Eng. J.*, p. 128346, 2020.
[461] H. Li, M. Qu, and Y. Hu, “Preparation of spherical Li4SiO4 pellets by novel agar method for high-temperature CO2 capture,” *Chem. Eng. J.*, vol. 380, no. July 2019, p. 122538, 2020.
[462] L. Martínez-dlCruz and H. Pfeiffer, “Cyclic CO2 chemisorption–desorption behavior of Na2ZrO3: Structural, microstructural and kinetic variations produced as a function of temperature,” *J. Solid State Chem.*, vol. 204, pp. 298–304, 2013.
[463] S. Munro, M. Åhlén, O. Cheung, and A. Sanna, “Tuning Na2ZrO3 for fast and stable CO2 adsorption by solid state synthesis,” *Chem. Eng. J.*, vol. 388, p. 124284, 2020.
[464] M. Z. Akram *et al.*, “Low-Temperature and Fast Kinetics for CO2 Sorption Using Li6WO6 Nanowires,” *Nano Lett.*, vol. 18, no. 8, pp. 4891–4899, Aug. 2018.
[465] Y. Duan *et al.*, “{CO2} capture properties of lithium silicates with different ratios of {Li2O/SiO2:} an ab initio thermodynamic and experimental approach,” *Phys. Chem. Chem. Phys.*, vol. 15, no. 32, p. 13538, 2013.
[466] F. Durán-Muñoz, I. C. Romero-Ibarra, and H. Pfeiffer, “Analysis of the {CO2} chemisorption reaction mechanism in lithium oxosilicate ({Li8SiO6):} a new option for high-temperature {CO2} capture,” *J. Mater. Chem. A*, vol. 1, no. 12, p. 3919, 2013.

[467] X.-S. Yin, S.-P. Li, Q.-H. Zhang, and J.-G. Yu, “Synthesis and CO2 Adsorption Characteristics of Lithium Zirconates with High Lithia Content,” *J. Am. Ceram. Soc.*, vol. 93, no. 9, pp. 2837–2842, Sep. 2010.
[468] Y. Duan, “Structural and electronic properties of {Li8ZrO6} and its {CO2} capture capabilities: an ab initio thermodynamic approach,” *Phys. Chem. Chem. Phys.*, 2013.
[469] X.-S. Yin, Q.-H. Zhang, and J.-G. Yu, “Three-Step Calcination Synthesis of High-Purity Li8ZrO6 with CO2 Absorption Properties,” *Inorg. Chem.*, vol. 50, no. 7, pp. 2844–2850, Apr. 2011.
[470] T. Avalos-Rendon, J. Casa-Madrid, and H. Pfeiffer, “Thermochemical Capture of Carbon Dioxide on Lithium Aluminates (LiAlO2 and Li5AlO4): A New Option for the CO2 Absorption,” *J. Phys. Chem. a*, vol. 113, no. 25, pp. 6919–6923, Jun. 2009.
[471] T. Avalos-Rendon, V. H. Lara, and H. Pfeiffer, “CO2 Chemisorption and Cyclability Analyses of Lithium Aluminate Polymorphs (alpha- and beta-Li5AlO4),” *Ind. Eng. Chem. Res.*, vol. 51, no. 6, pp. 2622–2630, Feb. 2012.
[472] M. V. Blanco, K. Kohopää, I. Snigireva, and F. Cova, “Low temperature solid state synthesis of Li5FeO4 and CO2 capture mechanism via real time in situsynchrotron X-ray diffraction,” *Chem. Eng. J.*, vol. 354, pp. 370–377, Dec. 2018.
[473] H. A. Lara-García, P. Sanchez-Camacho, Y. Duan, J. Ortiz-Landeros, and H. Pfeiffer, “Analysis of the CO 2 Chemisorption in Li 5 FeO 4 , a New High Temperature CO 2 Captor Material. Effect of the CO 2 and O 2 Partial Pressures,” *J. Phys. Chem. C*, vol. 121, no. 6, pp. 3455–3462, Feb. 2017.
[474] T. Ávalos-Rendón, V. H. Lara, and H. Pfeiffer, “CO 2 chemisorption and cyclability analyses of lithium aluminate polymorphs (α- and β-Li 5AlO 4),” *Ind. Eng. Chem. Res.*, vol. 51, no. 6, pp. 2622–2630, Feb. 2012.
[475] F. Durán-Muñoz, I. C. Romero-Ibarra, and H. Pfeiffer, “Analysis of the CO2 chemisorption reaction mechanism in lithium oxosilicate (Li8SiO6): A new option for high-temperature CO2 capture,” *J. Mater. Chem. A*, vol. 1, no. 12, pp. 3919–3925, Mar. 2013.
[476] M. Kato *et al.*, “Novel CO2 absorbents using lithium-containing oxide,” *Int. J. Appl. Ceram. Technol.*, vol. 2, no. 6, pp. 467–475, 2005.
[477] T. Harada and T. A. Hatton, “Tri-lithium borate (Li3BO3); a new highly regenerable high capacity CO2 adsorbent at intermediate temperature,” *J. Mater. Chem. A*, vol. 5, no. 42, pp. 22224–22233, 2017.
[478] P. V. Subha *et al.*, “Germanium-incorporated lithium silicate composites as highly efficient low-temperature sorbents for CO2 capture,” *J. Mater. Chem. A*, vol. 6, no. 17, pp. 7913–7921, 2018.
[479] C. Gauer and W. Heschel, “Doped lithium orthosilicate for absorption of carbon dioxide,” *J. Mater. Sci.*, vol. 41, no. 8, pp. 2405–2409, 2006.
[480] Y. Duan and J. Lekse, “Regeneration mechanisms of high-lithium content zirconates as CO 2 capture sorbents: Experimental measurements and theoretical investigations,” *Phys. Chem. Chem. Phys.*, vol. 17, no. 35, pp. 22543–22547, Aug. 2015.
[481] S. Wang, C. An, and Q.-H. Zhang, “Syntheses and structures of lithium zirconates for high-temperature {CO2} absorption,” *J. Mater. Chem. A*, vol. 1, no. 11, p. 3540, 2013.
[482] M. T. Dunstan *et al.*, “Ion Dynamics and CO2 Absorption Properties of Nb-, Ta-, and Y-Doped Li2ZrO3 Studied by Solid-State NMR, Thermogravimetry, and First-Principles Calculations,” *J. Phys. Chem. C*, vol. 121, no. 40, pp. 21877–21886, 2017.
[483] L.-C. Lin *et al.*, “In silico screening of carbon-capture materials,” *Nat. Mater.*, vol. 11, no. 7, pp. 633–641, May 2012.
[484] A. Ö. Yazaydın *et al.*, “Screening of Metal−Organic Frameworks for Carbon Dioxide Capture from Flue Gas Using a Combined Experimental and Modeling Approach,” *J. Am. Chem. Soc.*, vol. 131, no. 51, pp. 18198–18199, Dec. 2009.

[485] R. Krishna and J. R. Long, “Screening Metal--Organic Frameworks by Analysis of Transient Breakthrough of Gas Mixtures in a Fixed Bed Adsorber,” *J. Phys. Chem. C*, vol. 115, no. 26, pp. 12941–12950, Jul. 2011.
[486] R. Krishna and J. M. van Baten, “In silico screening of metal--organic frameworks in separation applications,” *Phys. Chem. Chem. Phys.*, vol. 13, no. 22, p. 10593, 2011.
[487] R. Banerjee *et al.*, “High-Throughput Synthesis of Zeolitic Imidazolate Frameworks and Application to CO2 Capture,” *Science (80-.).*, vol. 319, no. 5865, pp. 939–943, 2008.
[488] Y. Duan, “A first-principles density functional theory study of the electronic structural and thermodynamic properties of {M2ZrO3} and {M2CO3} (M = Na, K) and their capabilities for {CO2} capture,” *J. Renew. Sustain. Energy*, vol. 4, no. 1, p. 13109, 2012.
[489] S. G. Kang, “First-principles evaluation of the potential of using Mg2SiO4, Mg2VO4, and Mg2GeO4 for CO2 capture,” *J. CO2 Util.*, vol. 42, p. 101293, 2020.
[490] Y. Duan and D. C. Sorescu, “CO2 capture properties of alkaline earth metal oxides and hydroxides: A combined density functional theory and lattice phonon dynamics study,” *J. Chem. Phys.*, vol. 133, no. 7, p. 74508, 2010.
[491] Y. Duan, “Efficient Theoretical Screening of Solid Sorbents for {CO₂} Capture Applications,” *Int. J. Clean Coal Energy*, vol. 01, no. 01, pp. 1–11, 2012.
[492] A. Jain *et al.*, “Commentary: The materials project: A materials genome approach to accelerating materials innovation,” *APL Mater.*, vol. 1, no. 1, 2013.
[493] J. E. Saal, S. Kirklin, M. Aykol, B. Meredig, and C. Wolverton, “Materials design and discovery with high-throughput density functional theory: The open quantum materials database (OQMD),” *JOM*, vol. 65, no. 11, pp. 1501–1509, Nov. 2013.
[494] S. Kirklin *et al.*, “The Open Quantum Materials Database (OQMD): Assessing the accuracy of DFT formation energies,” *npj Comput. Mater.*, vol. 1, Dec. 2015.
[495] G. Pizzi, A. Cepellotti, R. Sabatini, N. Marzari, and B. Kozinsky, “AiiDA: automated interactive infrastructure and database for computational science,” *Comput. Mater. Sci.*, vol. 111, pp. 218–230, 2016.
[496] S. Curtarolo *et al.*, “AFLOW: An automatic framework for high-throughput materials discovery,” *Comput. Mater. Sci.*, vol. 58, pp. 218–226, Jun. 2012.
[497] D. D. Landis *et al.*, “The computational materials repository,” *Comput. Sci. Eng.*, vol. 14, no. 6, pp. 51–57, 2012.
[498] M. T. Dunstan *et al.*, “Large scale computational screening and experimental discovery of novel materials for high temperature CO2 capture,” *Energy Environ. Sci.*, vol. 9, no. 4, pp. 1346–1360, 2016.
[499] M. W. Gaultois, M. T. Dunstan, A. W. Bateson, M. S. C. Chan, and C. P. Grey, “Screening and Characterization of Ternary Oxides for High-Temperature Carbon Capture,” *Chem. Mater.*, vol. 30, no. 8, pp. 2535–2543, 2018.
[500] M. W. Chase, “NIST-JANAF Thermochemical Tables, 4th Edition | NIST,” *NIST-JANAF Thermochem. Tables 2 Vol. (Journal Phys. Chem. Ref. Data Monogr.*, Aug. 1998.
[501] B. J. McBride, M. J. Zehe, and S. Gordon, “NASA Glenn Coefficients for Calculating Thermodynamic Properties of Individual Species.” Cleveland, Ohio, 2002.
[502] I. Barin, O. Knacke, and O. Kubaschewski, *Thermochemical properties of inorganic substances: supplement*. Springer Science & Business Media, 2013.
[503] I.-H. Jung and M.-A. Van Ende, “Computational Thermodynamic Calculations: FactSage from CALPHAD Thermodynamic Database to Virtual Process Simulation,” *Metall. Mater. Trans. B*, vol. 51, no. 5, pp. 1851–1874, 2020.
[504] L. C. Buelens, H. Poelman, G. B. Marin, and V. V. Galvita, “110th Anniversary:

Carbon Dioxide and Chemical Looping: Current Research Trends," *Ind. Eng. Chem. Res.*, vol. 58, no. 36, pp. 16235–16257, 2019.
[505] A. F. Kazakov *et al.*, "Ionic Liquids Database - ILThermo (v2.0) | NIST," *Ion. Liq. Database - ILThermo*, Dec. 2013.
[506] Q. Dong *et al.*, "ILThermo: A free-access web database for thermodynamic properties of ionic liquids," *Journal of Chemical and Engineering Data*, vol. 52, no. 4. pp. 1151–1159, Jul-2007.
[507] V. Venkatraman, S. Evjen, K. C. Lethesh, J. J. Raj, H. K. Knuutila, and A. Fiksdahl, "Rapid, comprehensive screening of ionic liquids towards sustainable applications," *Sustain. Energy Fuels*, vol. 3, no. 10, pp. 2798–2808, 2019.
[508] R. H. Görke, W. Hu, M. T. Dunstan, J. S. Dennis, and S. A. Scott, "Exploration of the material property space for chemical looping air separation applied to carbon capture and storage," *Appl. Energy*, vol. 212, pp. 478–488, 2018.
[509] B. Xu, M. B. Toffolo, E. Boaretto, and K. M. Poduska, "Assessing Local and Long-Range Structural Disorder in Aggregate-Free Lime Binders," *Ind. Eng. Chem. Res.*, vol. 55, no. 30, pp. 8334–8340, 2016.
[510] S. Leukel *et al.*, "Trapping Amorphous Intermediates of Carbonates – A Combined Total Scattering and NMR Study," *J. Am. Chem. Soc.*, vol. 140, no. 44, pp. 14638–14646, Nov. 2018.
[511] S. Leukel *et al.*, "Mechanochemical Access to Defect-Stabilized Amorphous Calcium Carbonate," *Chem. Mater.*, vol. 30, no. 17, pp. 6040–6052, 2018.
[512] A. Benedetti, J. Ilavsky, C. Segre, and M. Strumendo, "Analysis of textural properties of CaO-based CO2 sorbents by ex situ USAXS," *Chem. Eng. J.*, vol. 355, no. July 2018, pp. 760–776, 2019.
[513] M. L. Grasso, M. V. Blanco, F. Cova, J. A. González, P. Arneodo Larochette, and F. C. Gennari, "Evaluation of the formation and carbon dioxide capture by Li 4 SiO 4 using: In situ synchrotron powder X-ray diffraction studies," *Phys. Chem. Chem. Phys.*, vol. 20, no. 41, pp. 26570–26579, 2018.
[514] F. Cova, G. Amica, K. Kohopää, and M. V. Blanco, "Time-Resolved Synchrotron Powder X-ray Diffraction Studies on the Synthesis of Li8SiO6 and Its Reaction with CO2," *Inorg. Chem.*, vol. 58, no. 2, pp. 1040–1047, Jan. 2019.
[515] R. Molinder, T. P. Comyn, N. Hondow, J. E. Parker, and V. Dupont, "In situ X-ray diffraction of CaO based CO2 sorbents," *Energy Environ. Sci.*, vol. 5, no. 10, pp. 8958–8969, Oct. 2012.
[516] M. T. Dunstan *et al.*, "In situ studies of materials for high temperature CO2 capture and storage," *Faraday Discuss.*, vol. 192, pp. 217–240, 2016.
[517] F. Lundvall *et al.*, "Characterization and evaluation of synthetic Dawsonites as CO 2 sorbents," *Fuel*, vol. 236, pp. 747–754, Jan. 2019.
[518] H. Sun, Y. Zhang, S. Guan, J. Huang, and C. Wu, "Direct and highly selective conversion of captured CO2 into methane through integrated carbon capture and utilization over dual functional materials," *J. CO2 Util.*, vol. 38, pp. 262–272, 2020.
[519] X. Chen, L. Yang, Z. Zhou, and Z. Cheng, "Core-shell structured CaO-Ca9Al6O18@Ca5Al6O14/Ni bifunctional material for sorption-enhanced steam methane reforming," *Chem. Eng. Sci.*, vol. 163, pp. 114–122, 2017.
[520] X. Yan, Y. Li, X. Ma, Z. Bian, J. Zhao, and Z. Wang, "CeO2-modified CaO/Ca12Al14O33 bi-functional material for CO2 capture and H2 production in sorption-enhanced steam gasification of biomass," *Energy*, vol. 192, 2020.
[521] S. Tian, F. Yan, Z. Zhang, and J. Jiang, "Calcium-looping reforming of methane realizes in situ CO2 utilization with improved energy efficiency," *Sci. Adv.*, vol. 5, no. 4, 2019.
[522] J. V. Evans and T. L. Whateley, "Infra-red study of adsorption of carbon dioxide and

water on magnesium oxide," *Trans. Faraday Soc.*, vol. 63, pp. 2769–2777, 1967.
[523] K. Wang, Y. Zhao, P. T. Clough, P. Zhao, and E. J. Anthony, "Structural and kinetic analysis of CO2 sorption on NaNO2-promoted MgO at moderate temperatures," *Chem. Eng. J.*, vol. 372, no. February, pp. 886–895, 2019.
[524] S. M. Ward, J. Braslaw, and R. L. Gealer, "Carbon dioxide sorption studies on magnesium oxide," *Thermochim. Acta*, vol. 64, no. 1–2, pp. 107–114, 1983.
[525] D. L. Meixner, D. A. Arthur, and S. M. George, "Kinetics of desorption, adsorption, and surface diffusion of CO2 on MgO(100)," *Surf. Sci.*, vol. 261, no. 1–3, pp. 141–154, 1992.
[526] C. Yu, J. Ding, W. Wang, and X. Wei, "Characteristics of alkali nitrates molten salt-promoted MgO as a moderate-temperature CO2 absorbent," *Energy Procedia*, vol. 158, pp. 5776–5781, 2019.
[527] K. J. Fricker and A. H. A. Park, "Effect of H2O on Mg(OH)2 carbonation pathways for combined CO2 capture and storage," *Chem. Eng. Sci.*, vol. 100, pp. 332–341, 2013.
[528] D. Peltzer, J. Múnera, and L. Cornaglia, "Operando Raman spectroscopic studies of lithium zirconates during CO2 capture at high temperature," *RSC Adv.*, vol. 6, no. 10, pp. 8222–8231, 2016.
[529] D. Peltzer, J. Múnera, and L. Cornaglia, "The effect of the Li:Na molar ratio on the structural and sorption properties of mixed zirconates for CO2 capture at high temperature," *J. Environ. Chem. Eng.*, vol. 7, no. 2, p. 102927, 2019.
[530] L. A. Salazar Hoyos, B. M. Faroldi, and L. M. Cornaglia, "K-doping effect in the kinetics of CO2 capture at high temperature over lithium silicates obtained from rice husks: In situ/operando techniques," *Ceram. Int.*, vol. 47, no. 2, pp. 1558–1570, 2021.
[531] G. Montes-Hernandez and F. Renard, "Time-Resolved in Situ Raman Spectroscopy of the Nucleation and Growth of Siderite, Magnesite, and Calcite and Their Precursors," *Cryst. Growth Des.*, vol. 16, no. 12, pp. 7218–7230, 2016.
[532] M. E. Smith, "Recent progress in solid-state nuclear magnetic resonance of half-integer spin low-γ quadrupolar nuclei applied to inorganic materials," *Magn. Reson. Chem.*, vol. n/a, no. n/a, Nov. 2020.
[533] F. Taulelle, J. P. Coutures, D. Massiot, and J. P. Rifflet, "High and very high temperature NMR," *Bull. Magn. Reson.*, vol. 11, no. 3–4, pp. 318–320, 1989.
[534] H. Ernst, D. Freude, T. Mildner, and I. Wolf, "Laser-supported high-temperature MAS NMR for time-resolved in situ studies of reaction steps in heterogeneous catalysis," *Solid State Nucl. Magn. Reson.*, vol. 6, no. 2, pp. 147–156, 1996.
[535] S. Indris, P. Heitjans, R. Uecker, and B. Roling, "Li Ion Dynamics in a LiAlO2 Single Crystal Studied by 7Li NMR Spectroscopy and Conductivity Measurements," *J. Phys. Chem. C*, vol. 0, no. 0, p. null.
[536] M. T. Dunstan, J. M. Griffin, F. Blanc, M. Leskes, and C. P. Grey, "Ion Dynamics in Li2CO3 Studied by Solid-State NMR and First-Principles Calculations," *J. Phys. Chem. C*, vol. 119, no. 43, pp. 24255–24264, 2015.
[537] J. M. Valverde, P. E. Sanchez-Jimenez, L. A. Perez-Maqueda, M. A. S. Quintanilla, and J. Perez-Vaquero, "Role of crystal structure on CO2 capture by limestone derived CaO subjected to carbonation recarbonation calcination cycles at Ca looping conditions," *Appl. Energy*, vol. 125, pp. 264–275, Jul. 2014.
[538] M. Benitez-Guerrero, J. M. Valverde, A. Perejon, P. E. Sanchez-Jimenez, and L. A. Perez-Maqueda, "Effect of milling mechanism on the CO2 capture performance of limestone in the Calcium Looping process," *Chem. Eng. J.*, vol. 346, pp. 549–556, Aug. 2018.
[539] P. E. Sánchez-Jiménez, J. M. Valverde, A. Perejón, A. De La Calle, S. Medina, and L. A. Pérez-Maqueda, "Influence of Ball Milling on CaO Crystal Growth during Limestone and Dolomite Calcination: Effect on CO2 Capture at Calcium Looping

Conditions," *Cryst. Growth Des.*, vol. 16, no. 12, pp. 7025–7036, 2016.
[540] C. Ping *et al.*, "Acquiring an effective CaO-based CO2 sorbent and achieving selective methanation of CO2," *RSC Adv.*, vol. 10, no. 36, pp. 21509–21516, 2020.
[541] H. J. Yoon, S. Mun, and K. B. Lee, "Facile reactivation of used CaO-based CO2 sorbent via physical treatment: Critical relationship between particle size and CO2 sorption performance," *Chem. Eng. J.*, p. 127234, 2020.
[542] A. Lopez Ortiz and D. P. Harrison, "Hydrogen Production Using Sorption-Enhanced Reaction," *Ind. Eng. Chem. Res.*, vol. 40, no. 23, pp. 5102–5109, Nov. 2001.
[543] S. L. Homsy, J. Moreno, A. Dikhtiarenko, J. Gascon, and R. W. Dibble, "Calcium Looping: On the Positive Influence of SO2 and the Negative Influence of H2O on CO2 Capture by Metamorphosed Limestone-Derived Sorbents," *ACS Omega*, vol. 5, no. 50, pp. 32318–32333, Dec. 2020.
[544] C. I. C. Pinheiro, A. Fernandes, C. Freitas, E. T. Santos, and M. F. Ribeiro, "Waste Marble Powders as Promising Inexpensive Natural CaO-Based Sorbents for Post-Combustion CO2 Capture," *Ind. Eng. Chem. Res.*, vol. 55, no. 29, pp. 7860–7872, 2016.
[545] J. M. Valverde, "A model on the CaO multicyclic conversion in the Ca-looping process," *Chem. Eng. J.*, vol. 228, pp. 1195–1206, 2013.
[546] V. Manovic and E. J. Anthony, "Thermal activation of CaO-based sorbent and self-reactivation during CO2 capture looping cycles," *Environ. Sci. {&} Technol.*, vol. 42, no. 11, pp. 4170–4174, 2008.
[547] G. A. Mutch *et al.*, "Carbon Capture by Metal Oxides: Unleashing the Potential of the (111) Facet," *J. Am. Chem. Soc.*, vol. 140, no. 13, pp. 4736–4742, 2018.
[548] X. Carrier, C. S. Doyle, T. Kendelewicz, and G. E. Brown, "REACTION OF CO 2 WITH MgO (100) SURFACES," vol. 6, no. 6, pp. 1237–1245, 1999.
[549] H. Onishi, C. Egawa, T. Aruga, and Y. Iwasawa, "Adsorption of Na atoms and oxygen-containing molecules on MgO(100) and (111) surfaces," *Surf. Sci.*, vol. 191, no. 3, pp. 479–491, 1987.
[550] J. Hu, K. Zhu, L. Chen, C. Kübel, and R. Richards, "MgO(111) Nanosheets with Unusual Surface Activity," *J. Phys. Chem. C*, vol. 111, no. 32, pp. 12038–12044, Aug. 2007.
[551] T. Xu, X. Zhou, Z. Jiang, Q. Kuang, Z. Xie, and L. Zheng, "Syntheses of nano/submicrostructured metal oxides with all polar surfaces exposed via a molten salt route," *Cryst. Growth Des.*, vol. 9, no. 1, pp. 192–196, 2009.
[552] A. Nambo, J. He, T. Quang Nguyen, V. Atla, T. Druffel, and M. Sunkara, "Ultrafast Carbon Dioxide Sorption Kinetics Using Lithium Silicate Nanowires," *Nano Lett.*, vol. 17, no. 6, pp. 3327–3333, May 2017.
[553] K. Wang, F. Gu, P. T. Clough, Y. Zhao, P. Zhao, and E. J. Anthony, "Molten shell-activated, high-performance, un-doped Li4SiO4 for high-temperature CO2 capture at low CO2 concentrations," *Chem. Eng. J.*, p. 127353, 2020.
[554] Y. Yang *et al.*, "Novel synthesis of tailored Li4SiO4-based microspheres for ultrafast CO2 adsorption," *Fuel Process. Technol.*, p. 106675, 2020.
[555] H. Lu, A. Khan, and P. G. Smirniotis, "Relationship between structural properties and CO2 capture performance of CaO-based sorbents obtained from different organometallic precursors," *Ind. {&} Eng. Chem. Res.*, vol. 47, no. 16, pp. 6216–6220, 2008.
[556] H. Lu, E. P. Reddy, and P. G. Smirniotis, "Calcium oxide based sorbents for capture of carbon dioxide at high temperatures," *Ind. Eng. Chem. Res.*, vol. 45, no. 11, pp. 3944–3949, 2006.
[557] W. Liu, N. W. L. Low, B. Feng, G. Wang, and J. C. Diniz da Costa, "Calcium Precursors for the Production of CaO Sorbents for Multicycle CO2 Capture," *Environ.*

Sci. Technol., vol. 44, no. 2, pp. 841–847, Jan. 2010.
[558] Y. Hu, H. Lu, and H. Li, "Single step fabrication of spherical CaO pellets via novel agar-assisted moulding technique for high-temperature CO2 capture," *Chem. Eng. J.*, vol. 404, p. 127137, 2021.
[559] H. Lu, P. G. Smirniotis, F. O. Ernst, and S. E. Pratsinis, "Nanostructured Ca-based sorbents with high CO2 uptake efficiency," *Chem. Eng. Sci.*, vol. 64, no. 9, pp. 1936–1943, 2009.
[560] Y. Li, R. Sun, H. Liu, and C. Lu, "Cyclic CO2 capture behavior of limestone modified with pyroligneous acid (PA) during calcium looping cycles," *Ind. Eng. Chem. Res.*, vol. 50, no. 17, pp. 10222–10228, 2011.
[561] F. N. Ridha, V. Manovic, Y. Wu, A. Macchi, and E. J. Anthony, "Pelletized CaO-based sorbents treated with organic acids for enhanced CO2 capture in Ca-looping cycles," *Int. J. Greenh. Gas Control*, vol. 17, pp. 357–365, 2013.
[562] Y. Hu *et al.*, "Structurally improved CaO-based sorbent by organic acids for high temperature CO2 capture," *Fuel*, vol. 167, pp. 17–24, 2016.
[563] H. R. Radfarnia and M. C. Iliuta, "Limestone acidification using citric acid coupled with two-step calcination for improving the CO2 sorbent activity," *Ind. Eng. Chem. Res.*, vol. 52, no. 21, pp. 7002–7013, 2013.
[564] F. N. Ridha, V. Manovic, Y. Wu, A. Macchi, and E. J. Anthony, "Post-combustion CO2 capture by formic acid-modified CaO-based sorbents," *Int. J. Greenh. Gas Control*, vol. 16, pp. 21–28, 2013.
[565] F. N. Ridha, V. Manovic, A. Macchi, M. A. Anthony, and E. J. Anthony, "Assessment of limestone treatment with organic acids for CO2 capture in Ca-looping cycles," *Fuel Process. Technol.*, vol. 116, pp. 284–291, 2013.
[566] R. Sun, C. W. Tai, M. Strømme, and O. Cheung, "The effects of additives on the porosity and stability of amorphous calcium carbonate," *Microporous Mesoporous Mater.*, vol. 292, no. August 2019, p. 109736, 2020.
[567] G. Y. Jung, E. Shin, J. H. Park, B. Y. Choi, S. W. Lee, and S. K. Kwak, "Thermodynamic Control of Amorphous Precursor Phases for Calcium Carbonate via Additive Ions," *Chem. Mater.*, vol. 31, no. 18, pp. 7547–7557, 2019.
[568] R. Sun *et al.*, "Amorphous Calcium Carbonate Constructed from Nanoparticle Aggregates with Unprecedented Surface Area and Mesoporosity," *ACS Appl. Mater. Interfaces*, vol. 10, no. 25, pp. 21556–21564, 2018.
[569] P. Opitz *et al.*, "Insights into the In Vitro Formation of Apatite from Mg-Stabilized Amorphous Calcium Carbonate," *Adv. Funct. Mater.*, vol. 31, no. 3, p. 2007830, Jan. 2021.
[570] Global Carbon Capture and Storage Institute Ltd, "Global CCS Institute - Facilities Database." [Online]. Available: https://co2re.co/FacilityData. [Accessed: 10-Jun-2020].
[571] C. Halliday, T. Harada, and T. Alan Hatton, "Toward a Mechanistic Understanding and Optimization of Molten Alkali Metal Borates (AxB1-xO1.5-x) for Higherature CO2 Capture," *Chem. Mater.*, vol. 32, no. 1, pp. 348–359, 2020.
[572] C. Halliday, T. Harada, and T. A. Hatton, "Bench scale demonstration of molten alkali metal borates for high temperature CO2 capture Bench scale demonstration of molten alkali metal borates for high temperature CO 2 capture," 2020.
[573] T. Harada, C. Halliday, A. Jamal, and T. A. Hatton, "Molten ionic oxides for CO2 capture at medium to high temperatures," *J. Mater. Chem. A*, vol. 7, no. 38, pp. 21827–21834, 2019.
[574] B. N. Nair, T. Yamaguchi, H. Kawamura, S.-I. Nakao, and K. Nakagawa, "Processing of Lithium Zirconate for Applications in Carbon Dioxide Separation: Structure and Properties of the Powders," *J. Am. Ceram. Soc.*, vol. 87, no. 1, pp. 68–74, Jan. 2004.
[575] J. F. Gómez-García and H. Pfeiffer, "Effect of Chemical Composition and Crystal

Phase of (Li,Na)FeO2 Ferrites on CO2 Capture Properties at High Temperatures," *J. Phys. Chem. C*, vol. 122, no. 37, pp. 21162–21171, Sep. 2018.
[576] J. Ida and Y. S. Lin, "Mechanism of high-temperature CO2 sorption on lithium zirconate," *Environ. Sci. Technol.*, vol. 37, no. 9, pp. 1999–2004, May 2003.
[577] Y. M. Kwon *et al.*, "Regenerable sodium-based lithium silicate sorbents with a new mechanism for CO2 capture at high temperature," *Renewable Energy*, Elsevier Ltd, 2018.
[578] L. C. Buelens, H. Poelman, C. Detavernier, G. B. Marin, and V. V. Galvita, "CO2 sorption properties of Li4SiO4 with a Li2ZrO3 coating," *J. CO2 Util.*, vol. 34, no. May, pp. 688–699, 2019.
[579] C. Galven, T. Pagnier, N. Rosman, F. Le Berre, and M. P. Crosnier-Lopez, "β-Na2TeO4: Phase Transition from an Orthorhombic to a Monoclinic Form. Reversible CO2 Capture," *Inorg. Chem.*, vol. 57, no. 12, pp. 7334–7345, Jun. 2018.
[580] F. Fujishiro, K. Fukasawa, and T. Hashimoto, "CO2 absorption and desorption properties of single phase Ba 2Fe2O5 and analysis of their mechanism using thermodynamic calculation," *J. Am. Ceram. Soc.*, vol. 94, no. 11, pp. 3675–3678, Nov. 2011.
[581] M. T. Dunstan *et al.*, "Reversible CO 2 Absorption by the 6H Perovskite Ba 4 Sb 2 O 9," vol. 4891, no. 2, 2013.
[582] P. Sánchez-Camacho, J. F. Gómez-García, and H. Pfeiffer, "Thermokinetic and conductivity analyzes of the high CO2 chemisorption on Li5AlO4 and alkaline carbonate impregnated Li5AlO4 samples: Effects produced by the use of CO2 partial pressures and oxygen addition," *J. Energy Chem.*, vol. 26, no. 5, pp. 919–926, Nov. 2017.
[583] P. Olavarría, E. Vera, E. J. Lima, and H. Pfeiffer, "Synthesis and evaluation as CO2 chemisorbent of the Li5(Al1−xFex)O4 solid solution materials: Effect of oxygen addition," *J. Energy Chem.*, vol. 26, no. 5, pp. 948–955, Nov. 2017.
[584] H. A. Lara-García, O. Ovalle-Encinia, J. Ortiz-Landeros, E. Lima, and H. Pfeiffer, "Synthesis of Li 4+: X Si 1- x Fe x O 4 solid solution by dry ball milling and its highly efficient CO 2 chemisorption in a wide temperature range and low CO 2 concentrations," *J. Mater. Chem. A*, vol. 7, no. 8, pp. 4153–4164, 2019.
[585] N. Gómez-Garduño and H. Pfeiffer, "Thermokinetic evaluation of iron addition on lithium metazirconate (Fe-Li 2 ZrO 3) for enhancing carbon dioxide capture at high temperatures," *Thermochim. Acta*, vol. 673, pp. 129–137, Mar. 2019.
[586] X. Zhan, Y. T. Cheng, and M. Shirpour, "Nonstoichiometry and Li-ion transport in lithium zirconate: The role of oxygen vacancies," *J. Am. Ceram. Soc.*, vol. 101, no. 9, pp. 4053–4065, Sep. 2018.
[587] E. Vera, J. F. Gómez-García, and H. Pfeiffer, "Enhanced CO2 chemisorption at high temperatures via oxygen addition using (Fe, Cu or Ni)-containing sodium cobaltates as solid sorbents," *J. CO2 Util.*, vol. 25, pp. 147–157, May 2018.
[588] J. Hilz, M. Helbig, M. Haaf, A. Daikeler, J. Ströhle, and B. Epple, "Long-term pilot testing of the carbonate looping process in 1 MWth scale," *Fuel*, vol. 210, no. May, pp. 892–899, 2017.
[589] M. Haaf, J. Hilz, J. Peters, A. Unger, J. Ströhle, and B. Epple, "Operation of a 1 MWth calcium looping pilot plant firing waste-derived fuels in the calciner," *Powder Technol.*, 2020.
[590] M. E. Diego and B. Arias, "Impact of load changes on the carbonator reactor of a 1.7 MWth calcium looping pilot plant," *Fuel Process. Technol.*, vol. 200, no. September 2019, p. 106307, 2020.
[591] M.-H. Chang *et al.*, "Design and Experimental Testing of a 1.9MWth Calcium Looping Pilot Plant," *Energy Procedia*, vol. 63, pp. 2100–2108, 2014.

[592] B. Arias *et al.*, “Demonstration of steady state CO2 capture in a 1.7MWth calcium looping pilot,” *Int. J. Greenh. Gas Control*, vol. 18, pp. 237–245, 2013.
[593] H. Cui *et al.*, “Ultrafast and Stable CO2 Capture Using Alkali Metal Salt-Promoted MgO-CaCO3 Sorbents,” *ACS Appl. Mater. Interfaces*, vol. 10, no. 24, pp. 20611–20620, 2018.
[594] H. Cui, Z. Cheng, and Z. Zhou, “Unravelling the role of alkaline earth metal carbonates in intermediate temperature CO2 capture using alkali metal salt-promoted MgO-based sorbents,” *J. Mater. Chem. A*, vol. 8, no. 35, pp. 18280–18291, 2020.
[595] E. Desmaele, N. Sator, R. Vuilleumier, and B. Guillot, “The MgCO3–CaCO3–Li2CO3–Na2CO3–K2CO3 melts: Thermodynamics and transport properties by atomistic simulations,” *J. Chem. Phys.*, vol. 150, no. 21, p. 214503, Jun. 2019.
[596] Y. Hu, H. Cui, Z. Cheng, and Z. Zhou, “Sorption-enhanced water gas shift reaction by in situ CO2 capture on an alkali metal salt-promoted MgO-CaCO3 sorbent,” *Chem. Eng. J.*, vol. 377, no. August 2018, p. 119823, 2019.
[597] M. L. T. Triviño, H. Jeon, A. C. S. Lim, V. Hiremath, Y. Sekine, and J. G. Seo, “Encapsulation of Phase-Changing Eutectic Salts in Magnesium Oxide Fibers for High-Temperature Carbon Dioxide Capture: Beyond the Capacity–Stability Tradeoff,” *ACS Appl. Mater. Interfaces*, vol. 12, no. 1, pp. 518–526, Jan. 2020.
[598] P. Zhang, J. Tong, and K. Huang, “Self-Formed, Mixed-Conducting, Triple-Phase Membrane for Efficient CO2/O2 Capture from Flue Gas and in Situ Dry-Oxy Methane Reforming,” *ACS Sustain. Chem. Eng.*, vol. 6, no. 11, pp. 14162–14169, Nov. 2018.
[599] L. Zhang, Y. Gong, K. S. Brinkman, T. Wei, S. Wang, and K. Huang, “Flux of silver-carbonate membranes for post-combustion CO2 capture: The effects of membrane thickness, gas concentration and time,” *J. Memb. Sci.*, vol. 455, pp. 162–167, 2014.
[600] R. Lan, S. M. M. Abdallah, I. A. Amar, and S. Tao, “Preparation of dense La0.5Sr0.5Fe0.8Cu0.2O3−δ–(Li,Na)2CO3–LiAlO2 composite membrane for CO2 separation,” *J. Memb. Sci.*, vol. 468, pp. 380–388, 2014.
[601] M. Kazakli *et al.*, “Controlling molten carbonate distribution in dual-phase molten salt-ceramic membranes to increase carbon dioxide permeation rates,” *J. Memb. Sci.*, no. August, p. 118640, 2020.
[602] L. Duan, C. Su, M. Erans, Y. Li, E. J. Anthony, and H. Chen, “CO2 Capture Performance Using Biomass-Templated Cement-Supported Limestone Pellets,” *Ind. Eng. Chem. Res.*, vol. 55, no. 39, pp. 10294–10300, 2016.
[603] F. N. Ridha, V. Manovic, E. J. Anthony, and A. Macchi, “The morphology of limestone-based pellets prepared with kaolin-based binders,” *Mater. Chem. Phys.*, vol. 138, no. 1, pp. 78–85, 2013.
[604] Y. Wu, V. Manovic, I. He, and E. J. Anthony, “Modified lime-based pellet sorbents for high-temperature CO2 capture: Reactivity and attrition behavior,” *Fuel*, vol. 96, pp. 454–461, 2012.
[605] T. Jiang, H. Zhang, Z. Xu, Y. Zhao, X. Ma, and S. Wang, “Scale-up production and process optimization of Zr-doped CaO-based sorbent for CO2 capture,” *Asia-Pacific J. Chem. Eng.*, vol. 15, no. 5, p. e2502, Sep. 2020.
[606] K. Wang, F. Gu, P. T. Clough, P. Zhao, and E. J. Anthony, “Porous MgO-stabilized CaO-based powders/pellets via a citric acid-based carbon template for thermochemical energy storage in concentrated solar power plants,” *Chem. Eng. J.*, p. 124163, 2020.
[607] Z. Xu, T. Jiang, H. Zhang, Y. Zhao, X. Ma, and S. Wang, “Efficient MgO-doped CaO sorbent pellets for high temperature CO2 capture,” *Front. Chem. Sci. Eng.*, 2021.
[608] J. Hilz, M. Haaf, M. Helbig, N. Lindqvist, J. Ströhle, and B. Epple, “Scale-up of the carbonate looping process to a 20 MWth pilot plant based on long-term pilot tests,” *Int. J. Greenh. Gas Control*, vol. 88, no. July, pp. 332–341, 2019.
[609] Y. Wang, L. Zhao, A. Otto, M. Robinius, and D. Stolten, “A Review of Post-

combustion CO2 Capture Technologies from Coal-fired Power Plants," *Energy Procedia*, vol. 114, pp. 650–665, 2017.
[610] R. Zhao, Goodwin James G., K. Jothimurugesan, J. J. Spivey, and S. K. Gangwal, "Comparison of Attrition Test Methods: ASTM Standard Fluidized Bed vs Jet Cup," *Ind. Eng. Chem. Res.*, vol. 39, no. 5, pp. 1155–1158, May 2000.
[611] F. Donat and C. R. Müller, "A critical assessment of the testing conditions of CaO-based CO2sorbents," *Chem. Eng. J.*, vol. 336, pp. 544–549, 2018.
[612] J. C. Abanades, G. Grasa, M. Alonso, N. Rodriguez, E. J. Anthony, and L. M. Romeo, "Cost structure of a postcombustion CO2 capture system using CaO," *Environ. Sci. {&} Technol.*, vol. 41, no. 15, pp. 5523–5527, 2007.
[613] A. MacKenzie, D. L. Granatstein, E. J. Anthony, and J. C. Abanades, "Economics of CO2 capture using the calcium cycle with a pressurized fluidized bed combustor," *Energy {&} Fuels*, vol. 21, no. 2, pp. 920–926, 2007.
[614] P. Fennell, "3 - Economics of chemical and calcium looping," in *Woodhead Publishing Series in Energy*, P. Fennell and B. B. T.-C. and C. L. T. for P. G. and C. D. (CO2) C. Anthony, Eds. Woodhead Publishing, 2015, pp. 39–48.
[615] G. Grasa, B. Gonzalez, M. Alonso, and J. C. Abanades, "Comparison of CaO-Based SyntheticCO(2) sorbents under realistic calcination conditions," *Energy {&} Fuels*, vol. 21, no. 6, pp. 3560–3562, 2007.
[616] J. C. Abanades, E. S. Rubin, and E. J. Anthony, "Sorbent cost and performance in CO2 capture systems," *Ind. {&} Eng. Chem. Res.*, vol. 43, no. 13, pp. 3462–3466, 2004.
[617] S. Michalski, D. P. Hanak, and V. Manovic, "Techno-economic feasibility assessment of calcium looping combustion using commercial technology appraisal tools," *J. Clean. Prod.*, vol. 219, pp. 540–551, 2019.
[618] D. P. Hanak and V. Manovic, "Economic feasibility of calcium looping under uncertainty," *Appl. Energy*, vol. 208, pp. 691–702, 2017.
[619] Y. C. Hu, W. Q. Liu, Y. D. Yang, J. Sun, Z. J. Zhou, and M. H. Xu, "Enhanced CO2 Capture Performance of Limestone by Industrial Waste Sludge," *Chem. Eng. Technol.*, vol. 40, no. 12, pp. 2322–2328, 2017.
[620] X. Yan, Y. Li, X. Ma, J. Zhao, Z. Wang, and H. Liu, "CO2 capture by a novel CaO/MgO sorbent fabricated from industrial waste and dolomite under calcium looping conditions," *New J. Chem.*, vol. 43, no. 13, pp. 5116–5125, 2019.
[621] F. Yan *et al.*, "Cyclic Performance of Waste-Derived SiO2 Stabilized, CaO-Based Sorbents for Fast CO2 Capture," *ACS Sustain. Chem. Eng.*, vol. 4, no. 12, pp. 7004–7012, Dec. 2016.
[622] Y. Wu *et al.*, "Syntheses of four novel silicate-based nanomaterials from coal gangue for the capture of CO2," *Fuel*, vol. 258, no. August 2019, 2019.
[623] X. Ma, Y. Li, C. Chi, W. Zhang, J. Shi, and L. Duan, "CO2 Capture Performance of Mesoporous Synthetic Sorbent Fabricated Using Carbide Slag under Realistic Calcium Looping Conditions," *Energy and Fuels*, vol. 31, no. 7, pp. 7299–7308, 2017.
[624] A. Nawar, H. Ghaedi, M. Ali, M. Zhao, N. Iqbal, and R. Khan, "Recycling waste-derived marble powder for CO2 capture," *Process Saf. Environ. Prot.*, vol. 132, pp. 214–225, 2019.
[625] T. Papalas, A. N. Antzaras, and A. A. Lemonidou, "Evaluation of Calcium-Based Sorbents Derived from Natural Ores and Industrial Wastes for High-Temperature CO2 Capture," *Ind. Eng. Chem. Res.*, vol. 59, no. 21, pp. 9926–9938, May 2020.
[626] J. Arcenegui-Troya, P. E. Sánchez-Jiménez, A. Perejón, J. M. Valverde, R. Chacartegui, and L. A. Pérez-Maqueda, "Calcium-Looping Performance of Biomineralized CaCO3 for CO2 Capture and Thermochemical Energy Storage," *Ind. Eng. Chem. Res.*, vol. 59, no. 29, pp. 12924–12933, Jul. 2020.
[627] Y. Tsuboi and N. Koga, "Thermal Decomposition of Biomineralized Calcium

Carbonate: Correlation between the Thermal Behavior and Structural Characteristics of Avian Eggshell," *ACS Sustain. Chem. Eng.*, vol. 6, no. 4, pp. 5283–5295, 2018.
[628] S. A. Salaudeen, S. H. Tasnim, M. Heidari, B. Acharya, and A. Dutta, "Eggshell as a potential CO2 sorbent in the calcium looping gasification of biomass," *Waste Manag.*, vol. 80, pp. 274–284, 2018.
[629] T. Wang, D.-C. Xiao, C.-H. Huang, Y.-K. Hsieh, C.-S. Tan, and C.-F. Wang, "CO2 uptake performance and life cycle assessment of CaO-based sorbents prepared from waste oyster shells blended with PMMA nanosphere scaffolds," *J. Hazard. Mater.*, vol. 270, pp. 92–101, 2014.
[630] R. J. Thorne *et al.*, "Environmental impacts of a chemical looping combustion power plant," *Int. J. Greenh. Gas Control*, vol. 86, pp. 101–111, 2019.
[631] F. García-Labiano, P. Gayán, J. Adánez, L. F. Diego, and C. R. Forero, "Solid Waste Management of a Chemical-Looping Combustion Plant using Cu-Based Oxygen Carriers," *Environ. Sci. Technol.*, vol. 41, no. 16, pp. 5882–5887, 2007.
[632] D. P. Hanak, M. Erans, S. A. Nabavi, M. Jeremias, L. M. Romeo, and V. Manovic, "Technical and economic feasibility evaluation of calcium looping with no CO2 recirculation," *Chem. Eng. J.*, vol. 335, pp. 763–773, 2018.
[633] C.-C. Cormos, "Economic evaluations of coal-based combustion and gasification power plants with post-combustion CO2 capture using calcium looping cycle," *Energy*, vol. 78, pp. 665–673, 2014.
[634] D. P. Hanak, E. J. Anthony, and V. Manovic, "A review of developments in pilot-plant testing and modelling of calcium looping process for CO2 capture from power generation systems," *Energy Environ. Sci.*, vol. 8, no. 8, pp. 2199–2249, 2015.
[635] A. Rolfe, Y. Huang, M. Haaf, S. Rezvani, A. Dave, and N. J. Hewitt, "Techno-economic and Environmental Analysis of Calcium Carbonate Looping for CO2 Capture from a Pulverised Coal-Fired Power Plant," *Energy Procedia*, vol. 142, pp. 3447–3453, 2017.
[636] A. Rolfe, Y. Huang, M. Haaf, S. Rezvani, D. McIlveen-Wright, and N. J. Hewitt, "Integration of the calcium carbonate looping process into an existing pulverized coal-fired power plant for CO2 capture: Techno-economic and environmental evaluation," *Appl. Energy*, vol. 222, no. April, pp. 169–179, 2018.
[637] M. Spinelli *et al.*, "Integration of Ca-Looping Systems for CO2 Capture in Cement Plants," *Energy Procedia*, vol. 114, pp. 6206–6214, 2017.
[638] C. C. Dean, D. Dugwell, and P. S. Fennell, "Investigation into potential synergy between power generation, cement manufacture and CO2 abatement using the calcium looping cycle," *Energy Environ. Sci*, vol. 4, no. 6, pp. 2050–2053, 2011.
[639] C. Dean, T. Hills, N. Florin, D. Dugwell, and P. S. Fennell, "Integrating Calcium Looping CO2 Capture with the Manufacture of Cement," *Energy Procedia*, vol. 37, pp. 7078–7090, 2013.
[640] E. De Lena *et al.*, "Techno-economic analysis of calcium looping processes for low CO2 emission cement plants," *Int. J. Greenh. Gas Control*, vol. 82, no. October 2018, pp. 244–260, 2019.
[641] S. Gardarsdottir *et al.*, "Comparison of Technologies for CO2 Capture from Cement Production—Part 2: Cost Analysis," *Energies*, vol. 12, no. 3, p. 542, Feb. 2019.
[642] N. Rodríguez, R. Murillo, and J. C. Abanades, "CO2 Capture from Cement Plants Using Oxyfired Precalcination and/or Calcium Looping," *Environ. Sci. Technol.*, vol. 46, no. 4, pp. 2460–2466, Feb. 2012.
[643] E. De Lena, M. Spinelli, and M. C. Romano, "CO2 capture in cement plants by 'tail-End' Calcium Looping process," *Energy Procedia*, vol. 148, pp. 186–193, 2018.
[644] P. Bayer and M. Aklin, "The European Union Emissions Trading System reduced CO₂ emissions despite low prices," *Proc. Natl. Acad. Sci.*,

vol. 117, no. 16, pp. 8804 LP – 8812, Apr. 2020.
[645] Y. A. Criado, B. Arias, and J. C. Abanades, “Calcium looping CO2 capture system for back-up power plants,” *Energy Environ. Sci.*, vol. 10, no. 9, pp. 1994–2004, 2017.
[646] B. Arias, Y. A. Criado, and J. C. Abanades, “Thermal Integration of a Flexible Calcium Looping CO2 Capture System in an Existing Back-Up Coal Power Plant,” *ACS Omega*, vol. 5, no. 10, pp. 4844–4852, Mar. 2020.
[647] G. Ji *et al.*, “Enhanced hydrogen production from thermochemical processes,” *Energy Environ. Sci.*, vol. 11, no. 10, pp. 2647–2672, 2018.
[648] L. Han *et al.*, “Catalytic Toluene Reforming with In Situ CO2 Capture via an Iron–Calcium Hybrid Absorbent for Promoted Hydrogen Production,” *Energy Technol.*, vol. 8, no. 6, p. 2000083, Jun. 2020.
[649] M. Shokrollahi Yancheshmeh, H. R. Radfarnia, and M. C. Iliuta, “High temperature CO2 sorbents and their application for hydrogen production by sorption enhanced steam reforming process,” *Chem. Eng. J.*, vol. 283, pp. 420–444, Jan. 2016.
[650] N. H. Florin and A. T. Harris, “Enhanced hydrogen production from biomass with in situ carbon dioxide capture using calcium oxide sorbents,” *Chem. Eng. Sci.*, vol. 63, no. 2, pp. 287–316, 2008.
[651] D. P. Harrison, “The role of solids in CO2 capture: A mini review,” *Greenh. Gas Control Technol.*, vol. 11, no. 225, pp. 1101–1106, 2005.
[652] D. P. Harrison, “Calcium enhanced hydrogen production with CO2 capture,” *Energy Procedia*, vol. 1, no. 1, pp. 675–681, 2009.
[653] D. P. Harrison, “Sorption-enhanced hydrogen production: A review,” *Ind. Eng. Chem. Res.*, vol. 47, pp. 6486–6501, 2008.
[654] W. Gao, T. Zhou, Y. Gao, and Q. Wang, “Enhanced water gas shift processes for carbon dioxide capture and hydrogen production,” *Appl. Energy*, vol. 254, p. 113700, 2019.
[655] F. Wu, P. A. Dellenback, and M. Fan, “Highly efficient and stable calcium looping based pre-combustion CO2 capture for high-purity H2 production,” *Mater. Today Energy*, vol. 13, pp. 233–238, 2019.
[656] C. R. Müller, R. Pacciani, C. D. Bohn, S. A. Scott, and J. S. Dennis, “Investigation of the Enhanced Water Gas Shift Reaction Using Natural and Synthetic Sorbents for the Capture of CO2,” *Ind. Eng. Chem. Res.*, vol. 48, no. 23, pp. 10284–10291, Dec. 2009.
[657] C. Ortiz, J. M. Valverde, R. Chacartegui, L. A. Perez-Maqueda, and P. Giménez, “The Calcium-Looping (CaCO3/CaO) process for thermochemical energy storage in Concentrating Solar Power plants,” *Renew. Sustain. Energy Rev.*, vol. 113, no. July, p. 109252, 2019.
[658] J. Sunku Prasad, P. Muthukumar, F. Desai, D. N. Basu, and M. M. Rahman, “A critical review of high-temperature reversible thermochemical energy storage systems,” *Appl. Energy*, vol. 254, no. August, p. 113733, 2019.
[659] H. Sun, Y. Li, X. Yan, Z. Wang, and W. Liu, “CaO/CaCO3 thermochemical heat storage performance of CaO-based micrometre-sized tubular composite,” *Energy Convers. Manag.*, vol. 222, p. 113222, 2020.
[660] M. Astolfi, E. De Lena, and M. C. Romano, “Improved flexibility and economics of Calcium Looping power plants by thermochemical energy storage,” *Int. J. Greenh. Gas Control*, vol. 83, no. February, pp. 140–155, 2019.
[661] Y. Yan, K. Wang, P. T. Clough, and E. J. Anthony, “Developments in calcium/chemical looping and metal oxide redox cycles for high-temperature thermochemical energy storage: A review,” *Fuel Process. Technol.*, vol. 199, no. June 2019, p. 106280, 2020.
[662] R. Han, J. Gao, S. Wei, F. Sun, Q. Liu, and Y. Qin, “Development of dense Ca-based, Al-stabilized composites with high volumetric energy density for thermochemical

energy storage of concentrated solar power," *Energy Convers. Manag.*, vol. 221, p. 113201, 2020.
[663] A. J. Carrillo, K. J. Kim, Z. D. Hood, A. H. Bork, and J. L. M. Rupp, "La0.6Sr0.4Cr0.8Co0.2O3Perovskite Decorated with Exsolved Co Nanoparticles for Stable CO2Splitting and Syngas Production," *ACS Appl. Energy Mater.*, vol. 3, no. 5, pp. 4569–4579, 2020.
[664] D. Sastre, D. P. Serrano, P. Pizarro, and J. M. Coronado, "Chemical insights on the activity of La1-xSrxFeO3 perovskites for chemical looping reforming of methane coupled with CO2-splitting," *J. CO2 Util.*, vol. 31, no. December 2018, pp. 16–26, 2019.
[665] R. Barker, "Reactivity of Calcium-Oxide Towards Carbon-Dioxide and Its Use for Energy-Storage," *J. Appl. Chem. Biotechnol.*, vol. 24, no. 4–5, pp. 221–227, 1974.
[666] L. Yang, Z. Huang, and G. Huang, "Fe- and Mn-Doped Ca-Based Materials for Thermochemical Energy Storage Systems," *Energy & Fuels*, Aug. 2020.
[667] B. Li, Y. Li, H. Sun, Y. Wang, and Z. Wang, "Thermochemical Heat Storage Performance of CaO Pellets Fabricated by Extrusion–Spheronization under Harsh Calcination Conditions," *Energy & Fuels*, vol. 34, no. 5, pp. 6462–6473, May 2020.
[668] C. Zhang, Y. Li, Y. Yuan, Z. Wang, T. Wang, and W. Lei, "Simultaneous CO2 capture and heat storage by a Ca/Mg-based composite in coupling calcium looping and CaO/Ca(OH)2 cycles using air as a heat transfer fluid," *React. Chem. Eng.*, vol. 6, no. 1, pp. 100–111, 2021.
[669] Hot Lime Labs Ltd., "Hot lime labs." [Online]. Available: https://hotlimelabs.com/technology/.
[670] F. Dashtestani, M. Nusheh, V. Siriwongrungson, J. Hongrapipat, V. Materic, and S. Pang, "CO2 Capture from Biomass Gasification Producer Gas Using a Novel Calcium and Iron-Based Sorbent through Carbonation–Calcination Looping," *Ind. Eng. Chem. Res.*, vol. 59, no. 41, pp. 18447–18459, Oct. 2020.
[671] A. Di Giuliano, F. Giancaterino, C. Courson, P. U. Foscolo, and K. Gallucci, "Development of a Ni-CaO-mayenite combined sorbent-catalyst material for multicycle sorption enhanced steam methane reforming," *Fuel*, vol. 234, no. July, pp. 687–699, 2018.
[672] A. Di Giuliano *et al.*, "Development of Ni- and CaO-based mono- and bi-functional catalyst and sorbent materials for Sorption Enhanced Steam Methane Reforming: Performance over 200 cycles and attrition tests," *Fuel Process. Technol.*, vol. 195, no. July, p. 106160, 2019.
[673] P. Xu, Z. Zhou, C. Zhao, and Z. Cheng, "Catalytic performance of Ni/CaO-Ca5Al6O14 bifunctional catalyst extrudate in sorption-enhanced steam methane reforming," *Catal. Today*, vol. 259, Part, pp. 347–353, Jan. 2016.
[674] L. Tan, C. Qin, Z. Zhang, J. Ran, and V. Manovic, "Compatibility of NiO/CuO in Ca–Cu Chemical Looping for High-Purity H2 Production with CO2 Capture," *Energy Technol.*, vol. 6, no. 9, pp. 1777–1787, Sep. 2018.
[675] Y. Ni *et al.*, "High purity hydrogen production from sorption enhanced chemical looping glycerol reforming: Application of NiO-based oxygen transfer materials and potassium promoted Li2ZrO3 as CO2 sorbent," *Appl. Therm. Eng.*, vol. 124, pp. 454–465, 2017.
[676] C. Dang, L. Liu, G. Yang, W. Cai, J. Long, and H. Yu, "Mg-promoted Ni-CaO microsphere as bi-functional catalyst for hydrogen production from sorption-enhanced steam reforming of glycerol," *Chem. Eng. J.*, vol. 383, no. October 2019, p. 123204, 2020.
[677] N. N. Mohd Arif, S. Z. Abidin, O. U. Osazuwa, D. V. N. Vo, M. T. Azizan, and Y. H. Taufiq-Yap, "Hydrogen production via CO2 dry reforming of glycerol over

Re[sbnd]Ni/CaO catalysts," *Int. J. Hydrogen Energy*, vol. 44, no. 37, pp. 20857–20871, 2019.
[678] N. D. Charisiou *et al.*, "Ni supported on CaO-MgO-Al2O3 as a highly selective and stable catalyst for H2 production via the glycerol steam reforming reaction," *Int. J. Hydrogen Energy*, vol. 44, no. 1, pp. 256–273, 2019.
[679] S. Sang *et al.*, "Promotional role of MgO on sorption-enhanced steam reforming of ethanol over Ni/CaO catalysts," *AIChE J.*, no. October, pp. 1–13, 2019.
[680] X. Qiao, P. Lisbona, X. Guo, Y. Lara, and L. M. Romeo, "Energy Assessment of Ethanol-Enhanced Steam Reforming by Means of Li4SiO4 Carbon Capture," *Energy and Fuels*, vol. 30, no. 3, pp. 1879–1886, 2016.
[681] S. A. Ghungrud and P. D. Vaidya, "Improved Hydrogen Production from Sorption-Enhanced Steam Reforming of Ethanol (SESRE) Using Multifunctional Materials of Cobalt Catalyst and Mg-, Ce-, and Zr-Modified CaO Sorbents," *Ind. Eng. Chem. Res.*, vol. 59, no. 2, pp. 693–703, 2020.
[682] Y. Xu, B. Lu, C. Luo, J. Chen, Z. Zhang, and L. Zhang, "Sorption enhanced steam reforming of ethanol over Ni-based catalyst coupling with high-performance CaO pellets," *Chem. Eng. J.*, vol. 406, p. 126903, 2021.
[683] G. Grasa, M. V Navarro, J. M. López, L. Díez-Martín, J. R. Fernández, and R. Murillo, "Validation of the H2 production stage via SER under relevant conditions for the Ca/Cu reforming process practical application," *Chem. Eng. J.*, vol. 324, pp. 266–278, 2017.
[684] G. Diglio *et al.*, "Feasibility of CaO/CuO/NiO sorption-enhanced steam methane reforming integrated with solid-oxide fuel cell for near-zero-CO2 emissions cogeneration system," *Appl. Energy*, vol. 230, no. May, pp. 241–256, 2018.
[685] J. R. Fernández, J. M. Alarcón, and J. C. Abanades, "Study of the calcination of CaCO3 by means of a Cu/CuO chemical loop using methane as fuel gas," *Catal. Today*, vol. 333, no. February 2018, pp. 176–181, 2019.
[686] L. Díez-Martín, J. M. López, J. R. Fernández, I. Martínez, G. Grasa, and R. Murillo, "Complete Ca/Cu cycle for H2 production via CH4 sorption enhanced reforming in a Lab-Scale fixed bed reactor," *Chem. Eng. J.*, vol. 350, pp. 1010–1021, 2018.
[687] M. Z. Memon *et al.*, "Alkali Metal CO2 Sorbents and the Resulting Metal Carbonates: Potential for Process Intensification of Sorption-Enhanced Steam Reforming," *Environ. Sci. Technol.*, vol. 51, no. 1, pp. 12–27, Jan. 2017.
[688] L. C. Buelens, V. V Galvita, H. Poelman, C. Detavernier, and G. B. Marin, "Super-dry reforming of methane intensifies CO2 utilization via Le Chatelier's principle," *Science (80-.).*, vol. 354, no. 6311, pp. 449–452, Oct. 2016.